8-4-2017

P2X7 Receptor Primes IL-1β and the NLRP3 Inflammasome in Astrocytes Subjected to Mechanical Strain

Farraj S. Albalawi
University of Pennsylvania, albalawi_f@hotmail.com

Wennan Lu

Jonarhan M. Beckel

Jason C. Lim

Stuart A. McCaughey

See next page for additional authors

P2X7 Receptor Primes IL-1β and the NLRP3 Inflammasome in Astrocytes Subjected to Mechanical Strain

Abstract
Inflammatory responses play a key role in many neural pathologies, with localized signaling from non-immune cells making critical contributions. The NLRP3 inflammasome is an important component of innate immune signaling and can link neural insult to chronic inflammation. Stimulation of the NLRP3 inflammasome is a two-stage process. The priming stage involves upregulation of the biosynthesis of the structural components while activation results in their assembly into the actual inflammasome complex and subsequent activation. The priming step can be rate limiting and can connect insult to chronic inflammation but our knowledge of the signals that regulate NLRP3 inflammasome priming in sterile inflammatory conditions is limited. This study examined the link between mechanical strain and inflammasome priming in neural systems. Transient non-ischemic elevation of intraocular pressure (IOP) increased mRNA for inflammasome components *IL-1β, NLRP3, ASC, CASP1* and *IL-6* in rat and mouse retinas. The P2X7 receptor was implicated in the *in vivo* mechanosensitive priming of IL-1*β* and IL-*6* transcription and translation. *In vitro* experiments with optic nerve head astrocytes demonstrated enhanced expression of the *IL-1β* and *IL-6* genes following stretching or swelling. The increase in *IL-1β* expression was inhibited by degradation of extracellular ATP with apyrase, blocking pannexin hemichannels with carbenoxolone, probenecid or ^{10}Panx1 peptide, P2X7 receptor antagonists (BBG, A839977 or A740003) as well inhibition of the NFκB transcription factor with Bay 11-7082. The swelling-dependent fall in expression of the NFκB inhibitor IκB-α was reduced by treatment of cells with A839977 and in P2X7 knockout mice. In summary, our data suggest that mechanical trauma to the retina results in priming of the NLRP3 inflammasome components and upregulated *IL-6* expression and release. This was dependent upon ATP release through pannexin hemichannels and autostimulation of the P2X7 receptor. Since the P2X7 receptor can also trigger inflammasome activation it appears to have a central role in linking mechanical strain to neuroinflammation.

Degree Type
Dissertation

Degree Name
DScD (Doctor of Science in Dentistry)

Primary Advisor
Dr. Claire Mitchell

Keywords
IL-1β, astrocytes, glaucoma, pannexin, ATP release, NFκB, IL-18, caspase 1, NLRP3

Subject Categories
Dentistry

Author
Farraj S. Albalawi, Wennan Lu, Jonarhan M. Beckel, Jason C. Lim, Stuart A. McCaughey, and Claire H. Mitchell

P2X7 receptor primes IL-1β and the NLRP3 inflammasome
in astrocytes subjected to mechanical strain

Farraj Albalawi

A Dissertation

Presented to the Faculties of the University of Pennsylvania

in

Partial Fulfillment of the Requirements for the

Degree of Doctor of Science in Dentistry

2017

Supervisor of Dissertation

_____

Claire H. Mitchell, Ph.D.
Professor of Anatomy and Cell Biology

Dissertation Committee

_____

Chair: Jonathan Korostoff, DMD, Ph.D. Professor of Periodontics and Director of Master of Science in Oral Biology Program
Member: Kelly Jordan-Sciutto, Ph.D. Chair and Professor, Department of Pathology
Member: Kenneth S. Shindler, MD, Ph.D. Associate Professor of Ophthalmology and Neurology

P2X7 receptor primes IL-1β and the NLRP3 inflammasome
in astrocytes subjected to mechanical strain

ACKNOWLEDGMENT

First and foremost, I would like to thank my mentor, Dr. Mitchell, for all her help throughout this journey. Without her, this project would not have been possible. Coming from a clinical background where I am used to answering the question, she has taught me how to ask the question and think like a scientist.

I would like to thank my committee members, Dr. Korostoff, Dr. Jordan-Sciutto and Dr. Shindler for taking the time to meet with me and guiding me. Your questions and comments encouraged me to think critically and have inspired me to pursue this research in the dental field.

I would also like to thank Dr. Graves and Dr. Jordan-Sciutto who granted me acceptance into the DSCD program.

I would like to thank all of the orthodontic department especially Dr. Chung, Dr. Vanarsdall, Dr. Greco, Dr. Coby and Dr. Guan for all their support and guidance.

I would like to thank Dr. Mitchell's lab members, past and present, for being patient and for offering your help along every step of the way.

Last but not least I would like to thank my family and friends, I couldn't have done this without you.

ABSTRACT

P2X7 receptor primes IL-1β and the NLRP3 inflammasome

in astrocytes subjected to mechanical strain

Farraj Albalawi

Claire H. Mitchell, Ph.D.

Inflammatory responses play a key role in many neural pathologies, with localized signaling from non-immune cells making critical contributions. The NLRP3 inflammasome is an important component of innate immune signaling and can link neural insult to chronic inflammation. Stimulation of the NLRP3 inflammasome is a two-stage process. The priming stage involves upregulation of the biosynthesis of the structural components while activation results in their assembly into the actual inflammasome complex and subsequent activation. The priming step can be rate limiting and can connect insult to chronic inflammation but our knowledge of the signals that regulate NLRP3 inflammasome priming in sterile inflammatory conditions is limited. This study examined the link between mechanical strain and inflammasome priming in neural systems. Transient non-ischemic elevation of intraocular pressure (IOP) increased mRNA for inflammasome components *IL-1β, NLRP3, ASC, CASP1* and *IL-6* in rat and

mouse retinas. The P2X7 receptor was implicated in the *in vivo* mechanosensitive priming of IL-1*β* and IL-*6* transcription and translation. *In vitro* experiments with optic nerve head astrocytes demonstrated enhanced expression of the *IL-1β* and *IL-6* genes following stretching or swelling. The increase in *IL-1β* expression was inhibited by degradation of extracellular ATP with apyrase, blocking pannexin hemichannels with carbenoxolone, probenecid or ^{10}Panx1 peptide, P2X7 receptor antagonists (BBG, A839977 or A740003) as well inhibition of the NFκB transcription factor with Bay 11-7082. The swelling-dependent fall in expression of the NFκB inhibitor IκB-α was reduced by treatment of cells with A839977 and in P2X7 knockout mice. In summary, our data suggest that mechanical trauma to the retina results in priming of the NLRP3 inflammasome components and upregulated *IL-6* expression and release. This was dependent upon ATP release through pannexin hemichannels and autostimulation of the P2X7 receptor. Since the P2X7 receptor can also trigger inflammasome activation it appears to have a central role in linking mechanical strain to neuroinflammation.

TABLE OF CONTENTS

LIST OF TABLES

LIST OF ILLUSTRATIONS

LIST OF ABBREVIATIONS

AIM2: absent in melanoma 2
ASC: Apoptosis-Associated Speck-Like Protein Containing CARD
ATP: adenosine triphosphate
BAX: bcl-2-like protein 4
BBG: Coomassie Brilliant Blue G
BzATP: (4-benzoyl-benzoyl)-ATP
CARD: caspase activation and recruitment domain
CASP1: Interleukin-1 converting enzyme/caspase1 gene
CEI: Controlled Elevation of IOP
CNS: central nervous system
COX-2: cyclooxygenase-2
DAMPs: danger-associated molecular patterns
EDTA: ethylenediaminetetraacetic acid
ELISA: enzyme-linked immunosorbent assay
FBS: Fetal bovine serum
GAPDH: glyceraldehyde 3-phosphate dehydrogenase
GFAP: Glial fibrillary acidic protein
gp 130: glycoprotein 130
HEPES: 4-(2-hydroxyethyl)-1-piperazineethanesulfonic acid
HP1: hypoxanthine phosphoribosyltransferase 1,
HRP: horseradish peroxidase
IFI16: interferon-inducible protein 16
IFN-γ : interferon gamma
IL-18: Interleukin 18
IL-1R: Interleukin- 1 receptors
IL-1β: interleukin 1 beta
IL-6: Interleukin 6
IL-6: Interleukin- 6 receptors
IOP: Intraocular pressure
JAK: Janus Kinase
JNK: c-Jun N-terminal kinases
LLR: leucine-rich repeat
LPS: lipopolysaccharide
MAPK: mitogen-activated protein kinase
mtDNA: mitochondrial DNA

MyD88: myeloid differentiation factor 88
NBD: nucleotide-binding domain
NFκB: nuclear factor kappa-light-chain-enhancer of activated B cells
NLRP3: NACHT, LRR and PYD domains-containing protein 3
NLRs: Nod-like receptors
NMDA: N-methyl-D-aspartate receptor
NOD2: Nucleotide-binding oligomerization domain-containing protein 2
NTPDase1: Ectonucleoside triphosphate diphosphohydrolase-1
ONH: optic nerve head
PAMPs: pathogen-associated molecular patterns
PBS: phosphate buffered saline
PRRs: pattern-recognition receptors
PYD: pyrin domain
qPCR: quantitative polymerase chain reaction
RGC: retinal ganglion cell
RIPA: Radioimmunoprecipitation assay buffer
ROS: reactive oxygen species
SDS: sodium dodecyl sulfate polyacrylamide gel electrophoresis
SEM: standard error of the mean
STAT: signal transducers and activators of transcription
TBI: traumatic brain injury
TLRs: Toll-like receptors
TMD: transmembrane domain
TMJ: temporomandibular joint
TNFR: tumor necrosis factor receptor
TRIF: TIR-domain-containing adapter-inducing interferon- β

Chapter 1 : Introduction

Mechanical strain can induce complex pathological changes in many anatomic compartment of the body including epithelium, bone, cartilage and neural tissue (Corps et al., 2015; Heppner et al., 2015; Le Guen et al., 2016; Xiao et al., 2016). These changes can lead to several disorders such as atherosclerosis (Quigley and Addicks, 1980), temporomandibular joint (TMJ) disorders (Balaratnasingam et al., 2007), periodontal diseases (Liu et al., 2017), traumatic brain injury (TBI) (Lau et al., 2006), encephalitis (Kumar et al., 2009) and glaucoma (Sigal and Ethier, 2009) amongst others. In several acute and chronic disorders, inflammatory signaling is increasingly recognized as contributing to pathology. However, the exact mechanism through which mechanical strain leads to inflammation is still not fully understood. Thus, we hypothesized that purinergic signaling pathways link mechanical strain to inflammatory signaling. In particular, the mechanosensitive release of ATP and autostimulation of P2X7 receptors play a key role in priming the NLRP3 inflammasome. While these studies were carried out in an effort to expand the existing knowledge regarding inflammatory signaling in glaucoma, the findings have wider-ranging implications. By extension, the results can be used to explain the ability of mechanical strain to induce sterile chronic inflammation throughout the body in general and the stomatognathic system in particular.

“Inflammation is generally defined as a response to infection, tissue injury or tissue stress that aims to restore homeostasis” (Tehrani et al., 2014). Microbes interact with receptors of the innate immune system to induce an inflammatory response that eradicates the microbe and induces protective immunity. On the other hand, inflammation triggered by sterile tissue stress or injury aims to repair the damaged tissue and adapt to the stress leading to restoration of homeostasis (Medzhitov, 2008). Therefore, depending on the trigger, inflammatory responses have different physiological purposes and when uncontrolled, potential pathological consequences. Several studies have focused on the inflammatory response to microbial infection (e.g. (Gianchecchi and Fierabracci, 2015; Jimenez-Dalmaroni et al., 2016; Rhee, 2011; Takeda and Akira, 2004), yet less is known about the signaling pathway and inflammatory mediators of sterile inflammation especially in the central nervous system (CNS).

Mechanical strain is frequently associated with changes in purinergic signaling, with ATP release associated with cell swelling and stretching (Corriden and Insel, 2010; Praetorius and Leipziger, 2009). Purinergic signaling has been implicated in regulating the production of multiple inflammatory cytokines by a variety of cell types. For example, IL-6 has been shown to be regulated by ATP-mediated activation of purinergic receptors in fibroblasts (Inoue et al., 2007), macrophages (Hanley et al., 2004) and microglia (Shieh et al., 2014). IL-1β release and inflammasome activation is closely linked to P2X7 receptor stimulated by ATP in non-neural cells (Ferrari et al., 2006; Franceschini et al.,

2015; Gombault et al., 2012). In both cases, the signals leading to IL-6 release or inflammasome priming, which is required before IL-1β release, are not well understood, particularly in sterile inflammation. Since chronic inflammatory conditions in CNS may involve pathways activated by mechanical strain, the goal of this study was to determine the mechanism through which mechanical strain leads to priming of the inflammasome and enhanced expression of IL-6,

The master proinflammatory cytokine IL-1β is released after priming, assembly and activation of the inflammasome, which is a component of the innate immune system. The innate immune system is specialized to perform receptor-mediated surveillance for microbial pathogens or tissue injury (Patel et al., 2017). This system acts at the front line of the broader immune response by sensing pathogen-associated molecular patterns (PAMPs) and danger-associated molecular patterns (DAMPs) via pattern-recognition receptors (PRRs). PAMPs are associated with external pathogens, while DAMPs are associated with host-derived molecules, and both can interact with and activate PRRs. The presence of DAMPs such as mitochondrial DNA, uric acid, chromatin, ATP and β-amyloid have been reported in CNS chronic inflammatory diseases, but their role is still unclear (Martinon, 2008; Thundyil and Lim, 2015). PRRs are expressed by several immune and non-immune cells, but in the CNS they are primarily expressed by astrocytes, microglia and macrophages (Walsh et al., 2014). These molecules are either membrane bound or located within the cytoplasm. Membrane bound PRRs such as Toll-like receptors (TLRs) sense extracellular or

endosomally located signals, while the cytosolic receptors such as Nod-like receptors (NLRs) sense intracellular signals and are involved in the assembly of the inflammasome (Bezbradica et al., 2017; Walsh et al., 2014). The pathogenesis of many sterile chronic inflammatory diseases including glaucoma involve the inflammasome (Chi et al., 2015; Chi et al., 2014), but our knowledge regarding the mechanism(s) that results in its priming is not well understood (Figure 1.1).

Inflammasome structure:

The inflammasome concept was initially described in the early 2000's by Tschopp and colleagues when a crucial link between tissue injury, innate immune response, and caspase 1-dependent responses was revealed (Martinon et al., 2002; Martinon et al., 2000). The inflammasome is a cytosolic multiprotein platform that enables the activation of pro-inflammatory caspases, mainly caspase 1 (Figure 1.1) (Rathinam et al., 2012). Caspase 1 leads to the maturation and release of pro-inflammatory cytokines and therefore to a strong inflammatory response against infectious agents and physiological abnormality (Man and Kanneganti, 2015). Inflammasome complexes have three main components: a cytosolic pattern-recognition receptor, the enzyme caspase 1 and an adaptor protein that enables the interaction between the two. The receptor is a member of either the NLR family of proteins such as NLRP1, NLRP2 and NLRP3 or a member of the pyrin and HIN domain-containing (PYHIN) family of

proteins, such as absent in melanoma 2 (AIM2) and interferon-inducible protein 16 (IFI16) (Man and Kanneganti, 2015).

The NLRs contain a carboxy-terminal leucine-rich repeat (LRR), nucleotide-binding domain (NBD) and variable amino-terminal domain that defines several NLR subfamilies. There are several inflammasomes subfamilies, but the NLRP3 inflammasome is most well understood and regulates caspase 1 activation. Therefore, our work focused on the NLRP3 inflammasome. The NLRP3 family is recognized by its pyrin domain (PYD) in the amino-terminal region. Following activation and oligomerization, NLRP3 recruit, via homotypic protein interactions, the adaptor ASC (Apoptosis-associated speck-like protein containing a caspase activation and recruitment domain), the second component of most inflammasomes. ASC, which is composed of a (PYD) and a caspase activation and recruitment domain (CARD), acts as an adaptor between the PYD of the NLRP3 protein and the CARD of pro-caspase 1, the third component of inflammasomes (Figure 1.2) (Agostini et al., 2004). Caspase 1 is produced from the 45 kDa pro-caspase in the cytoplasm. Pro-caspase 1 is constitutively expressed, but requires post-translational processing to form active 20 and 10 kDa forms of caspase 1 (Ho et al., 2014). Activation of caspase-1 occurs following assembly and activation of the NLRP3 inflammasome, and subsequently leads to proteolytic activation of IL-1β and IL-18 within the inflammasome protein complex.

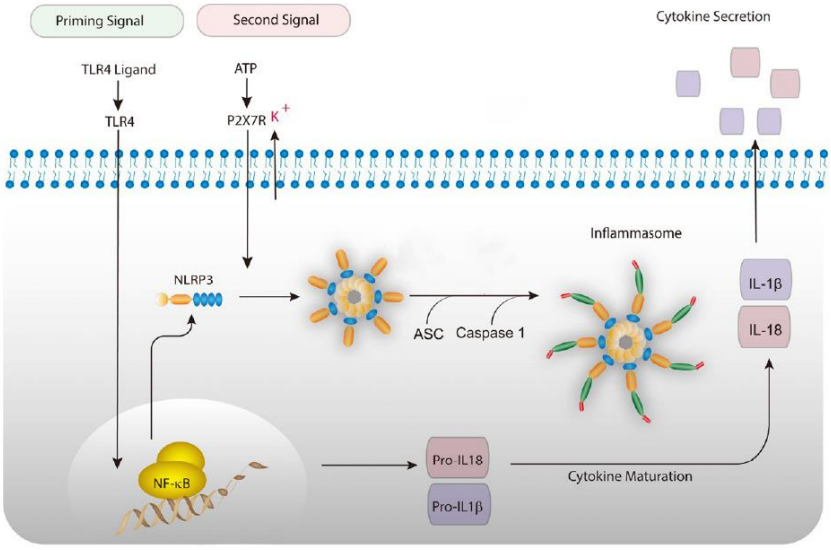

Figure 1.1 Inflammasome priming and activation.

NLRP3 inflammasome requires 2 signals to prime and activate, resulting in activation of caspase 1 and subsequent maturation and release of IL-1β. A priming signal, traditionally ascribed to a TLR activates the NFκB dependent transcription of pro-IL-1β and in some cases NLRP3 and IL-18. The second signal involves the activation of the inflammasome. The P2X7 receptor is a common trigger for the second step, with stimulation by extracellular ATP triggering potassium ion (K^+) efflux. *Modified from* (Choi and Ryter, 2014)

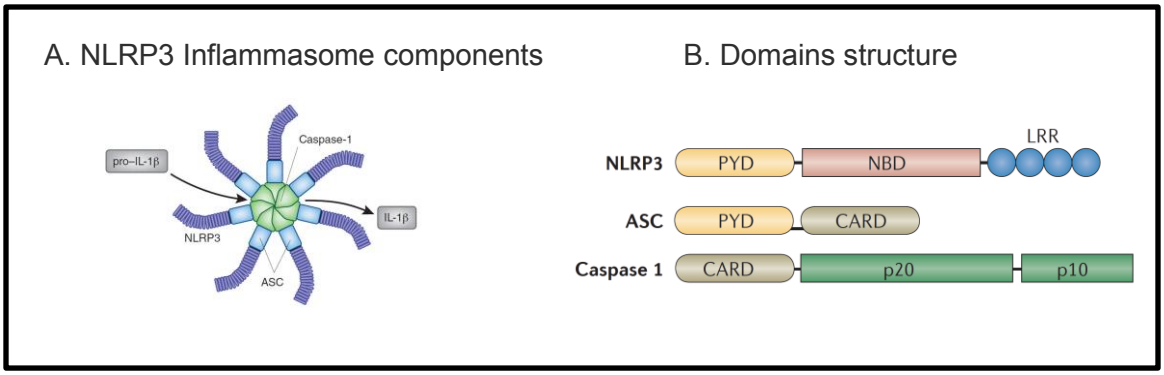

Figure 1.2 NLRP3 Inflammasome components.

A. The assembled NLRP3 inflammasome forms a wheel-like structure that has 3 components; the receptor NLRP3 protein, the adaptor protein ASC and the enzyme caspase 1. *Modified from (Hansson and Klareskog, 2011).*
B. The receptor NLRP3 protein has a sensory component formed by the carboxy-terminal leucine-rich repeat (LRR). Oligomerization of NLRP3 is mediated by the nucleotide-binding domain (NBD). The pyrin domain (PYD) of the receptor NLRP3 mediates protein–protein interactions between (PYD) of the adaptor ASC. The caspase activation and recruitment domain (CARD) mediate the protein–protein interactions of ASC with pro-caspase 1, which also contains a (CARD). The recruitment of pro-caspase 1 into the inflammasome induces cleavage of the pro-caspase1 into active subunits. *Modified from (Walsh et al., 2014)*.

Inflammasome priming and activation:

In immune cells, the NLRP3 inflammasome signaling pathway is described as a two-step process that uses two signals (Figure 1.1). The first step is priming, which increases the level of the pro-IL-1β to suitable levels (Johansson, 1988), and in some cases NLRP3 at the transcriptional and translational level (Bauernfeind et al., 2009; Halle et al., 2008; Mariathasan et al., 2006). The second step, activation, is much better understood. Basically, a signal triggers the oligomerization and formation of the wheel-like inflammasome structure (Figure 1.2) (Broz, 2015). This process is induced by a wide range of stimuli including bacterial toxins, prokaryotic mRNA, crystalline materials, protein aggregates, Ca^{2+} influx, mitochondrial reactive oxygen species (ROS), mitochondrial DNA (mtDNA), ATP and efflux of K^+ through the P2X7 purinergic receptor (Bernier, 2012; Karmakar et al., 2016; Man and Kanneganti, 2015; Mariathasan et al., 2006; Petrilli et al., 2007). The final outcome of NLRP3 inflammasome assembly is the proteolytic cleavage of cytosolic inactive pro-IL-1β and pro-IL-18 into the mature inflammatory cytokines IL-1β and IL-18 by the activated caspase 1 (Lamkanfi and Dixit, 2012; Martinon et al., 2002). The fact that various stimuli lead to NLRP3 activation suggests that it acts as a general sensor of cellular damage or stress (Figure 1.1).

In immune cells such as macrophages, priming of the NLRP3 inflammasome can be accomplished by activation of receptors that signal via MyD88 (myeloid

differentiation factor 88) and TRIF (TIR-domain-containing adapter-inducing interferon-β) or other NFκB activating pathways, including TLRs, Interleukin- 1 receptors (IL-1R), tumor necrosis factor receptor (TNFR) and Nucleotide-binding oligomerization domain-containing protein 2 (NOD2)(Deguine and Barton, 2014). In several species, the expression of both IL-1β and NLRP3 is transcriptionally regulated (Broz et al., 2010) and thought to prime the inflammasome before it is activated by a second stimulus. TLR4 ligands, such as lipopolysaccharide (LPS), are commonly used to study priming of the NLRP3 inflammasome and upregulate IL-1β and NLRP3 expression (Bezbradica et al., 2017). Many sterile chronic inflammatory diseases involve inflammasome activation. However, our knowledge concerning the mechanism that leads to its' priming in the absence of signals associated with microbial pathogens is limited. Non-immune cells such as neurons and astrocytes have been shown to be involved in immunologic reactions and to release inflammatory cytokines (Choi et al., 2014; Lim et al., 2016). Thus, their inflammasome priming may have a different signaling pathway relative to that of immune cells. Unraveling the priming process in these cells will therefore have significant implications regarding our understanding of sterile chronic inflammation.

When the inflammasome is primed and activated the final products are mature IL-1β and IL-18. IL-1β is a part of IL-1 family, which is a central player in the inflammatory cascade. IL-1 has two isoforms, IL-1α and IL-1β, which both bind to the same receptors and are biologically active (Hattori and Gouaux, 2012). IL-1β

is produced as 31 kDa precursors within the cell; this precursor form remains within the cell and cleaved to its mature active form through the action of the active caspase 1 from the NLRP3 inflammasome. IL-1β is only active once it is cleaved to its 17 kDa mature form. IL-1β has been the focus of numerous studies due to its highly pro-inflammatory effect, especially in humans (Dinarello, 2011). and has been implicated in a variety of CNS pathologies including stroke, traumatic brain injury and spinal cord injury (Walsh et al., 2014).

IL-18 is also a member of the IL-1 family and can mediate inflammatory reactions and the host response to infection (Dinarello, 2002, 2007). Unlike IL-1β, IL-18 is constitutively produced as a precursor protein in several cell types (Dinarello, 2007). Pro-IL-18 is cleaved by caspase 1 to form mature active IL-18, which is released along with mature IL-1β. LPS signaling can prime IL-18 above baseline levels, but another stimulus is needed to activate the inflammasome and lead to the release. While IL-1β priming is crucial for its processing and release, the role of IL-18 priming is not well understood, perhaps related to its constitutive expression (Dinarello, 2007; Ferrari et al., 2006).

The biological activities of IL-1β, IL-18 and pyroptosis are largely beneficial to the host during an infection. IL-1β and IL-18 have a wide range of effects on their target cells via induction of distinct signal transduction pathways. IL-1β activates NFκB, resulting in upregulation of several gene products in the inflammatory process, such as, IL-6, cyclooxygenase-2 (COX-2), chemokines, and cellular

adhesion molecules (Arulkumaran et al., 2011; Dinarello, 2002). IL-18 induces enhanced production of interferon gamma (IFN-γ) and upregulates IL-6, and IL-8 through activation mitogen-activated protein kinase (MAPK) pathway (Lee et al., 2004). In synergy with cells of the immune system the beneficial result is eradication of the microbial pathogen. However, IL-1β and IL-18 induced by endogenous danger signals can also trigger sterile inflammation, a risk factor for the development of autoinflammatory and neuroinflammatory disorders and metabolic diseases (Man and Kanneganti, 2015). This priming signal can be the rate-limiting step in inflammatory responses and may connect the initial insult to situations of sterile chronic inflammation associated with traumatic brain injuries and glaucoma.

While the NLRP3 inflammasome proteolytically cleaves IL-1β and IL-18, IL-6 release does not necessarily require inflammasome activation. This pleiotropic cytokine belongs to the IL-6 family and interacts with cells through either glycoprotein 130 (gp 130) (Heinrich et al., 2003) or the soluble IL-6 receptor (Chalaris et al., 2007). Janus Kinase (JAK), signal transducers and activators of transcription (STAT) and the MAPK cascade, are all known to be activated by IL-6. These molecules and pathway mediate several physiological and pathological conditions in the CNS (Scheller et al., 2014; Tsakiri et al., 2008). IL-6 upregulation has been confirmed in multiple neuroinflammatory conditions, including traumatic brain injury (TBI) and spinal cord injury, with levels of IL-6 correlating with pathological progression of the conditions (Guptarak et al., 2013;

Kumar et al., 2015; Yang et al., 2013). In addition, IL-6 has been detected in patients with chronic glaucoma and in a glaucoma model with IOP elevation (Chen et al., 1999; Johnson et al., 2011; Zenkel et al., 2010).

While IL-6 is traditionally known as a proinflammatory cytokine, it can also induce neurogenesis and protect neural cells after damage (Erta et al., 2012; Penkowa et al., 2003). IL-6 increases both the number and length of neuronal processes from isolated retinal ganglion cells (Chidlow et al., 2012) protects retinal ganglion cells from pressure-induced cell death *in vitro* (Sappington et al., 2006). While these observations suggest IL-6 has an important role in response to increased pressure, the signaling mechanisms linking the mechanical strain to the IL-6 response are not well understood.

Mechanical strain and inflammation:

Mechanical strain can be translated into important physiological signals, but overstimulation of these pathways can induce complex pathological changes to neural tissue via inflammation (Corps et al., 2015; Heppner et al., 2015). For example, stretching neurons in a model of traumatic brain injury leads to apoptosis (Lau et al., 2006). In encephalitis, which involves elevated intracranial pressure (Kaushik et al., 2012; Kumar et al., 2009) the inflammatory reaction is mediated by the inflammasome and IL-1β (Tamai et al., 2017). Similarly, in glaucoma, increased intraocular pressure (IOP) produces complex mechanical deformations that contribute to glaucomatous optic neuropathy (Sigal and Ethier,

2009). The pathological changes in glaucoma occur in what is usually considered a sterile environment. As such, glaucoma provides an ideal model to examine the relationship between strain, purines, and inflammasome priming in neural tissue. Previous work suggests that the NLRP1/NLRP3 inflammasomes and production of IL-1β play a critical role in cell death in mouse models of acute glaucoma with high levels of IOP that induce ischemia (Chi et al., 2015; Chi et al., 2014). While this indicates a possible link between mechanical strain and inflammasome involvement in neuronal inflammation, the model makes it difficult to separate the complex effects of ischemia from those due to mechanical strain resulting from more modest IOP elevations representative of most forms of glaucoma.

"Glaucoma is the second most common cause of blindness" (Resnikoff et al., 2004), affecting approximately 80 million people worldwide (Plantinga et al., 2013). It is a group of ocular disorders sharing a characteristic neuropathy of the optic nerve, with the most common risk factor being an elevation of the IOP. The elevation in IOP is most commonly associated with a block in the drainage of aqueous humor through the trabecular meshwork. Since the eye is a relatively closed system, this increased resistance to drainage leads to an increase in IOP (Casson et al., 2012). In patients with glaucoma and in experimental glaucoma models where IOP is elevated, an inflammatory response including activation of the complement system and upregulation of TNF-α (Plantinga et al., 2013) and IL-6 (Johnson et al., 2011; Lu et al., 2017), occurs at early stages of disease progression. The physical strains produced by IOP elevation are focused at the

optic nerve head (ONH) and in particular at the region of the lamina cribrosa (Bellezza et al., 2003; Burgoyne, 2011; Sigal and Ethier, 2009). The optic nerve head astrocytes that reside here have been identified as a critical intermediary in the pathogenesis of glaucoma (Hernandez 2000; Downs et al. 2008).

Astrocytes are star-shaped glial cells that are the most abundant cell type in the ONH and most parts of the brain. (Nedergaard et al., 2003; Tehrani et al., 2014). Astrocytes are in contact with neurons and provide both metabolic and structural support to neurons as part of normal physiology (Plantinga et al., 2013). In addition, they can regulate synaptic transmission and can also release gliotransmitters such as glutamate and ATP (Hamilton and Attwell, 2010). Neuronal stress or injury can trigger a coordinated multicellular inflammatory response that involves astrocytes as well as neurons and other CNS cells (Liddelow and Barres, 2017). Astrocytes can undergo reactive hypertrophy of the cell body and processes in response to these stimuli (Sofroniew, 2009). These morphological changes are associated with changes in cytoskeletal proteins, such as glial fibrillary acidic protein (GFAP) and actin (Ho et al., 2014). Recent studies have shown that various insults to the CNS can elicit dissimilar reactive astrocyte types each exhibiting distinct properties (Liddelow and Barres, 2017).

Axons in the ONH receive mechanical and biochemical support from astrocytes that envelop axon bundles with their processes (Morrison et al., 2011). Astrocytes are emerging as central mediators of mechanical strain and the ability

of astrocytes to release ATP upon stretch or swelling has implications for neuronal signaling in various regions. (Bennett et al., 2012; Darby et al., 2003; Halassa et al.,2009; Ostrow and Sachs, 2005; Perez-Ortiz et al., 2008). Astrocytes are mechanosensitive to stretch (Beckel et al., 2014) and optic nerve head astrocytes are particularly well situated to examine the signals induced by these forces. Elevated pressure in a closed system leads to a stretch of cells and their membranes (Landsman et al., 1995). As glaucomatous eyes have both an increase in baseline IOP and an increased magnitude of the daily IOP fluctuations (Gao et al., 2012), optic nerve head astrocytes are subjected to considerable mechanical stretch. Astrocytes from patients showed morphological changes before marked loss of retinal ganglion cells (Lye-Barthel et al., 2013). They have also been identified as contributing to the inflammatory response in the glaucomatous eye (Johnson and Morrison, 2009) and have been implicated in the damage to retinal ganglion cells in chronic glaucoma (Hernandez et al., 2008; Morgan, 2000). Currently, the progression towards blindness can be delayed mainly by reducing the IOP (Scemes et al., 2009). Therefore, understanding how mechanical strain in the ONH is translated into inflammatory signals by astrocytes is a major challenge in glaucoma research. Accumulating evidence implicates a central role for purinergic signaling through ATP.

Purinergic signaling:

Throughout the body, mechanical strain triggers the release of the transmitter adenosine triphosphate (ATP) from both neural and non-neural cell types

(Burnstock, 1999; Grygorczyk et al., 2013). ATP was originally recognized as the main metabolic fuel for cells. Burnstock subsequently identified ATP as a neurotransmitter in nerves of the peripheral and central nervous systems (Burnstock, 1972, 2009). Later, the discovery of purinergic receptors demonstrated that ATP mediates autocrine and paracrine signaling actions via receptors located on the plasma membrane (Burnstock, 1980, 2012, 2014). At least one form of purinergic receptors is found on nearly every cell in the body. The receptors are excited by ATP released into the extracellular space or degraded into adenosine by ecto-ATPases.

Extracellular ATP is a possible candidate to link the elevated IOP in glaucoma to inflammatory signaling in the retina and optic nerve. ATP is found to be released with shear stress, stretch and swelling of the cells. The released ATP has been postulated act as a “messenger” to induce cellular responses to mechanical strain (Burnstock, 1999; Mitchell, 2001). It has been shown that release of ATP can result in various physiological and pathological responses such as cell death, volume regulation, pain, inflammatory responses and neuroprotective signals (Lazarowski et al., 2003; Lu et al., 2015). Elevated extracellular ATP was confirmed in mouse, primate and rat models of chronic IOP elevation (Lu et al., 2015) and detected in the eyes of humans with chronic glaucoma (Li et al., 2011) illustrating a clear link between increased IOP and excessive ATP release in the retina.

In astrocytes, ATP can be released by multiple pathways. Amongst these are lytic release through a compromised plasma membrane as a part of programmed cell death (Dahl, 2015), vesicular release by exocytosis (Silinsky, 1975) or transport down an electrochemical gradient through ion channels such as connexin hemichannels, pannexin hemichannels, maxi-anion channels and CALMH1 channels (Cotrina et al., 1998; Iglesias et al., 2009; Liu et al., 2008; Taruno et al., 2013). In astrocytes isolated from the optic nerve head, moderate strain from stretch or swelling leads to a release of ATP through pannexin hemichannels (Beckel et al., 2014). Expression of pannexin 1 is increased *in vitro* by cell stretch and *in vivo* in a model of chronic intraocular pressure (IOP) elevation, implicating ATP release in response to sustained mechanical strain.

Pannexin hemichannels include pannexin 1, 2 and 3 that are expressed in both vertebrates and invertebrates (Panchin et al., 2000). Pannexins belong to the family of mammalian gap junction proteins which include the connexin channels in vertebrates and innexin channels in invertebrates. Despite the difference in the amino acid sequence between the pannexin and connexin hemichannels, they both have similar membrane topology: four transmembrane domains (TMDs) with two extracellular loops with intracellular N and C termini (Scemes et al., 2009). However, pannexin proteins have only two extracellular cysteines and are extensively glycosylated on their second extracellular loop at Asn^{254}, preventing gap junction formation, while connexins have conserved cysteine residues on their extracellular loops (Boassa et al., 2007; Boassa et al.,

2008; Scemes et al., 2009). Pannexin 1 can conduct molecules up to 1 kDa in size across the plasma membrane. As ATP and UTP are 507 and 484 daltons, respectively, they can permeate the channel (Chekeni et al., 2010).

Pannexin hemichannels are mechanosensitive and can be opened by application of negative pressure applied via a patch pipette (Bao et al., 2004). This channel property could be the basis for the observed swelling-induced ATP release in response to hypotonic stress in airway epithelial cells (Ransford et al., 2009). In addition, swelling has been shown to activate pannexins in several cell types, including neurons (Xia et al., 2012b) and astrocytes (Beckel et al., 2014). Therefore, investigating the role of pannexins in inflammasome priming that accompanies the mechanosensitive release of ATP is justified.

Extracellular ATP can induce physiological responses by binding to P2 purinergic receptors of which there are two major groups; ionotropic P2X receptors and metabotropic P2Y receptors (Burnstock, 2004). P2X receptors are found only in eukaryotes and are expressed throughout the human body including the nervous, cardiovascular and immune systems. P2X receptors are implicated in a wide range of physiological processes such as synaptic transmission, muscle contraction, taste and inflammation (Burnstock and Kennedy, 2011; Hattori and Gouaux, 2012; Surprenant and North, 2009). Multiple P2X family subunits have been identified which form functional ligand-gated ion channels as homo- and/or hetero-oligomeric protein complexes

(Sperlagh et al., 2006). Within the P2X receptor family, P2X7 receptors are known to have key physiological and pathological functions in the CNS because of their widespread involvement in neuroinflammatory diseases (Sperlagh et al., 2006).

The ATP-gated P2X7 receptor is a homotrimeric, non-selective cation channel. The basic structure of the P2X7 receptor exhibits two transmembrane domains (TM1, TM2), a large, glycosylated, cysteine-rich extracellular loop, a short intracellular N- terminal domain and an intracellular C-terminal domain which is longer than that of other P2X receptor subunits (Jiang et al., 2013; Sperlagh and Illes, 2014). Pharmacologically, P2X7 receptors have a low sensitivity for ATP. Unlike other members of the P2X receptor family, P2X7 receptors require submillimolar to millimolar concentrations of ATP for activation. This is far greater than the micromolar concentration required for other P2X receptors (EC50 of ATP for P2X7 receptor = 2-4 mM and for other P2X receptors = 1–10 μM) (Rodrigues et al., 2015 ; Soares-Bezerra et al., 2015). Moreover, they have a higher affinity for 4-benzoyl-benzoyl-ATP (BzATP) than ATP (Klapperstuck et al., 2001 ; Young et al., 2007). While the requirement for a high concentration of ATP can limit activation, ATP release from pannexin hemichannels has been proposed as a pathway for physiologic activation; if the pannexin channel is adjacent to the P2X7 receptor, a release of fewer ATP molecules is required to achieve the concentration necessary to activate the P2X7 receptor (Poornima et al., 2012; Silverman et al., 2009).

Stimulation of the P2X7 receptor by endogenous agonist ATP enables the efflux of K^+ and the influx of Ca^{2+}, Na^+, resulting in membrane depolarization. This, in turn, can modulate multiple signaling pathways and alter the rate of neurotransmitter release. Over-activation of P2X7 receptors can lead to membrane blebbing and apoptotic or necrotic cell death (Bellezza et al., 2003; Burgoyne, 2011; Pelegrin and Surprenant, 2006; Perregaux and Gabel, 1994; Tsukimoto et al., 2006; Virginio et al., 1999). The role of the P2X7 receptor in mediating apoptosis makes it a major target for therapeutic intervention for neuroprotection and peripheral diseases. In addition, the P2X7 receptor is well known for its ability to activate the NLRP3 inflammasome following the efflux of K^+ through its opened pore (Mariathasan et al., 2006; Petrilli et al., 2007). This leads to IL-1β release from macrophages, microglia, dendritic cells and monocytes primed by LPS (Ferrari et al., 2006; Mingam et al., 2008; Pizzirani et al., 2007 ; Takenouchi et al., 2009). However, it is currently unclear if the P2X7 receptor also plays a role in priming the inflammasome. This is crucially important as priming is often the rate-limiting step in chronic sterile inflammation.

Hypothesis

The NLRP3 inflammasome is a key component of the localized innate immune system, leading to the cleavage and release of pro-inflammatory cytokines (Rathinam et al., 2012). This cytoplasmic oligoprotein complex has been implicated in neural disorders associated with mechanical strain or elevated pressure (Walsh et al., 2014) including traumatic brain injury, encephalitis, and glaucoma (Chi et al., 2015; Kaushik et al., 2012; Liu et al., 2013). **We hypothesized that, mechanical strain induced by IOP triggers release of ATP through pannexin 1 hemichannels on optic nerve head astrocytes, leading to autostimulation of the P2X7 receptors and priming of the NLRP3 inflammasome**. Studies in this thesis have identified a novel role for the P2X7 receptor in priming the inflammasome. Thus, this represents and alternative mechanism to the Toll-like receptor pathways traditionally associated with this process. The demonstration that mechanosensitive ATP release and inflammasome priming occur in optic nerve head astrocytes may help delineate the events that link mechanical strain to inflammatory signaling in glaucoma as well as provide a paradigm for neuroinflammation that occurs in response to other general types of mechanical strain in the nervous system (Figure 1.3).

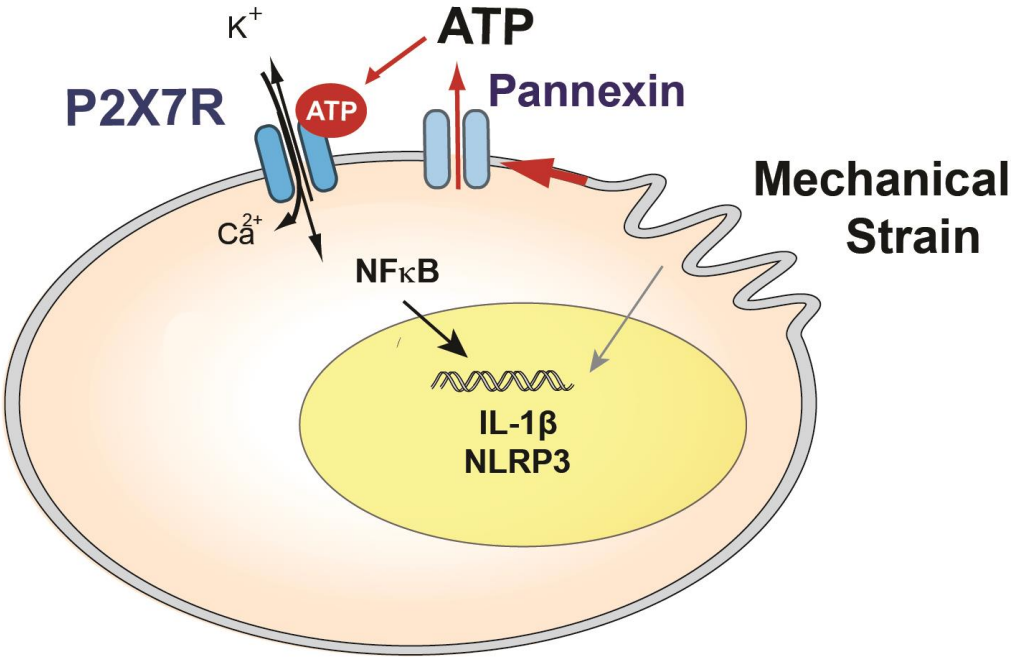

Figure 1.3 Hypothesized model

Model summarizing the hypothesized role of the P2X7 receptor in the priming of inflammasome genes after mechanical strain. Membrane stretch leads to ATP release through pannexin hemichannels. The resulting extracellular ATP can autostimulate P2X7 receptors leading to NFκB activation and transcriptional elevation of IL-1β and NLRP3 in optic nerve head astrocytes. Swelling may also activate inflammasome genes through additional pathways.

Chapter 2 : The P2X7 receptor primes IL-1β and the NLRP3 inflammasome in astrocytes exposed to mechanical strain

Farraj Albalawi,[1,2] Wennan Lu[1], Jonathan M. Beckel,[1,5] Jason C. Lim[1], Stuart A. McCaughey[1], Claire H. Mitchell[1,3,4*]

Author affiliation: Departments of [1]Anatomy and Cell Biology, [2]Orthodontics, [3]Physiology, [4]Ophthalmology, University of Pennsylvania, Philadelphia, PA 19104; [5]Department of Pharmacology and Chemical Biology, Pittsburgh University, Pittsburgh, PA

This chapter represents my main project and I helped design, carry out, analyze and interpret all experiments performed in this section. The results identify a novel role for the P2X7 receptor in the priming of IL-1β and NLRP3.

This chapter has been submitted for publication in Frontiers in Cellular Neuroscience. The version reprinted here has been resubmitted in response to reviewers' comments. A more detailed Material and Methods section and additional figures 2.1, 2.2 and 2.3 were added to improve the manuscript.

Introduction

Mechanical trauma can induce complex pathological changes to neural tissue via inflammation (Corps et al., 2015; Heppner et al., 2015). While recruitment of immune cells to the injured region can contribute, localized inflammatory signaling between glia and neurons can also initiate or enhance inflammatory damage. The NLRP3 inflammasome is a key component of the localized innate immune system, leading to the cleavage and release of pro-inflammatory cytokines (Rathinam et al., 2012), and it has been implicated in neural disorders associated with mechanical strain or elevated pressure (Walsh et al., 2014), including traumatic brain injury, encephalitis, and glaucoma (Chi et al., 2015; Kaushik et al., 2012; Liu et al., 2013).

The involvement of the NLRP3 inflammasome is a two-step process. In the first stage, referred to as the priming step, expression of inflammasome components such as pro-IL-1β and NLRP3 is increased at the transcriptional and translational level (Mariathasan et al., 2006; Patel et al., 2017). This priming stage can be the rate-limiting step in inflammatory responses and may connect the initial insult to chronic inflammation. During the second stage, inflammasome components are assembled and activated, turning on caspase 1 which subsequently catalyzes the maturation of cytokines IL-1β and IL-18 (Stutz et al., 2009). This later step has been linked to efflux of K^+ through the P2X7 purinergic receptor (Bernier, 2012; Karmakar et al., 2016; Mariathasan et al., 2006; Petrilli et al., 2007), even for activation associated with lysosomal rupture (Zode et al.,

2011), and can be mimicked by the K^+ ionophore nigericin (Zode et al., 2015). While activation of the NLRP3 inflammasome has been the subject of intense investigation (e.g. (Freeman and Ting, 2016; Guo et al., 2015; Yilmaz and Lee, 2015), the signals leading to inflammasome priming are less well understood. Standard models attribute priming to microbial molecules or other toll-like receptor agonists that are rarely detected in sterile neural environments.

The central role of aberrant purinergic signaling in the neuropathology triggered by mechanical strain has been outlined for the retina (Mitchell et al., 2009). In astrocytes isolated from the optic nerve head, moderate strain leads to a release of ATP through pannexin hemichannels (Beckel et al., 2014). This released ATP then autostimulates P2X7 receptors on these astrocytes to regulate cytoplasmic Ca^{2+} and other physiological responses. Expression of pannexins is increased *in vitro* by cell stretch and *in vivo* in a model of chronic intraocular pressure (IOP) elevation, consistent with a role for ATP release in the neural response to sustained mechanical strain. Elevated extracellular ATP was confirmed in primate, rat, and mouse models of chronic IOP elevation (Lu et al., 2015) and detected in the eyes of humans with chronic glaucoma (Li et al., 2011).

This study asks whether extracellular ATP release through pannexins and autostimulation of the P2X7 receptor are involved in the priming of the NLRP3 inflammasome. The data are consistent with a role for the P2X7 receptor in

priming IL-1β and NLRP3 in retina following activation of NFκB in optic nerve head astrocytes. This identifies a new pathway for priming the inflammasome in sterile neural environments subject to mechanical strain.

Materials and Methods:

Animal care and use: All procedures were performed in strict accordance with the National Research Council's "Guide for the Care and Use of Laboratory Animals" and were approved by the University of Pennsylvania Institutional Animal Care and Use Committee (IACUC). All animals were housed in temperature-controlled rooms on a 12:12 light:dark cycle with food and water *ad libitum*. Long–Evans and Sprague Dawley rats (Harlan Laboratories/Envigo, Fredrick, MD), and mice (C57BL/6J wildtype and $P2X7^{-/-}$) of both sexes were utilized. Both the wildtype C57BL/6J and the $P2X7^{-/-}$ B6.129P2-P2rx7tm1Gab/J Pfizer mice were from Jackson Laboratories (Bar Harbor, ME). Tg-$Myoc^{Y437H}$ mice provide a model of chronic glaucoma and were received as a gift from Val Sheffield (Lu et al., 2015).

Model of moderate temporally-controlled intraocular pressure elevation: The IOP was elevated in adult Sprague-Dawley rats as previously reported (Lu et al., 2017) based on the Control Elevation of IOP (CEI) protocol developed by John Morrison and colleagues (Morrison et al., 2010; Morrison et al., 2014). This procedure enables the effects of increased pressure to be separated from cell death to focus specifically on the consequences of mechanical strain. Pressures were selected so that retinal blood flow was maintained and ischemia avoided; studies suggest this protocol leads to minimal loss of neurons, and allows the separation of pressure and cell death (Crowston et al., 2015; Lu et al., 2017).

This model was therefore chosen to investigate the mechanosensitive priming of the inflammasome in neural tissue *in vivo*.

After receiving 2 mg/kg meloxicam, rats were deeply anesthetized with 1.5% isoflurane or intraperitoneal injection of ketamine (80 mg/kg) and xylazine (10 mg/kg). After administration of proparacaine (0.5%) and tropicamide (0.5-1%), one eye was cannulated with a 27-gauge shielded wing needle (Becton Dickinson, NJ) inserted into the anterior chamber, connected to a 20ml syringe filled with sterile phosphate buffered saline (PBS). IOP was increased to 50-60 mmHg by elevating the reservoir to the appropriate height; blood flow through the retina was maintained throughout to avoid ischemic complications. The contralateral eye without cannulation served as a normotensive control. After 4 hrs, pressure was returned to normal, the needle removed and 0.3% gentamicin ointment or 0.5% erythromycin applied to the cornea. Rats were sacrificed 22 hrs later and the retina, including the optic nerve head material, was dissected. Experiments on mice were performed using procedures similar to those described elsewhere (Crowston et al., 2015). Mice were anesthetized with 1.5% isoflurane, and IOP was increased to 60 mmHg for 4 hours; pressure was then returned to normal, the needle (33-gauge) removed and 0.5% erythromycin applied to the cornea. Mice were either sacrificed 22 hrs later or immediately (depending on the experiment), and the retina, including the optic nerve head material, was dissected. In some experiments mice were sacrificed immediately after the pressure was returned to normal (Figure 2.1).

A. Rat eye with IOP elevated

B. Schematic time course

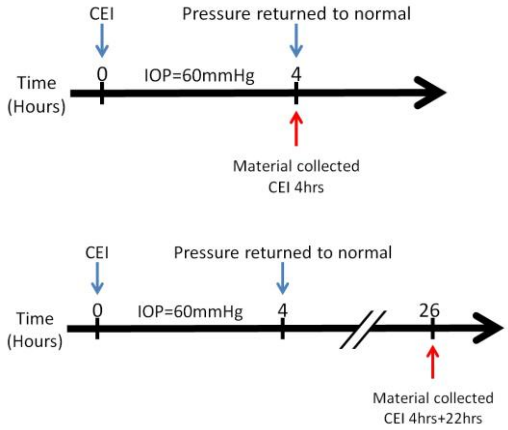

Figure 2.1 Model of moderate temporally-controlled intraocular pressure elevation (CEI):

A. The anterior segment of the eye from an anesthetized Sprague Dawley rat was cannulated with a 27 gauge needle. IOP was increased to 60 mmHg for 4 hrs without signs of ischemia by raising the reservoir connected to the cannulating needle. B. Schematic of experimental time course. IOP was elevated to 60 mmHg for 4 hours, and then pressure was returned to normal. Mice and rats were sacrificed immediately or 22 hrs later and the retina, including the optic nerve head material, was dissected.

Chronic glaucoma model: The Tg-Myoc mouse provides a model of chronic glaucoma and was generated and initially characterized by Sheffield and colleagues. A colony was established at the University of Pennsylvania. Tg-Myoc^{Y437H} mice were bred with C56BL/6N mice and the offspring were genotyped to identify those with the human transgene. Human *Tg-MYOC^{Y437H}* mutant myocilin expressed in the trabecular meshwork led to ER stress, IOP elevation, and loss of ganglion cell axons. IOP measured from genotyped littermates indicated a significant elevation in IOP of Tg-Myoc mice (15.5 ± 0.5 mmHg vs. 12.2 ± 1.0 in WT controls, N=3, P=0.043), consistent with previous reports (Lu et al., 2015).

Intravitreous injection: Intravitreal injections were performed in rat eyes under a dissecting microscope using a micropipette connected to a microsyringe (Drummond Scientific Co., Broomall, PA) as described elsewhere (Hu et al., 2010). A glass pipette filled with P2X7 receptor antagonist Brilliant Blue G (BBG, 0.8%) dissolved in saline was passed through the superior nasal region of sclera into the vitreous cavity, ~1 mm from the limbus, with a total volume of 5 µl injected over a 30 sec time period. The antagonist was delivered 1-3 days before IOP elevation. C57BL/6J wild type mice were injected with either P2X7 receptor agonist Bz-ATP (2 µl, 250 µM) or sterile saline.

Astrocyte cell culture: Primary rat optic nerve head astrocyte cultures were grown based on a protocol modified from Mandal et al. (Mandal et al., 2009). The

optic nerve proximal to the sclera, defined as the optic nerve head, was obtained from rat pups PD3-5 of both genders. This optic nerve head tissue was digested for 1 h using 0.25% trypsin (Invitrogen), with periodic trituration to create a cell suspension. Cells were washed once with Dulbecco's modified Eagle's medium (DMEM)/F12 containing 10% of fetal bovine serum (FBS), re-suspended in DMEM/F12, 10% FBS, 1% penicillin/streptomycin, and 25 ng/mL epidermal growth factor (#E4127, Sigma-Aldrich), plated on 35mm culture dishes and grown at 37˚C, 5.5% CO_2. Cultures were found to contain >99% astrocytes, as defined by glial fibrillary acidic protein (GFAP) immunofluorescence staining. Cells were generally at passages 2 to 5 when used. Mouse optic nerve head astrocyte tissue was collected from 3-month-old animals, due to the limited material from the neonatal mice. C57BL/6J and $P2X7^{-/-}$ mice of both genders were prepared similarly to the rat protocol, but the optic nerve head tissue was digested for only 35 min using 0.25% trypsin (Invitrogen).

Swelling isolated astrocytes: Rat and mouse optic nerve head astrocytes were subcultured onto plastic 6-well plates and grown until confluent. Cells were incubated in 2ml of control isotonic solution containing (in mM) 105 NaCl, 5 KCl, 4 NaHEPES, 6 HEPES acid, 1.3 $CaCl_2$, 5 glucose, 5 $NaHCO_3$, 60 mannitol and 0.25 $MgCl_2$ pH 7.4) or in 30% hypotonic solution for 4 hours in the tissue culture incubator. Cells were pretreated with inhibitors Bay 11-7082 (4μM) Brilliant Blue G (BBG, 10 μM), A839977 (50 nM, Tocris Bioscience), A740003 (5 μM, Tocris Bioscience), carbenoxolone (10μM, #C4790), Probenecid (1mM, #P8761) or

[10]Panx1 and scrambled peptide (100μM, #3348 and #3708, Tocris Bioscience) for 1 hr before adding test solutions. RNA was extracted immediately after the 4 hrs treatment.

In vitro stretch experiments: Isolated rat optic nerve head astrocytes were plated on 6 well plates with 0.05 mm silicone substrates coated with collagen 1 (Flexcell biaxial six-well plate #BF-3001C, Flexcell International Corp.) for 6-7 days until confluent. After replacing medium with isotonic solution, cells were exposed to mechanical cyclic tensile strain of 16% at 0.3 Hz for 4hrs in the tissue culture incubator using a vacuum provided by the Flexcell FX-5000 Tension System (Figure 2.2) (Flexcell International Corp.). Control cells were cultured and grown under the same conditions on similar plates and kept in the same incubator without mechanical stretching. RNA was extracted immediately after stretch.

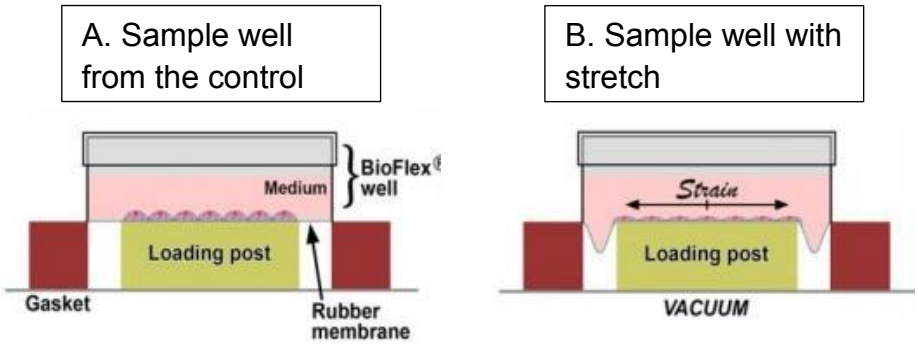

Figure 2.2 Stretching wells of the Flexcell FX-5000 Tension System

A. Diagram of the silicon membrane in control condition (No stretch).
B. Diagram of the silicon membrane in stretch condition. In these experiments astrocytes were exposed to cyclic tensile strain of 16% at 0.3 Hz for 4hrs. *Modified from (Flexcell, 2011)*

RNA isolation: RNA was extracted from astrocytes plated on six well plates or whole retina including the optic nerve head by homogenizing in 1 ml TRIzol reagent per sample (#15596026, Invitrogen). Samples were sonicated for 10 sec on ice, then 200µl Chloroform was added to each sample, vortexed for 15 sec and incubated for 5 min at room temperature. The samples were centrifuged at 1200g at 4˚C for 10 min then the upper aqueous solution (around 400-450µl) was transferred to a new 1.5 ml tube. One volume of 70% ethanol was added to the

solution, and the mix was transferred to an RNeasy spin column with a silica membrane placed in a 2 ml collection tube RNeasy mini kit (#79254, Qiagen, Inc., MD, USA). After adding the solution to the spin column, manufacturer instructions were followed. Samples were treated with RNase free DNase set. (#79254 Qiagen, Inc., MD, USA) to remove the remaining DNA. At the final step, RNA was eluted with 30µl RNase free water. RNA concentration and purity were assessed using a Nanodrop spectrophotometer (Thermo Scientific).

Quantitative PCR: cDNA was synthesized from 1µg of total RNA per reaction using the High Capacity cDNA Reverse Transcription Kit (#4368814, Applied Biosystems) at 25 °C for 10 min, 37 °C for 120 min and terminated at 85 °C for 5 min. The Quantitative Polymerase Chain Reaction (qPCR) was performed using SYBR Green and the 7300 RealTimePCR system (Applied Biosystems Corp.), starting with 50°C for 2 min and 95°C for 10 min, followed by 40 cycles at 95°C for 15 sec and 60°C for 1 min, and concluding with 15 sec at 95°C, 60°C for 1 min and 95°C for 15 sec to ensure a single product on melting curves; 0.5µl of cDNA was used per well, except for *in vitro* analysis of *IL-1β* in which 1.0 µl was used. GAPDH expression did not differ between control and experimental groups. To control for genomic DNA contamination, in addition to the DNase treatment during the RNA isolation, PCR was also performed on samples from reverse transcriptase reactions in without the enzyme. Any product from these samples indicated a DNA contamination and results were excluded. All experiments were performed in triplicate and data were analyzed using the delta-

delta Ct approach. As $\Delta Ct = Ct_{Target} - Ct_{GAPDH}$, $\Delta\Delta Ct = \Delta Ct_{experiment} - \Delta Ct_{Control}$ and, relative expression (RQ) = $2^{-\Delta\Delta Ct}$. Primers used are described in Table 2-1.

For the PCR gel used in genotyping, RNA was extracted from confluent wild type and $P2X7^{-/-}$ mouse optic nerve head astrocytes and converted to cDNA as above. The PCR amplification reaction included 10µl REDExtract-N-Amp PCR Reaction mixture (# XNATS, Sigma-Aldrich) with 4 µl of the cDNA, 2 µl H2O and 2µl of the P2X7 receptor primer (10µM) (Table 2.1). cDNA was denatured at 94°C for 3 min, followed by 35 PCR cycles. Each consisted of three steps: 94°C for 45 sec, 65°C for 1 min, and 72°C for 1 min. Final extension was set at 72°C for 10 min. PCR products were detected by 1% (w/v) agarose gels using 100bp DNA Ladder (#15628-019, Invitrogen).

Immunocytochemistry: Astrocytes were grown to 80% of confluence, fixed with 4% formaldehyde for 20 min at 25˚C, permeabilized with 0.1% Triton X-100 (Bio-Rad, USA) for 15 min then blocked with 20% Superblock (ThermoFisher Scientific Inc) in PBS with 0.1% Tween 20 (Bio-Rad, USA) (PBS/T) for 1 hour. Coverslips were incubated with anti-GFAP monoclonal antibody (#MABH360, 1:250: Chemicon Int.) overnight at 4˚C, followed by donkey anti-mouse IgG Alexa-Fluor 488 for 60 min (#A21202, 1:500; Invitrogen). For pannexin 1, cells were incubated with goat polyclonal (#ab124131, 1:200, Abcam), followed by rabbit anti-goat 594 nm. For P2X7 receptor staining, cells were incubated overnight with rabbit polyclonal (#APR-008, 1:100, Alomone), followed by donkey

anti-rabbit IgG Alexa Flour 488 for 1 hour (#A21206, 1:500, Invitrogen). Cells were incubated with Alexa Fluor 568 Phalloidin (#A12380, 1:100; Invitrogen) for 15 min. After incubation with DAPI (#D9542, Sigma-Aldrich) for 10 min, coverslips were washed and mounted using SlowFade Gold Anti-fade Media (Invitrogen). Images were acquired using a Nikon Eclipse microscope (Nikon, USA) and ImagePro software (MediaCybernetics). ImageJ was used to subtract background, modify intensity and combine pseudocolored images, with parallel processing for all images. Mouse astrocytes were stained with the anti-GFAP monoclonal antibody used for rat cells.

For retinal sections, mice were transcardially perfused with 4% formaldehyde in PBS. After enucleation, eyes were fixed with 4% formaldehyde overnight then incubated in 30% sucrose for 2 h. Eyes were embedded in OCT compound (Tissue-Tek #62550-1), cryosectioned at 9 µm and mounted on Colorfrost Plus slides (ThermoFisher # 9991001). Sections were fixed with 4% formaldehyde for 10 min, permeabilized with 0.1% Triton-X-100 for 10 min, then blocked with 20% Superblock with PBS/T plus 10% donkey serum. Sections were incubated in 5µg/ml IL-1β primary antibody (goat polyclonal antibody #AF-401-NA R&D systems, Lot# NP2715111) and anti-GFAP monoclonal antibody (#MABH360, 1:250: Chemicon Int.) overnight at 4°C, followed by secondary donkey anti-goat Alexa555-conjugated antibody (# A21432) and donkey anti-mouse IgG Alexa-Fluor 488 for 60 min (# A21432, #A21202, 1:500; Invitrogen). Images were obtained as described above.

Immunoblots: Whole retinas or astrocytes grown on 6 well plates were washed twice with cold PBS and lysed in RIPA buffer containing 50 mM Tris-HCl, 150 mM NaCl, protease inhibitor cocktail (Complete; Roche Diagnostics, Germany), 1% Triton X-100, 0.1% SDS, and 10% glycerol. Sonicated samples were centrifuged (14,000g, 10 min, 4°C) and quantified using a BCA Protein Assay (Pierce/ThermoFisher). 10 to 20 µg of protein was loaded into each lane of 4–15% Mini-PROTEAN® TGX™ Gel, 10 well, 50 µl (#4561084, Bio-Rad, USA). Precision Plus Protein™ Dual Color Standards molecular weight ladder (#1610374, Bio-Rad, USA) was run on each gel. After separation, proteins were transferred onto Polyvinylidene difluoride membrane (PVDF) and blocked in PBS with 0.1% Tween 20 (PBS/T) and 5% non-fat milk for 60 minutes at RT. PVDF membranes were incubated overnight at 4°C with primary antibodies in PBS/T + 1% non-fat milk. Primary antibodies used were 0.25µg/ml IL-1β goat polyclonal antibody (#AF-401-NA R&D systems, Lot# NP2715111) and IκBα rabbit polyclonal antibody (#9242, 1:1000; Cell Signaling). PVDF membranes were washed with PBS/T, then incubated with corresponding secondary antibodies at 1:5000 dilution in PBST + 1% non-fat milk: donkey anti-goat IgG-HRP (1:5000; sc-2020, Santa Cruz Biotechnology) or Rabbit IgG, HRP-linked whole AB from donkey (1:5000, #NA934, amersham Bioscience Corp.). Blots were developed using a chemiluminescence detection kit (ECL detection system; Amersham Biosciences Corp.) and visualized with the ImageQuant LAS 4100 imager and Image Quant software (GE Healthcare Lifesciences).

ATP measurement: Rat astrocytes were grown to confluence into white-walled, clear-bottom 96-well plates (#3610, Corning Inc.). The border wells were avoided and treatments were randomized across the plate (Figure 2.3). Growth medium was replaced with isotonic solution and cells were allowed to recover for 30 min at 37°C before measurements were taken. A bioluminescent luciferin/luciferase assay was used to measure ATP levels (Reigada et al., 2005). The ATP mix Luciferin/Luciferase (#FLAAM, Sigma-Aldrich) was stored frozen as a stock solution with 450 µl of control solution/50 µl of dH_2O per vial and diluted 20-fold in isotonic solution. Each well contained 20 µl of the assay with 50 µl isotonic base and 30 µl of either isotonic, dH_2O, dH_2O with Apyrase (1U/ml, A6535; Sigma-Aldrich) or 10µM carbenoxolone to achieve 30% hypotonic. Isotonic solution was removed from the cells, and prepared mixes were added to the cells carefully. ATP was then quantified using the Luminoskan Ascent luminometer (ThermoFisher), integrating over 200 ms and sampling in succession every 10 s for 18 min at 25°C. The ATP released was calculated at the different time points indicated in the results with the use of a standard curve to transform the arbitrary light units to an ATP concentration, then normalized to mean levels for isotonic solution.

A. Randomization of groups

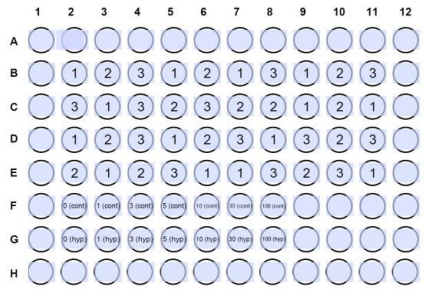

B. ATP measurement

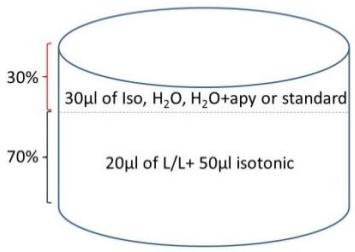

Figure 2.3 ATP measurements

A. Layout of 96-well plates. The treatment groups were randomized across the plate and the borders wells were avoided
B. Each well contained 20 µl of the assay, with 50 µl of isotonic base and 30 µl of either isotonic, dH2O, dH2O with Apyrase or 10µM carbenoxolone added to achieve 30% hypotonic.

Data Analysis: Data are reported as mean ± SEM. Analysis was performed in a masked fashion whenever possible. Statistical analysis used a 1-way ANOVA with post-hoc Holm-Sidak (all pairway) method, student t-test, or paired t-test when appropriate. Analyses were performed using Systat Software Inc. (San Jose, CA). Sample size was predicted by power analysis, and numbers take into account a 15% failure rate in animal experiments. Sample sizes are consistent with those reported in similar studies and provide sufficient power to detect

changes. When data were not normally distributed analysis were performed on ranks. Results with $p<0.05$ were considered significant.

Table 2-1 Primers used for qPCR of NLRP3 Inflammasome-related genes

Gene Name	GenBank Accession	Forward Primer (5' to 3')	Reverse Primer (5' to 3')	Size (bp)
Rat IL-1β 1	NM_031512.2	GGGATTTTGTCGTTGCTTGT	CTGTGACTCGTGGGATGATG	211
Rat IL-1β 2	NM_031512.2	CACCTCTCAAGCAGAGCACAG	GGGTTCCATGGTGAAGTCAAC	83
Rat NLRP3	NM_001191642	CCATGAGCTCCCTTAAGCTG	TTGCACAGGATCTTGCAGAC	283
Rat CASP1	NM_012762	TATGGAAAAGGCACGAGACC	CAGCTGATGGACCTGACTGA	137
Rat ASC	NM_172322.1	CCCATAGACCTCACTGATAAAC	AGAGCATCCAGCAA ACCA	260
Rat IL-18	NM_019165.1	GGACTGGCTGTGACCCTATC	TGTCCTGGCACACGTTTCTG	152
Mouse IL-1β 1	NM_008361.4	GAAGATGGAAAAACGGTTTG	GTACCAGTTGGGGAACTCTGC	85
Mouse IL-1β 2	NM_008361.4	CAAGCTTCCTTGTGCAAGTGTCTG	AGGACAGCCCAGGTCAAAGGTT	161
Mouse NLRP3	NM_145827.3	AGAGCCTACAGTTGGGTGAAATG	CCACGCCTACCAGGAAATCTC	116
Mouse CASP1	NM_009807.2	TGGTCTTGTGACTTGGAGGA	TGGCTTCTTATTGGCACGAT	172
Mouse ASC	NM_023258.4	GGAGTCGTATGGCTTGGAGC	CGTCCACTTCTGTGACCCTG	204
Mouse IL-18	NM_008360.1	CAGTGAACCCCAGACCAGAC	TGTTGTGTCCTGGAACACGT	212
Mouse P2X7R	NM_001284402.1	TGGAACCCAAGCCGACGTTGA	CTCGGGCTGTCCCCGGACTT	250
Mouse Bax	NM_007527.3	TGCAGAGGATGATTGCTGAC	GATCAGCTCGGGCACTTTAG	154
GAPDH	NM_017008	TCACCACCATGGAGAAGGC	GCTAAGCAGTTGGTGGTGCA	195

Results:

Priming of inflammasome genes after elevation of IOP

We first examined whether mechanical strain primed inflammasome components *in vivo*. IOP was unilaterally elevated in rats to between 50-60 mmHg for 4 hrs using a variant of the Controlled Elevation of IOP (CEI) procedure. RNA was extracted from the retina of treated and contralateral control eyes soon after return of IOP to baseline, and qPCR was used to compare expression of genes associated with the NLRP3 inflammasome. There was a significant elevation in the expression of mRNA for *IL-1β, NLRP3,* Interleukin-1 converting enzyme/caspase1 gene (*CASP1)* and Apoptosis-Associated Speck-Like Protein Containing CARD (*ASC*), but not in expression of cytokine *IL-18* (Figure 2.4.A).

The procedure was also performed in mice to determine whether the response occurred across species. In material extracted immediately after IOP was returned to baseline, *IL-1β* was elevated moderately (Figure S 2.1.A). Expression was substantially increased in material extracted 22 hrs after IOP returned to baseline, with *IL-1β, NLRP3, CASP1,* and *ASC* levels elevated significantly (Figure 2.4.B). The increased expression was greatest for *IL-1β*, with mRNA levels increasing over 80-fold. At neither time point did the CEI procedure elevate message for the pro-apoptotic marker *BAX* (Figure S 2.1.B), consistent with the lack of cell death found previously with this procedure (Crowston et al., 2015).

Expression was also examined in retinas from Tg-Myoc^{Y437H} mice; these mice had a sustained, moderate elevation in IOP of 15.5 ± 0.5 mmHg, as compared to 12.2 ± 1.0 in wildtype controls at 14-18 months, similar to the IOP difference measured previously at 8 months (Lu et al., 2015). Expression of *IL-1β* mRNA was increased in retinas from Tg-Myoc^{Y437H} mice compared to littermate controls (Figure S 2.1.C), but the rise in *NLRP3* or *CASP1* was not significant.

Inflammasome priming at protein level

Given that the elevation of *IL-1β* was substantially greater than that of other inflammasome components, further efforts were focused on this cytokine. Immunoblots were performed to probe for pro-IL-1β protein to confirm the mRNA results. Expression of 31kDa pro-IL-1β protein was significantly elevated in mouse eyes when examined 22 hrs after IOP elevation (Figure 2.5.A, B). Immunohistochemistry was used to localize the rise in IL-1β induced by IOP elevation. Staining for IL-1β was low under control conditions, but increased substantially in eyes exposed to IOP elevation (Figure 2.5.C, Figure S 2.2). The increased staining was greatest in the nerve fiber bundle of the retina and throughout the optic nerve. Closer inspection of the staining pattern in the optic nerve head showed increased expression of IL-1β in bands through the optic nerve head that colocalized with GFAP, suggesting IL-1β expression was increased in optic nerve head astrocytes.

P2X7 receptor is involved in IL-1β priming in vivo

We hypothesized that the increased expression of IL-1β following IOP elevation might relate to the release of ATP and autostimulation of P2X7 receptors found in optic nerve head astrocytes exposed to mechanical strain (Beckel et al., 2014). This possibility was supported by recent findings implicating the P2X7 receptor in the mechanosensitive upregulation of cytokines IL-3 (Lim et al., 2016) and IL-6 (Lu et al., 2017) in the retina. To determine if the P2X7 receptor was involved in IOP-sensitive priming of IL-1β, the P2X7 receptor antagonist BBG (0.8%) was injected intravitreally 1-3 days before the IOP rise, then retinas were collected 22 hrs after the IOP returned to baseline. Pretreatment with BBG prevented the upregulation of *IL-1β* mRNA triggered by IOP elevation (Figure 2.6.A).

P2X7 receptor involvement was examined further by evaluating *IL-1β* mRNA levels in P2X7$^{-/-}$mice. Elevation of IOP significantly increased *IL-1β* mRNA levels in control C57BL/6J mouse eyes, but not P2X7$^{-/-}$ mice (Figure 2.6.B). A similar reduction was observed in levels of NLRP3 in tissue from the P2X7$^{-/-}$ mice (Figure 2.6.C). P2X7 receptor stimulation was itself sufficient to increase *IL-1β* expression; the P2X7 agonist BzATP was injected intravitreally in C57BL/6J mice with sterile saline injected into the contralateral eye as a control. Retinas collected 1 day after the injections showed that BzATP significantly increased the expression of *IL-1β* (Figure 2.6.D). The effect of BzATP on other inflammasome

genes was much smaller (Figure 2.6.D). Together, the data suggested the P2X7 receptor primes *IL-1β* in response to mechanical strain *in vivo*.

Mechanical strain primes inflammasome genes in isolated astrocytes

The optic nerve head has been identified as a focal center of mechanical strain that accompanies IOP elevation (Burgoyne et al., 2005; Downs et al., 2008), with optic nerve head astrocytes involved in several signaling pathways implicated in glaucomatous pathology (Hernandez, 2000; Morgan, 2000; Tehrani et al., 2016). Mild stretch to optic nerve head astrocytes leads to a release of ATP and autostimulation of P2X7 receptors (Beckel et al., 2014), and the immunohistochemical staining in (Figure 2.5.C) indicated an increase in IL-1β in optic nerve head astrocytes. As such, the mechanosensitive priming of *IL-1β* and the contribution of the P2X7 receptor to this priming was examined further in isolated optic nerve head astrocytes.

Primary rat optic nerve head astrocytes were plated on a silicon sheet and subjected to 16% strain at 0.3 Hz for 4 hrs. Cells subjected to this stretch protocol looked identical to controls cells on a macroscopic level, with very similar patterns of F-actin staining (Figure 2.7.A). The level of *IL-1β* mRNA was significantly increased in stretched cells (Figure 2.7.B). Expression of *IL-1β* was also elevated by applying strain to the cells by swelling in a 30% hypotonic solution (Figure 2.7.C). The rise in other inflammasome genes induced by

swelling astrocytes was variable, with small increases in *NLRP3*, *ASC* and *IL-18*, but not *CASP1* (Figure S 2.3.A).

ATP release through pannexin channels required for mechanosensitive priming of IL-1β in astrocytes

The measurements of *IL-1β* mRNA from optic nerve head astrocytes *in vitro* allowed further investigation of the mechanisms linking mechanical strain to *IL-1β* upregulation. First, the ability of astrocytes to release ATP when swollen, and of the soluble ectoATPase apyrase to prevent the extracellular elevation in ATP was confirmed (Figure 2.8.A, B). The ability of apyrase to prevent the swelling-induced rise in *IL-1β* expression supported a role for extracellular ATP in this pathway (Figure 2.8.C).

Previous work suggests that pannexin hemichannels are a conduit for the mechanosensitive release of ATP from these cells (Beckel et al., 2014). Carbenoxolone is reported to be relatively specific for pannexin channels at 10 μM (Bruzzone et al., 2005), and this concentration led to a moderate, but significant reduction in the swelling-induced release of ATP (Figure 2.8.D). This concentration of carbenoxolone reduced the rise in *IL-1β* mRNA expression by a similar amount (Figure 2.8.E). The swelling-induced rise in *IL-1β* was also blocked by probenecid and the peptide blocker ^{10}Panx1, while the scrambled peptide control had no effect on expression (Figure 2.8.F). The expression of

pannexin 1 in these astrocytes (Figure 2.8.G), combined with the reduction by three pannexin blockers, implicated pannexins in the *IL-1β* response.

P2X7 receptor necessary and sufficient for mechanosensitive priming of IL-1β in vitro

ATP released after swelling can autostimulate astrocytes, with P2X7 antagonists blocking the rise in cytoplasmic Ca^{2+} induced by swelling (Beckel et al., 2014). To determine whether this autostimulation contributed to the priming of IL-1β, the effect of P2X7 antagonists on the swelling-dependent rise in IL-1β was examined. The expression of the P2X7 receptor in astrocytes was confirmed using immunocytochemistry (Figure 2.9.A). Three P2X7 antagonists, BBG, A839977, and A740003, significantly prevented the mechanosensitive *IL-1β* priming in optic nerve astrocytes (Figure 2.9.B). To support this pharmacological identification of the P2X7 receptor, experiments were pursued on astrocytes isolated from C57Bl/6J mice and $P2X7^{-/-}$ mice. PCR confirmed the absence of the P2X7 receptor message in astrocytes obtained from knockout mice while immunocytochemistry supported the absence of P2X7 protein (Figure S 2.4.A, B). The increased in expression of *IL-1β* mRNA after 4 hrs of swelling was significantly lower in astrocytes from the $P2X7^{-/-}$ mice as compared to the C57BL/6J mice (Figure 2.9.C). Treatment of astrocytes with the P2X7 receptor agonist BzATP was sufficient to upregulate *IL-1β* mRNA (Figure 2.9.D). Similar

results were found with *NLRP3*; the response was reduced in astrocytes from P2X7$^{-/-}$ mice (Figure S 2.4.C), while addition of BzATP induced a significant, albeit small, rise in *NLRP3* (Figure S 2.4.D).

NFκB is involved in priming of NLRP3 and IL-1β after mechanical strain

While many different transcription factors could be involved in the upregulation of IL-1β, we focused on the contribution of NFκB, as it is linked to the transcription of inflammasome genes including IL-1β (Cogswell et al., 1994) and can be activated by P2X7 stimulation (Liu et al., 2011). The NFκB inhibitor Bay 11-7082 prevented the swelling-induced upregulation of *IL-1β* in rat astrocytes (Figure 2.10.A). Upregulation of *NLRP3* was similarly blocked by Bay 11-7082 (Figure 2.10.B). While neither swelling nor Bay 11-7082 had any effect on expression of *CASP1* (Figure 2.10.C).

To confirm a role for NFκB in the transcriptional changes, levels of nuclear factor of kappa light polypeptide gene enhancer in B-cells inhibitor, alpha (IκBα) in extracts from control and swollen astrocytes from C57BL/6J were probed with immunoblots. Reduction in Iκbα levels correspond to activation of NFκB (Finco and Baldwin, 1995). Swelling reduced levels Iκbα in astrocytes from control mice, but not in cells from P2X7$^{-/-}$ mice (Figure 2.11.A). Quantification showed the reduction in Iκbα induced by swelling was significantly less in astrocytes from P2X7$^{-/-}$ mice (Figure 2.11.B). The P2X7 receptor antagonist A839977 also

reduced the ability of swelling to activate IκBα (Figure 2.11.C,D), supporting a role for the P2X7 receptor in the swelling-dependent activation of NFκB.

Discussion:

This study suggests that mechanical strain can increase expression of certain components of the NLRP3 inflammasome in neural tissue and identifies a role for ATP release and the P2X7 receptor in this priming. The cytokine IL-1β was linked through this pathway most strongly, with supportive evidence for upregulation of NLRP3. Given that priming is the initial step in NLRP3 inflammasome involvement, this study implicates a role for the P2X7 receptor in linking mechanical strain to innate immune responses in neural tissues.

Role of purinergic signaling

Evidence linking the P2X7 receptor with priming of IL-1β comes from *in vivo* and *in vitro* assays of mRNA and protein. The P2X7 antagonist BBG prevented the rise in *IL-1β* expression *in vivo* in rat retinas exposed to a transient rise in IOP. The rise in IL-1β following transient IOP increase was significantly less in $P2X7^{-/-}$ mice as compared to control, while the rise in *IL-1β* expression following intravitreal injection of P2X7 agonist BzATP suggests receptor stimulation is sufficient to increase *IL-1β* expression.

In vitro work using isolated astrocytes provides additional support and implicates the P2X7 receptor more specifically, with the use of more selective antagonists A839977 and A740003 (Honore et al., 2009; Honore et al., 2006), in addition to BBG. The pressure-induced rise in *IL-1β* expression was prevented by these agents and was not present in $P2X7^{-/-}$ mice, while the P2X7 agonist

BzATP was sufficient to elevate *IL-1β*. Together, the combined evidence from pharmacological and genetic methods, and in both isolated astrocytes and whole retina, strongly implicate a role for the P2X7 receptor in priming of IL-1β. The identification of a P2X7 receptor contributions in both rats and mice suggests receptor involvement may be widespread, particularly given the differences in the receptor across these species (Donnelly-Roberts et al., 2009b).

Involvement of extracellular ATP in IL-1β priming was supported by the ability of the soluble ectoATPase apyrase to block gene upregulation. The ability of pannexin channel blockers carbenoxolone, probenecid and the ^{10}Panx1 peptide to prevent a rise in *IL-1β* strongly implicates the release of ATP through the hemichannel in priming, as these drugs inhibited the ATP release induced by astrocyte swelling (Beckel et al., 2014). Overall, these studies suggest a model in which mechanical strain leads to release of ATP through pannexin hemichannels, autostimulation of the P2X7 receptor and subsequent priming of IL-1β (Figure 1.3).

Transcription factors and gene variation

The transcription factor NFκB was implicated in the upregulation of IL-1β and NLRP3 in astrocytes. Increased expression of both genes in swollen astrocytes was blocked by NFκB antagonist Bay 11-7082. The P2X7 receptor was implicated by data showing the swelling-dependent decreased in NFκB inhibitor Iκbα was reduced in astrocytes from P2X7$^{-/-}$ mice and by the P2X7 receptor

antagonist A839977. Elevation of hydrostatic pressure leads to translocation of NFκB to the nucleus in retinal astrocytes (Sappington and Calkins, 2006), while NFκB regulates transcription of NLRP3 and IL-1β in other cells (Boaru et al., 2015; Cogswell et al., 1994; Lawrence, 2009). The P2X7 receptor has been shown to activate NFκB through contact with MyD88 in HEK cells (Liu et al., 2011). This makes the activation of NFκB by P2X7 receptor a likely route to connect mechanical strain with increased expression of *IL-1β* and *NLRP3*. While the residual activation in astrocytes from $P2X7^{-/-}$ mice may reflect the involvement of other pathways, the presence of P2X7 splice variants may provide additional possibilities (Valentin et al., 2009).

The increase in *IL-1β* in response to mechanical strain was particularly consistent, observed both in rat and mouse *in vivo* models, and in cultured astrocytes from rat and mouse tissues; the increase in the 31 kDa pro-form in immunoblots confirmed this on a protein level. While expression of *NLRP3, CASP1,* ASC and *IL-18* were all increased by some model of mechanical strain, the effects in these genes were less consistent. Some of this variation may have been time-dependent, as the expression of most genes was substantially larger in mouse retina 22 hrs after IOP elevation was returned to baseline. The diverse responses to swelling and stretching were not unexpected given that *IL-1β, IL-18, NLRP3, CASP1,* and *ASC* are all regulated by a different combination of transcription factors. Regardless, the priming of *IL-1β* and *NLRP3* may be rate limiting in inflammasome activation as CASP1 and IL-18 are constitutively

expressed in monocytes and epithelial cells (Dinarello, 2007; Thornberry et al., 1992).

Contribution of astrocytes

The P2X7 receptor was implicated in priming *IL-1β* in both *in vivo* experiments, where material from the entire retina was analyzed, and during the *in vitro* experiments using isolated optic nerve head astrocytes. These optic nerve head astrocytes make up a small proportion of retinal material, however, and increased staining for IL-1β in various parts of the retina after elevated IOP suggests additional cell types may contribute to the retinal response. For example, our staining was consistent with increased expression in Muller glial cells. Neuronal involvement is also likely; the increased staining above is supported by recent results showing increased *IL-1*β expression in isolated retinal ganglion cells exposed to stretch (Lim et al., 2016); these neurons release ATP and autostimulate their P2X7 receptors, suggesting a parallel pathway may be involved (Xia et al., 2012b). However, the optic nerve head is a focal center of mechanical strain in the glaucomatous eye (Burgoyne et al., 2005), and astrocytes from patients showed morphological changes before marked loss of retinal ganglion cells (Lye-Barthel et al., 2013). The astrocytes express mechanosensitive channels (Choi et al., 2015) and contribute to the inflammatory response in glaucomatous eye (Johnson and Morrison, 2009). As such, the identification of the P2X7 receptor linking mechanical strain to inflammasome priming in optic nerve head astrocytes is particularly relevant.

ATP as endogenous trigger linking mechanical strain to inflammation in neural tissues

Inflammation has emerged as a critical component of chronic neurodegeneration, with the NLRP3 inflammasome a major contributor (Freeman and Ting, 2016). While priming of the NLRP3 inflammasome traditionally has been attributed to stimulation of toll-like receptors (Patel et al., 2017), these receptors are primarily activated by pathogens, and the endogenous triggers linking neural insult to inflammasome priming are largely unknown.

Our identification of the P2X7 receptor as a trigger for NLRP3 inflammasome priming in the retina builds on evidence linking mechanical strain to aberrant purinergic signaling in the retina and allows this endogenous trigger to be placed in a physiological context. Extracellular ATP is elevated after increased IOP in bovine, mouse, rat, primate and human samples (Lu et al., 2015; Reigada et al., 2008; Zhang et al., 2007). Stimulation of P2X7 receptors can damage retinal ganglion cells *in vitro* and *in vivo* (Hu et al., 2010; Zhang et al., 2005), and ATP release through pannexin hemichannels following mechanical strain can autostimulate P2X7 receptors on optic nerve head astrocytes (Beckel et al., 2014). As pannexin hemichannels are upregulated by prolonged stretch *in vitro* and *in vivo*, this provides a source of the sustained extracellular ATP found in the chronic glaucoma models. The present study suggests this may also provide a mechanism for chronic priming of inflammasome genes.

The P2X7 receptor is traditionally known for its ability to activate the NLRP3 inflammasome following the efflux of K^+ through the open channel (Katsnelson et al., 2015). The present study identifies a novel role for the P2X7 receptor in the priming of IL-1β and NLRP3. The ability of one receptor to mediate both steps of inflammasome involvement identifies a potentially central role for purinergic signaling in the link between mechanical strain and innate inflammation in neural tissues. Future studies focused on the contributions of the P2X7 receptor to inflammasome activation following its role in priming will clarify how this “double punch” impacts the inflammatory state of the retina.

Portions of this work have previously been presented in abstract form (Albalawi et al., 2016; Lu et al., 2013; Mitchell et al., 2016; Mitchell et al., 2017)

Acknowledgments:

We thank Wennan Lu for teaching me how to perform the CEI model. This work is supported by grants from the NIH EY015537 and EY013434 and core grant EY001583 (CHM). NIH DK106115 (JMB), Jody Sack Fund (WL) King Saud bin Abdulaziz University for Health Sciences (FA).

Figures

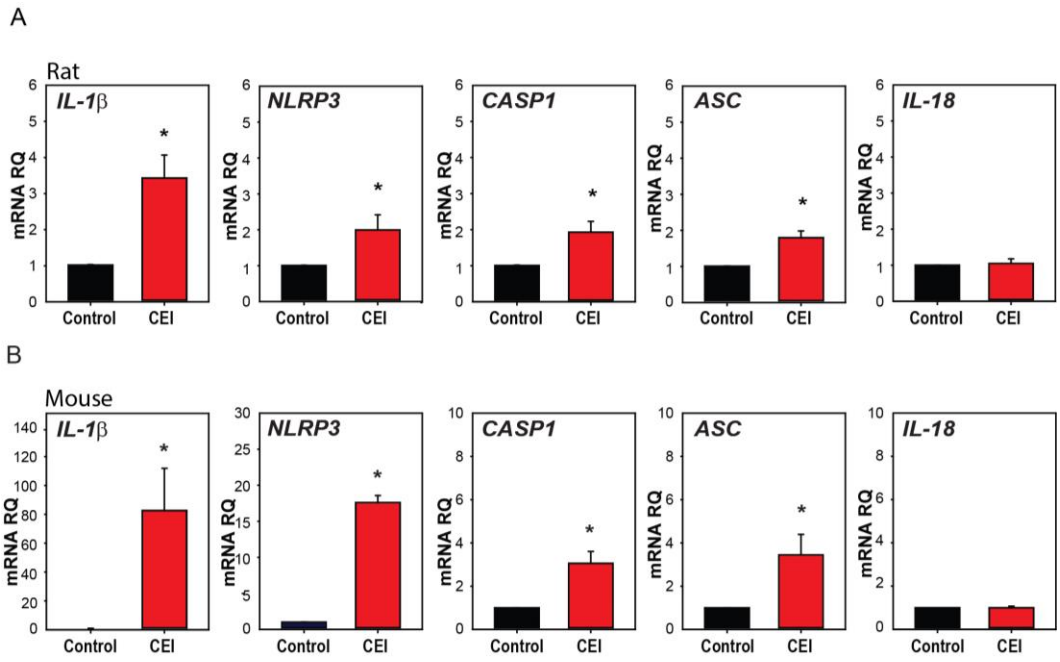

Figure 2.4 Increased expression of inflammasome-associated genes in rat retina after controlled elevation of IOP (CEI).

A. RNA was extracted from the retina soon after IOP returned to baseline following an elevation to 50-60 mmHg for 4 hrs. The IOP rise led to increased expression of *IL-1β* (*p=0.004, n=10), *NLRP3* (*p=0.045, n=10), *CASP1* (*p=0.014, n=10), and *ASC* (*p=0.008, n=5) as compared to contralateral control eye. There was no detectable rise in *IL-18* (n=5).
B. Mouse retina exposed to CEI showed increased expression of *IL-1β* (*p=0.049, n=5), *NLRP3* (*p=0<0.001, n=3), *CASP1* (*p =0.021, n=3) and *ASC* (*p=0.029, n=4), but not *IL-18* (n=4). Note the scale difference for *IL-1β*. RNA from retina (including the optic nerve head material) was extracted 22 hrs after returning IOP to baseline from an elevation to 60 mmHg for 4 hrs.

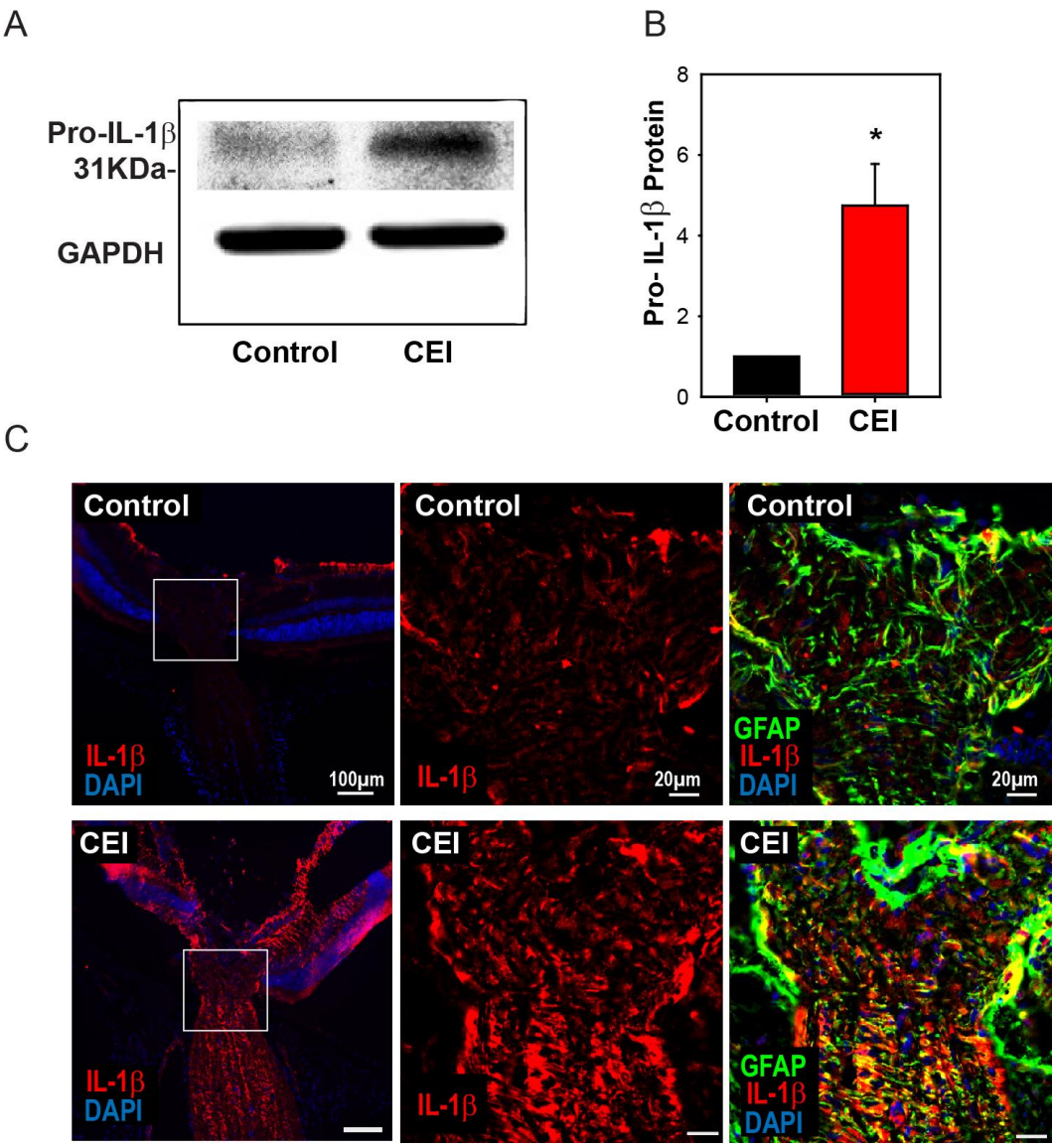

Figure 2.5 Elevation of IL-1β at the protein level

A. Representative immunoblots from mouse whole retina lysates probed for pro-IL-1β, at the expected 31 kDa size. Protein levels increased in eyes subject to controlled elevation of IOP (CEI) to 60 mmHg for 4 hrs and sacrificed 22 hrs after IOP returned to baseline, as compared to the contralateral non-pressurized control eye. Levels of housekeeping protein GAPDH (37 kDa) were similar between conditions.

B. Summary of relative protein expression in response to IOP elevation, as quantified with densitometry and normalized to GAPDH levels (*p=0.006, n=5).
C. Immunohistochemistry sections of mouse retina stained for IL-1β (red), GFAP (green) and with the nuclear stain DAPI (blue). The top row shows representative images from the non-pressurized eye, while the bottom row is from a contralateral eye exposed to the CEI procedure as in panel “A”. Increased staining for IL-1β was apparent in the nerve fiber layer, optic nerve and to a lesser extent throughout the retina (left). Higher magnification of the boxed area shows horizontal bands stained for IL-1β throughout the optic nerve head (center). These bands colocalize with GFAP (right), consistent with optic nerve head astrocytes (representative images from 3 animals).

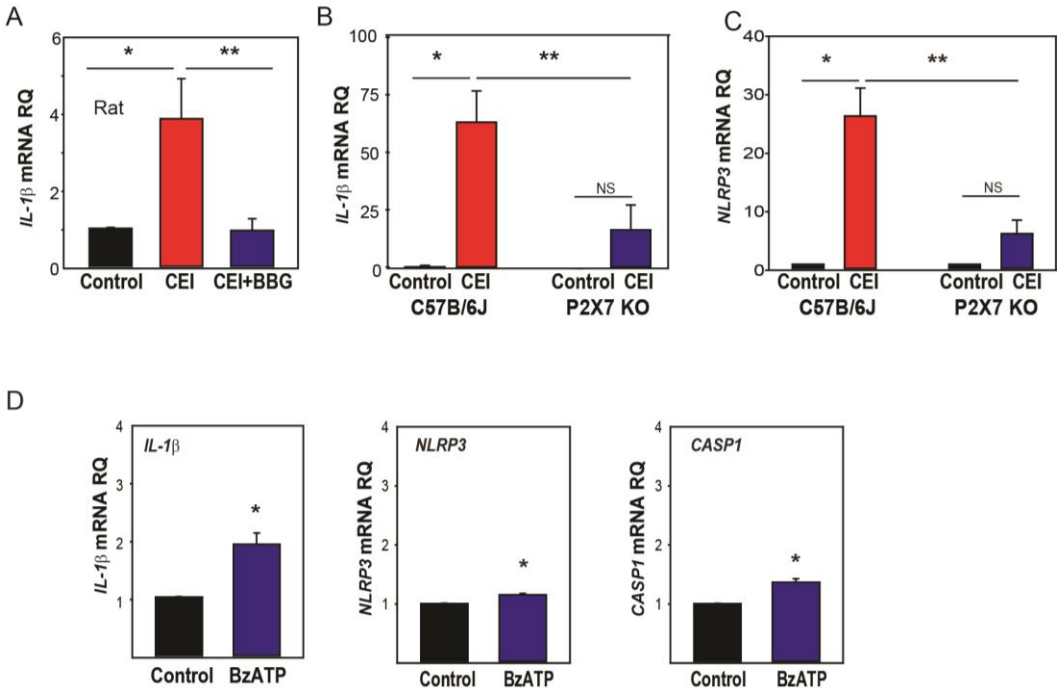

Figure 2.6 Involvement of the P2X7 receptor in inflammasome priming *in vivo*

A. The pressure-dependent rise in *IL-1β* mRNA in rat retinas exposed to moderate elevation of IOP (CEI) was not present following injection of the P2X7 antagonist BBG. Data are expressed as relative gene expression in the non-pressurized (Control) vs pressurized retina for eyes injected with 0.8% BBG (CEI + BBG) or saline (CEI) 1-3 days before the elevation of IOP to 50 mmHg for 4 hrs (n=4-5. *p<0.05 vs. saline pressurized).
B. In C57BL/6J mice, the CEI procedure increased retina levels of *IL-1β* mRNA relative to contralateral untreated eyes (*p=0.018). In P2X7 knockout mice, the elevation in IOP did not significantly (NS) increase levels of *IL-1β*. Levels of *IL-1β* mRNA in pressurized eyes of P2X7 knockout mice were significantly less than in wildtype pressurized eyes (**p=0.036). Data are expressed as gene expression of untreated eyes (Control) relative to pressurized eyes (CEI). Retina including optic nerve head was extracted 22 hrs after returning IOP to baseline from an elevation to 60 mmHg for 4 hrs (n=4).
C. Similarly, the levels of NLRP3 mRNA relative to paired untreated eyes is upregulated in C57BL/6J mice (*p<0.01). In P2X7 knockout mice, the elevation in IOP did not significantly increase levels of NLRP3. Levels of NLRP3 mRNA from P2X7 knockout mice pressurized eyes were significantly

less than in wildtype pressurized eyes (**p<0.01). Data are expressed as gene expression of pressurized eyes (CEI) relative to untreated eyes (Control). Retina including optic nerve head was extracted 22 hrs after returning IOP to baseline from an elevation to 60 mmHg for 4 hrs. n=4 in all cases.

D. Intravitreal injection of P2X7 agonist BzATP was sufficient to increase levels *IL-1β, NLRP3 and CASP1* mRNA in mouse retina when extracted 24 hrs after injection. Data are expressed as relative gene expression of contralateral non-injected eye (Control) vs injected eye (BzATP; *p<0.01, n=3 in all cases).

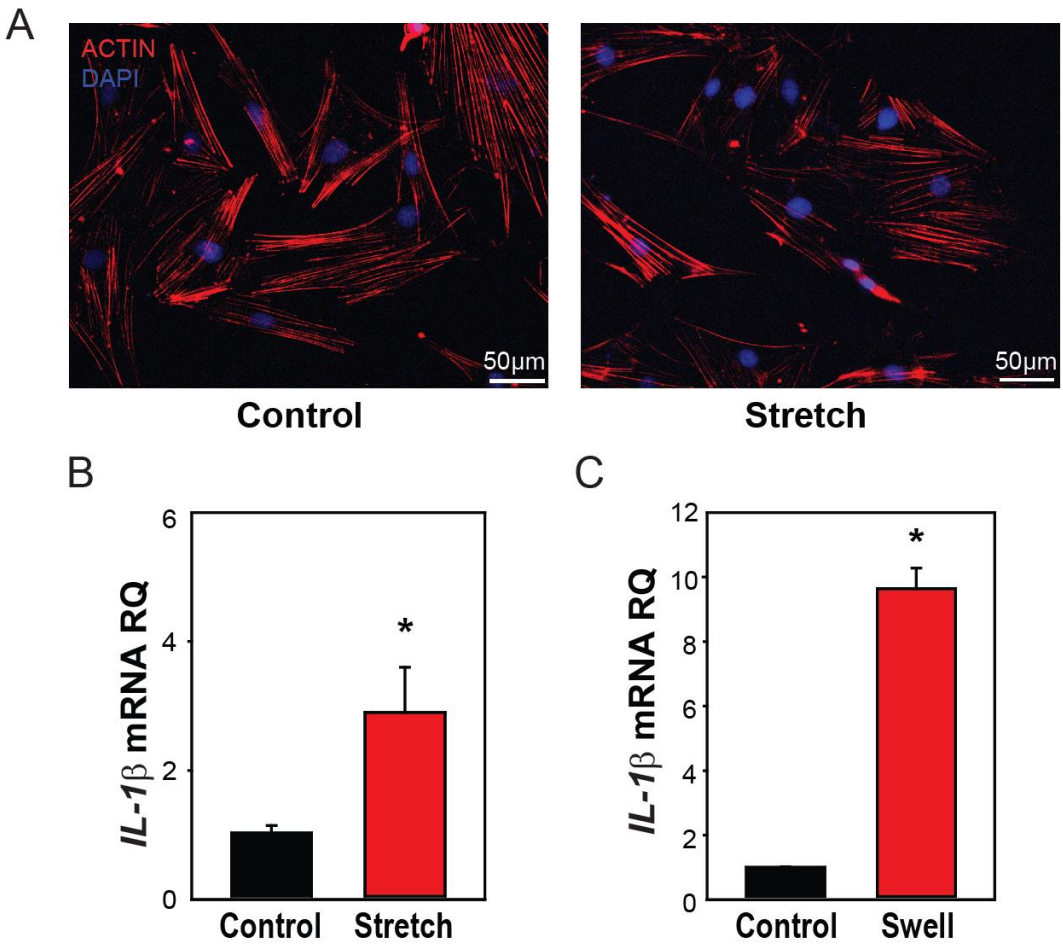

Figure 2.7 Mechanical strain primes IL-1β in optic nerve head astrocytes

A. Astrocytes plated on silicon substrates and fixed after 4 hrs in control conditions (left, Control) or after 16% cyclical strain at 0.3 Hz (right, Stretch). Staining for actin with Phalloidin (red) showed no obvious changes to the cytoskeleton.
B. Application of 16% cyclical strain for 4 hrs increased expression of *IL-1β* mRNA (n=5, *p<0.03).
C. Astrocytes exposed to moderate swelling induced by 30% hypotonicity (Swell) showed increased expression of *IL-1β* mRNA relative to untreated cells maintained in isotonic solution (Control; n=3, *p=0.009).

Figure 2.8 ATP release through pannexin channels required for mechano-sensitive priming of IL-1β in astrocytes

A. Swelling rat astrocytes in hypotonic solution led to a release of ATP into the extracellular medium, as detected by the luciferin/luciferase assay. The ATP hydrolase apyrase (1U/ml) substantially reduced the response. Symbols represent mean ±SEM, n=10.
B. Quantification of extracellular ATP levels 18 min after exposure to solutions (*Control vs Swell or Swell+apyrase, $p<0.05$, ** Swell vs Swell + Apyrase, $p<0.05$, n=10).
C. Swelling astrocytes in the presence of apyrase also prevented the rise in *IL-1β* mRNA (*p=0.02 Swell vs Control, **p=0.03 Swell vs Swell+Apyrase, n=3)
D. The swelling-induced release of ATP was inhibited by pannexin channel blocker carbenoxolone (CBX, 10μM, *$p<0.05$, Control vs Swell or Swell+CBX, **$p<0.05$ Swell vs Swell+CBX, n=20, normalized to swell).
E. The swelling-induced rise in *IL-1β* mRNA was also inhibited by 10 μM carbenoxolone (*$p<0.05$, Control vs Swell or Swell+CBX, **$p<0.05$ Swell vs Swell+CBX, n=7, normalized to swell from 2 experiments).
F. Pannexin blocker probenecid (Prob, 1 mM) reduced the swelling-induced rise of *IL-1β* in astrocytes (p=0.029). The peptide blocker ^{10}Panx1 (100μM) reduced the expression of *IL-1β* as compared to the scrambled peptide control (^{10}Panx1scr, *p=0.003). Swelling alone raised *IL-1β* (p=0.03, n=3 for all). No significate difference between control, probenecid and ^{10}Panx1.
G. Left: Astrocytes stained for pannexin 1 (green), actin (red) and DAPI (blue). Right: No signal was detected in the absence of pannexin 1 antibody.

Figure is located on following page.

Figure 2.8.

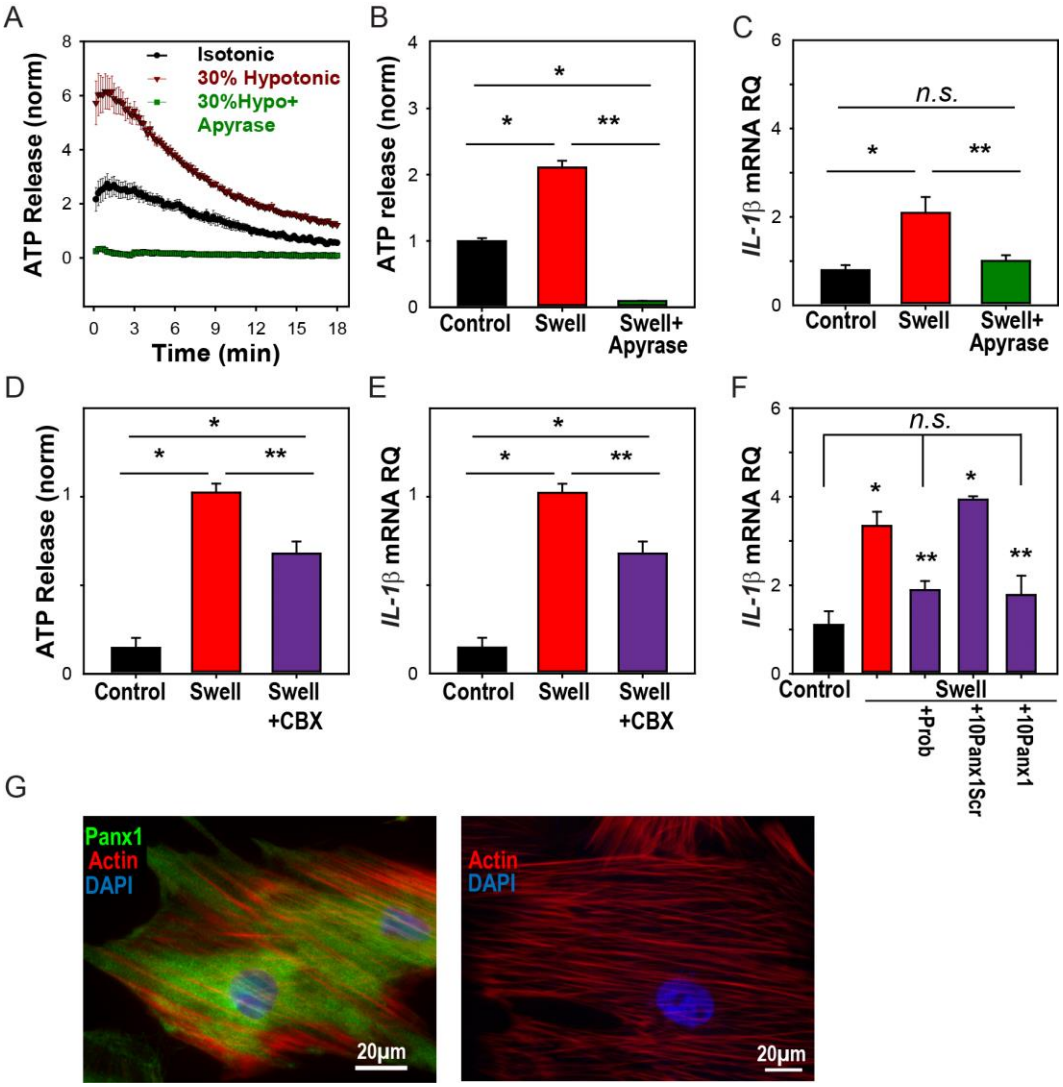
A
ATP Release (norm)
Isotonic
30% Hypotonic
30%Hypo+ Apyrase
Time (min)
B
ATP release (norm)
Control
Swell
Swell+ Apyrase
C
IL-1β mRNA RQ
n.s.
Control
Swell
Swell+ Apyrase
D
ATP Release (norm)
Control
Swell
Swell +CBX
E
IL-1β mRNA RQ
Control
Swell
Swell +CBX
F
IL-1β mRNA RQ
n.s.
Control
Swell
+Prob
+10Panx1Scr
+10Panx1
G
Panx1
Actin
DAPI
20μm
Actin
DAPI
20μm

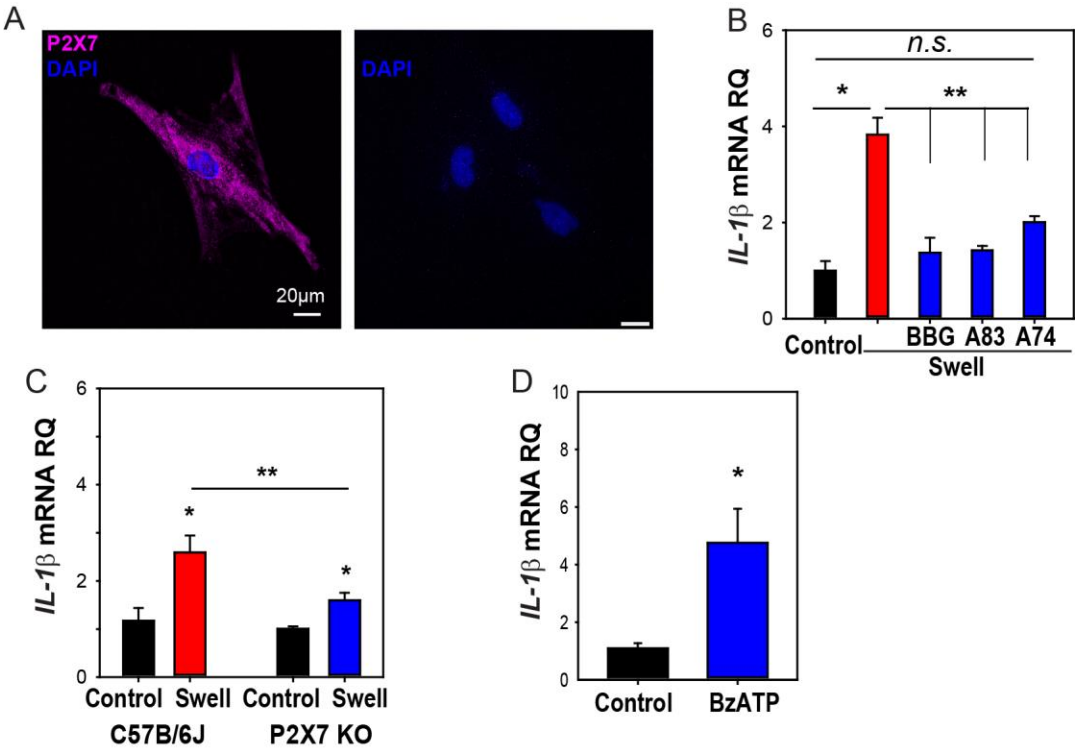

Figure 2.9 P2X7 receptor involved in priming of IL-1β in astrocytes

A. Immunocytochemistry showing expression of the P2X7 in cultured optic nerve head astrocytes (left). No signal was detected in the absence of the primary antibody (right).
B. The swelling-induced rise in *IL-1β* mRNA was inhibited by P2X7 antagonists BBG (10 μM), A839977 (50 nM) and A740003 (5 μM). Cells were pretreated with drugs for 1 hr before swelling (*p<0.001 Swell vs. control, **p<0.001 Swell vs. Swell+drugs, n=4).
C. The swelling-induced rise in *IL-1β* was reduced in astrocytes from P2X7$^{-/-}$ mice as compared to C57BL/6J mice. Data are expressed relative to the matched control group (*p<0.01, ** p=0.026, n=6).
D. Application of BzATP (400 μM) for 4 hrs increased *IL-1β* expression (*p<0.01, n=7,).

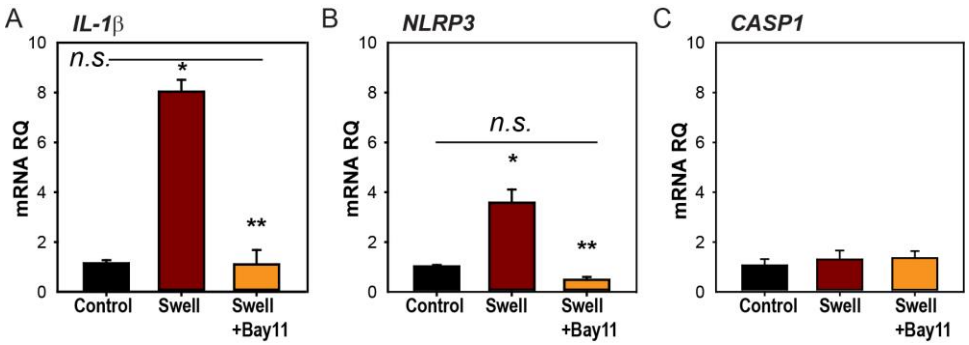

Figure 2.10 NFκB is involved in inflammasome priming after mechanical strain

A. NFκB inhibitor Bay11-7082 (Bay11, 4μM) prevented *IL-1β* upregulation in rat astrocytes. Bay11-7082 was present for 1 hr before and during the 4 hr swelling (*p<0.001 Control vs Swell, **p<0.001, Swell vs Swell+Bay11; n=4, from 2 experiments).
B. The NFκB inhibitor Bay 11-7082 (Bay11, 4μM) reduced *NLRP3* mRNA upregulation in swollen rat astrocytes. Bay11-7082 was present for 1 hr before and during the 4 hr swelling. (*p<0.001 Control vs Swell, **p≤0.001 Swell vs Swell+Bay11; n=4, from 2 experiments)
C. Neither swelling nor Bay 11-7082 had any effect on expression of *CASP1*.

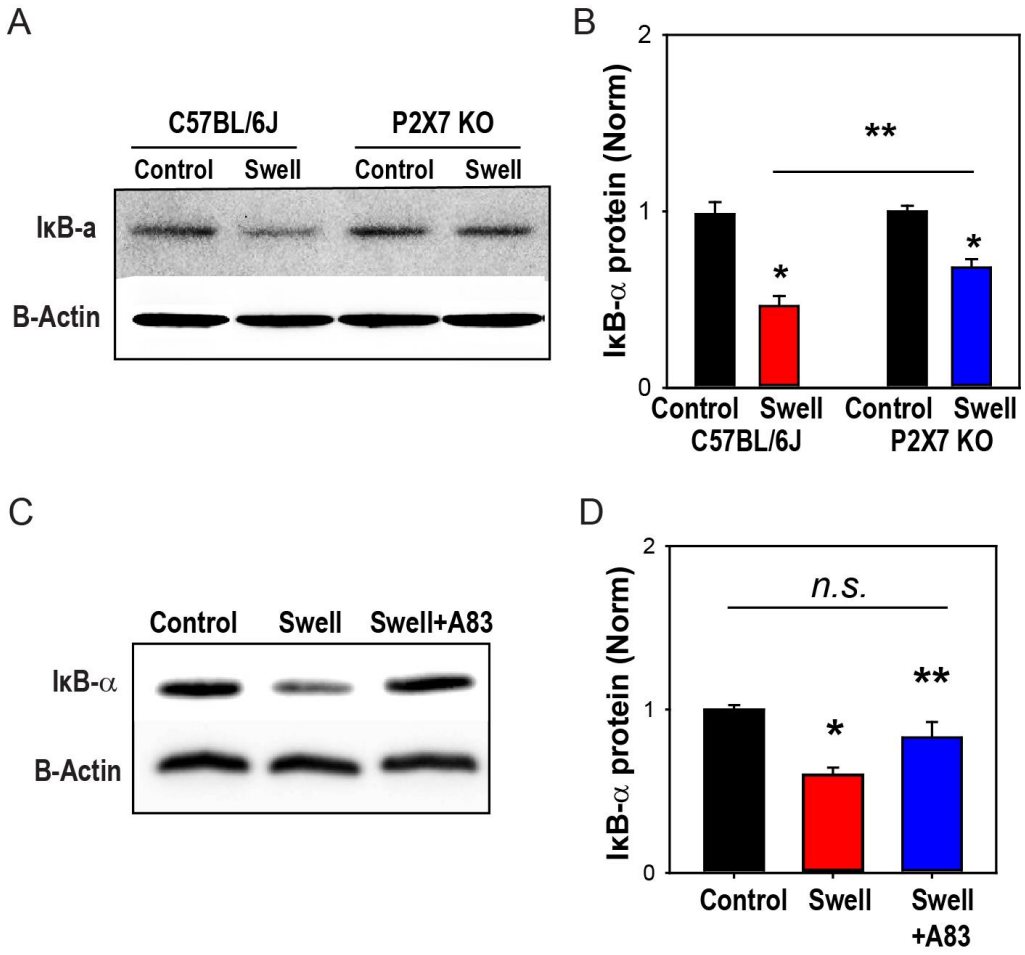

Figure 2.11 P2X7 receptor is involved in NFκB activation after mechanical strain.

A. Representative immunoblots from mouse optic nerve head astrocyte lysates from control C57BL/6J and P2X7$^{-/-}$ mice probed for IκB-α (39 kDa) and housekeeping protein β-actin (42 kDa). Expression of IκB-α was reduced following 4 hrs of swelling in control astrocytes, consistent with the activation of NFκb.
B. Summary of relative IκB-α protein expression from experiments illustrated in panel B quantified with densitometry. The effect of swelling on IκB-α was significantly less in astrocytes from P2X7$^{-/-}$ mice (*p<0.001 Swell vs. Control C57BL/6J, *p=0.011 Swell vs. Control P2X7$^{-/-}$, **p=0.038 Swell C57BL/6J vs Swell P2X7$^{-/-}$; n=3).
C. Representative immunoblots from mouse optic nerve head astrocyte lysates from control mice probed for IκB-α (39 kDa) and housekeeping

protein β-actin (42 kDa). The reduction in IκB-α triggered by swelling was reduced in the presence of P2X7 antagonist A839977 (100 nM).

D. Mean densitometry values for IκB-α protein expression from immunoblots like those in panel “D”. (*p=0.002, **p=0.043; n=6 from 2 experiments)

Supplemental figures

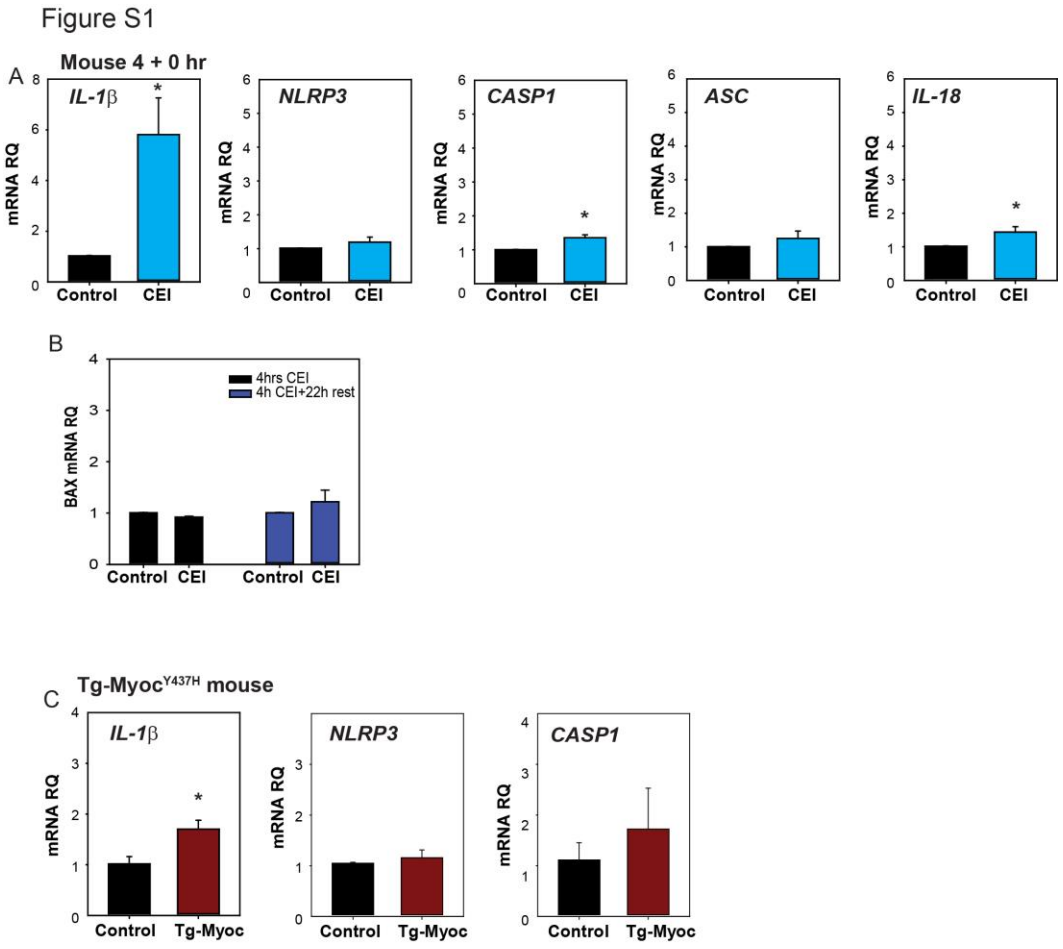

Figure S 2.1.

A. Expression of genes obtained from mouse retinas (including the optic nerve head material) immediately after a 4 hr elevation of IOP to 60 mmHg as compared to levels in the contralateral unpressurized eye. Expression of *IL-1β* (*p=0.006, n=6) *CASP1* (*p = 0.002, n=6), and *IL-18* rose modestly (*p = 0.038), n=4) while expression of *NLRP3* and *ASC* did not change.
B. The CEI procedure did not increase the apoptosis regulator *BAX* at the mRNA level immediately after the transient elevation of IOP to 60 mmHg for 4 hrs or if allowed to rest for 22hrs before extraction (n=3).

C. In retina obtained from 14-18-month-old Tg-Myoc^{Y437H} mice (Tg-Myoc), *IL-1β* mRNA expression was greater than in controls (*p=0.02, n=3). Neither the rise in *NLRP3* nor *CASP1* were significant (n=3).

Figure S2

A. Negative controls of IL-1b and GFAP staining

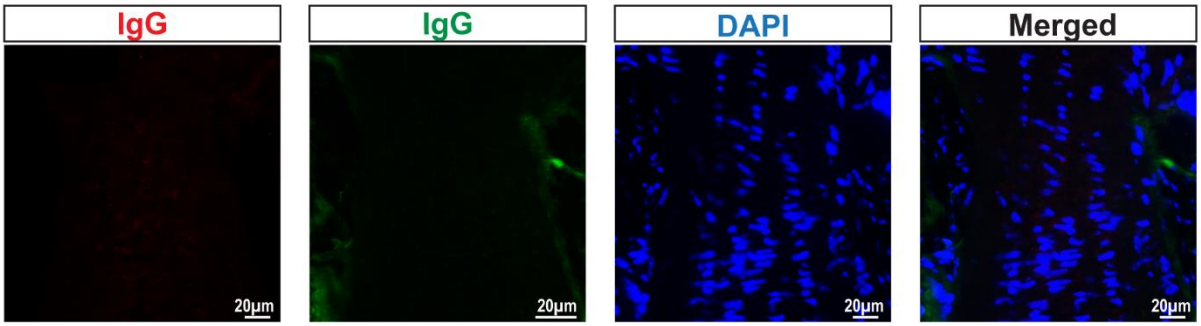

Figure S 2.2

Representative negative controls for the immunohistochemistry of mouse retina treated with the goat IgG then the secondary donkey anti-goat Alexa555-conjugated and donkey anti-mouse IgG Alexa-Fluor 488 in parallel to the immunostaining in Figure 2.5.C. ImageJ was used to modify intensity and combine pseudocolored images, with parallel processing for all images in Figure 2.5 and S.2.2 Scale bar = 20µm.

Figure S3

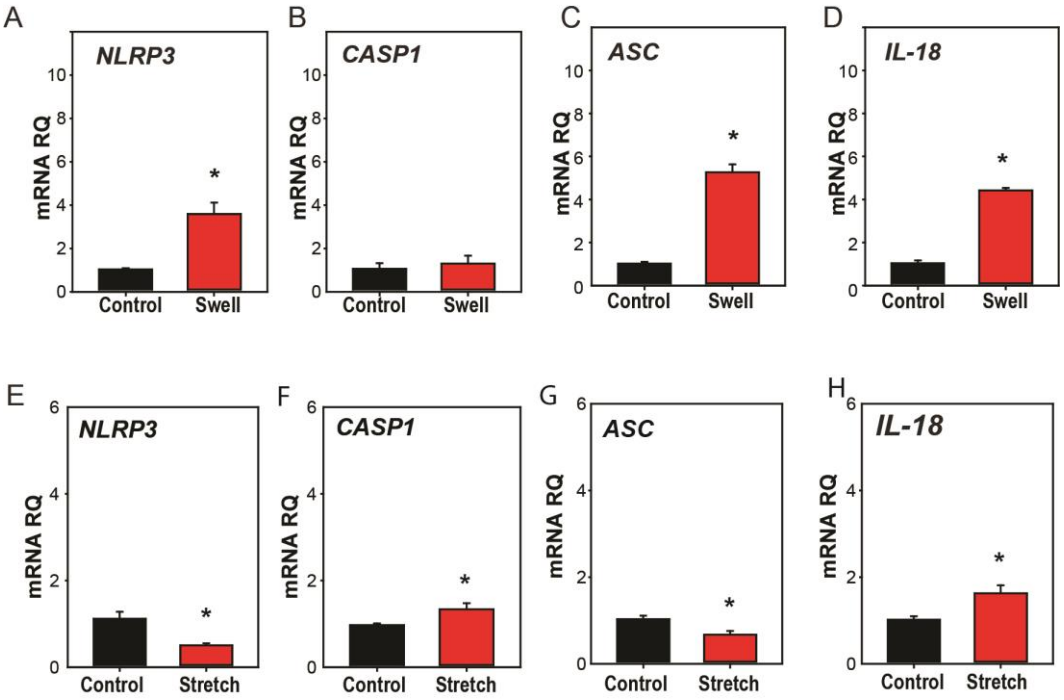

Figure S 2.3

1. A-D. Astrocytes exposed to moderate swelling induced by 30% hypotonicity (Swell) showed increased expression, relative to untreated cells (Control), of mRNA for *NLRP3* (A), *ASC* (C) and (D) *IL-18*, but swelling had no effect on *CASP1* expression (B); n=3 and *p≤0.009 in all cases.
2. E-H. Astrocytes stretched by 16% (Strain) showed greater expression, relative to unstretched cells (Control), of, *CASP1*, and *IL-18*, whereas expression of *NLRP* and *ASC* was smaller with stretching. N=5 and *P<0.03 in all cases.

Figure S4

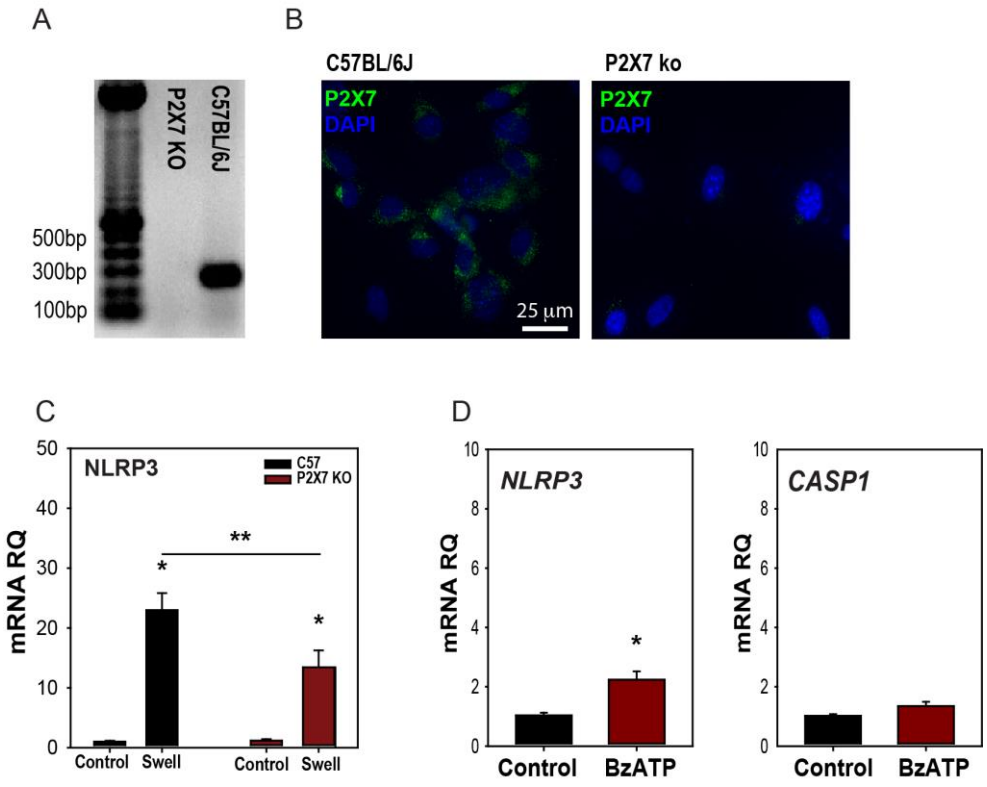

Figure S 2.4

A. PCR of astrocytes obtained from P2X7 knockout and C57BL/6J mice confirmed the absence of the expected 246 bp band in cells from the knockout animals.
B. Immunohistochemistry showing staining for P2X7 in astrocytes cultured from control C57BL6J mice but not from P2X7$^{-/-}$ mice.
C. The swelling-dependent rise in *NLRP3* expression was significantly reduced in astrocytes from P2X7 $^{-/-}$ mice (n=6, *p=0.04)
D. The P2X7 receptor agonist BzATP (400 µM) led to a slight increase in *NLRP3* but not *CASP1* (n=7, *p<0.01).

Chapter 3 : The P2X7 receptor links mechanical strain to cytokine IL-6 upregulation and release in neurons and astrocytes

Wennan Lu[1], **Farraj Albalawi**[1,2] Jonathan M. Beckel[1,5], Jason C. Lim[1], Alan M. Laties[3], Claire H. Mitchell[1,3,4]

Author affiliation: Departments of [1]Anatomy and Cell Biology, [2]Orthodontics, [3]Ophthalmology and [4]Physiology, University of Pennsylvania, Philadelphia, PA 19104; [5]Department of Pharmacology and Chemical Biology, University of Pittsburgh, PA 15261

The work in this chapter started before I joined Dr. Mitchell's lab. However, I was involved in the *in vivo* rat and mouse experiments and the *in vitro* astrocytes experiments. This chapter formed the foundation of my main work in chapter 2.
This work was originally published in J Neurochemistry. 2017 May (Lu et al., 2017), It is reprinted here with some modification to the figures. Experiments in Figures 1 and 4 in the published paper were performed by the other authors, therefore they will be excluded from the figure section in this chapter but will still be in the text and referred to the paper in the appendix.
A copy of the published paper is included in the Appendix with all figures, and at 10.1111/jnc.13998.

Abstract:

Background: Mechanical strain in neural tissues can lead to the upregulation and release of multiple cytokines including IL-6. In the retina, the mechanosensitive release of ATP can autostimulate P2X7 receptors on both retinal ganglion cell neurons and optic nerve head astrocytes. Here we asked whether the purinergic signaling contributed to the IL-6 response to increased intraocular pressure (IOP) *in vivo*, and stretch or swelling *in vitro*. Methods: Rat and mice eyes were exposed to non-ischemic elevations in IOP to 50-60 mmHg for 4 hrs. A PCR array was used to screen cytokine changes, with quantitative (q)PCR used to confirm mRNA elevations and immunoblots used for protein levels. P2X7 antagonist Brilliant Blue G (BBG) and agonist BzATP were injected intravitreally. ELISA was used to quantify IL-6 release from optic nerve head astrocytes or retinal ganglion cells. Receptor identity was confirmed pharmacologically and in $P2X7^{-/-}$ mice Results: Acute elevation of IOP altered retinal expression of multiple cytokine genes. Elevation of *IL-6* was greatest, with expression of *IL1m*, *IL24*, *Tnf*, *Csf1* and *Lif* also increased more than two-fold, while *Tnfsf11*, *Gdf9* and *Tnfsf4* were reduced. qPCR confirmed the rise in IL-6 and extracellular ATP marker *ENTPD1,* but not pro-apoptotic genes. Intravitreal injection of P2X7 receptor antagonist BBG prevented the pressure-dependent rise in *IL-6* mRNA and protein in the rat retina, while injection of P2X7 receptor agonist BzATP was sufficient to elevate *IL-6* expression. IOP elevation increased *IL-6* in wild type but not P2X7 receptor knockout mice. Application of mechanical

strain to isolated optic nerve head astrocytes increased *IL-6* levels. This response was mimicked by agonist BzATP, but blocked by antagonists BBG and A839977. Stretch or BzATP led to IL-6 release from both astrocytes and isolated retinal ganglion cells. Conclusions: The mechanosensitive upregulation and release of cytokine IL-6 from the retina involves the P2X7 receptor, with both astrocytes and neurons contributing to the response.

Graphical abstract

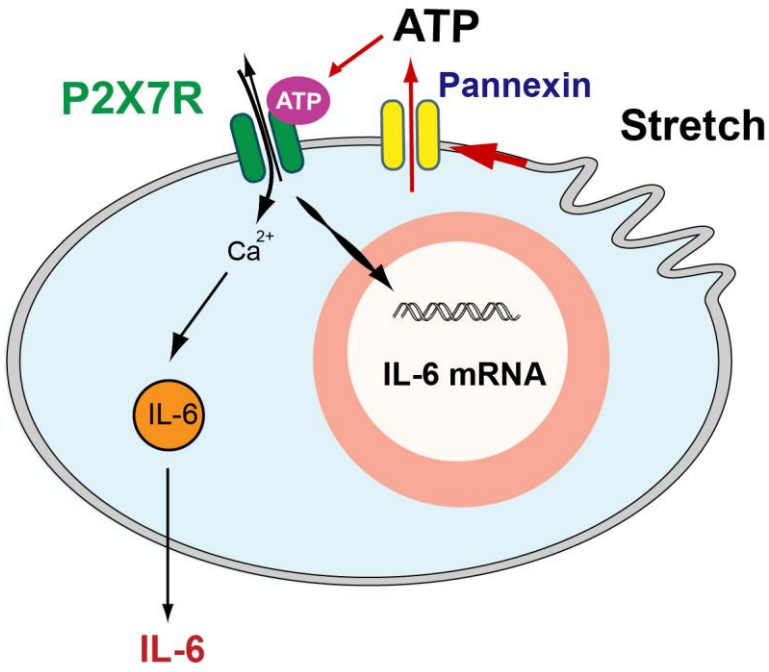

Up-regulation of IL-6 by mechanical strain involves pannexin-mediated ATP release and autostimulation of P2X7 receptors. Increased expression of IL-6 mRNA and protein in the retina following transient increase in intraocular pressure *in vivo*, and instretched/swollen optic nerve head astrocytes was blocked by P2X7 receptor antagonists. Stretch or P2X7 receptor stimulation raised calcium and released IL-6 from astrocytes and retinal ganglion cell neurons.

Introduction

Mechanical strain to neurological tissues frequently leads to both inflammatory and protective responses (Corps et al., 2015). The cytokine interleukin 6 (IL-6) is of particular relevance as it can mediate pathological or protective actions in neural systems depending on context (Erta et al., 2012). IL-6 can lead to neuroinflammation after traumatic brain injury (TBI) and cerebrospinal fluid levels of IL-6 correlate with pathological progression after TBI (Kumar et al., 2015; Yang et al., 2013). However, IL-6 can also induce neurogenesis and protect neural cells after damage (Erta et al., 2012; Penkowa et al., 2003). A better understanding of the pathways linking mechanical strain to IL-6 may help determine the mechanism for the shift of IL-6 from detrimental to protective actions.

The purinergic system has been implicated in regulation of IL-6 in several cell types including fibroblasts (Inoue et al., 2007), skeletal muscle cells (Bustamante et al., 2014), macrophages (Hanley et al., 2004) and microglia (Shieh et al., 2014). Purinergic signaling is particularly sensitive to mechanical strain, with ATP release accompanying increases in shear stress, stretch, and swelling (Corriden and Insel, 2010; Praetorius and Leipziger, 2009). In neural tissue, ATP can be released through pannexin hemichannels in response to mechanical strain (Iglesias et al., 2009; Xia et al., 2012b). The release of ATP and stimulation of the P2X7 receptor is closely linked with inflammatory responses in non-neural cell types (Gombault et al., 2012), leading to inflammasome activation and IL-1β

release (Ferrari et al., 2006; Franceschini et al., 2015). Of particular relevance is the priming and release of IL-6 in microglial cells in response to stimulation of the P2X7 receptor (Shieh et al., 2014).

The retina provides an ideal model with which to examine the relationship between strain, purines and IL-6 in neural tissue. Mechanical strain is experienced by neurons and glial cells in the retina when the intraocular pressure (IOP) rises during glaucoma (Downs, 2015; Sigal and Ethier, 2009). Retinal ganglion cells are the most susceptible to neuropathological changes and death in response to elevated IOP, while the focal point for mechanical strain is the optic nerve head, with optic nerve head astrocytes identified as a critical intermediary (Downs et al., 2008; Hernandez, 2000).

Perturbed purinergic signaling is implicated in response to glaucoma and elevated IOP. For example, human patients with both acute and chronic glaucoma have elevated levels of extracellular ATP in ocular fluids (Li et al., 2011; Zhang et al., 2007). Primate, rat and mouse models of sustained IOP elevation show elevated extracellular ATP (Lu et al., 2015). These models also demonstrated increased expression of the ectoATPase NTPDase1, previously identified to act as a marker for sustained elevation of extracellular ATP (Lu et al., 2007). The pressure-dependent ATP release from retina is inhibited by blockers of pannexin hemichannels and not linked to lactase dehydrogenase, suggesting it is a physiological response (Reigada et al., 2008). Both optic nerve

head astrocytes (Beckel et al., 2014) and retinal ganglion cells (Xia et al., 2012a) release ATP through pannexin hemichannels when subjected to mechanical strain. This released ATP can autostimulate the P2X7 receptor in both cell types.

Alterations in cytokine IL-6 have also been recognized as an important response to elevated IOP. Levels of IL-6 have been detected in the aqueous humor of patients with chronic glaucoma (Chen et al., 1999; Zenkel et al., 2010). In the hypertonic saline model of chronic IOP elevation, *IL-6* was the most upregulated gene in the optic nerve head tissue (Johnson et al., 2011), while *IL-6* was also elevated following transient elevation of IOP (Cepurna et al., 2008). Several observations suggest IL-6 confers protection to retinal ganglion cells; exposure of isolated ganglion cells to high hydrostatic pressure *in vitro* led to apoptotic death that was attenuated by addition of recombinant IL-6 (Sappington et al., 2006), and IL-6 increased both the number and the length of neurites sprouting from isolated retinal ganglion cells (Chidlow et al., 2012). While these observations suggest IL-6 has an important role in the response to increased pressure, the signaling mechanisms linking the mechanical strain to the IL-6 response are largely unknown.

Given the link between mechanical strain, ATP release and P2X7 receptor autostimulation in the retina, the connection between the purinergic signaling and IL-6 activation, and evidence implicating IL-6 in glaucoma, this study was based on the hypothesis that mechanosensitive stimulation of the P2X7 receptor was

involved in the IL-6 response to elevated IOP in the retina. To distinguish between responses due to elevated IOP and those due to cell death, an *in vivo* model of acute but non-ischemic IOP elevation was employed as studies indicate it is generally not lethal to retinal neurons (Abbott et al., 2014; Crowston et al., 2015). Isolated optic nerve head astrocytes and retinal ganglion cells were also utilized to investigate the response in more mechanistic detail *in vitro*.

Methods

Animals: All experiments protocols were approved by the Institutional Animal Care and Use Committee of the University of Pennsylvania. The P2X7 knockout (P2X7-/-) mice originally generated from Pfizer (B6.129P2-P2rx7tm1Gab/J), along with age matched 9 month-old C57Bl6J wild type controls were obtained from Jackson Laboratories (Bar Harbor, ME). Sprague-Dawley and Long-Evans rats were obtained from Harlan Laboratories (Fredrick, MD). Mice and rats of both sexes were utilized.

Model of moderate temporally-controlled IOP elevation: Acute elevation of IOP experiments were performed using adult Sprague-Dawley rats based on the Control Elevation of IOP (CEI) protocol developed by John Morrison and colleagues (Morrison et al., 2010; Morrison et al., 2014). Adult rats were given a prior dose of 2 mg/kg meloxicam and then deeply anesthetized with intraperitoneal injection of ketamine (80 mg/kg) and xylazine (10 mg/kg). Proparacaine (1%) was added to the ocular surface and one drop of Tropicamide (1%) was administered into each eye for pupil dilation. Once anesthesia had taken effect, one eye was cannulated with a 27 gauge shielded wing needle (Becton Dickinson, NJ) inserted into the anterior chamber and connected to a 20 ml syringe filled with sterile phosphate buffered saline (PBS). IOP was increased to 50 mmHg by positioning the syringe at the appropriate height (68cm H_2O), while the contralateral eye without cannulation served as a normotensive control. During the initial development of the model, IOP was calibrated with a TonoLab

tonometer (Colonial Medical Supply, VT) at the beginning and end of the elevation of the reservoir. As IOP was found to be remarkably consistent both throughout the 4 hrs of elevation and between animals, it was usually just measured at the end of the 4 hr period during experiments to avoid excessive force on the needle tip inside the eye. The retina was carefully observed under an operating microscope to ensure that blood flow through the retinal vessels was maintained. After 4 hrs IOP elevation, pressure was returned to normal, the needle was removed and 0.3-0.5% gentamycin ointment or erythromycin (0.5%) was applied to the cornea. Animals were sacrificed 20 hrs (i.e. 1 day) or 5 days later and the retina, including the optic nerve head material, was dissected.

Experiments were also performed on mice using procedures similar to those used for rat with parallels to those described by Crowston and colleagues (Crowston et al., 2015). Mice were given a prior dose of meloxicam and then anesthetized with 1.5% isofluorane. IOP was increased to 50-60 mmHg for 4 hours. Mice were sacrificed immediately after the pressure was returned to baseline, or 20 hrs later. The contralateral eye without cannulation served as a normotensive control.

PCR Array: Expression of mRNA for 84 rat interferons, cytokines and interleukins in the retina was determined using the Rat Common Cytokine RT2 Profiler™ PCR Array (#PARN-021A, SABiosciences Corp., Frederick, MD). Samples were processed according to the manufacturer's protocol. In brief, total

RNA was isolated from the control and pressurized retinas using Trizol and RNeasy mini kit (Qiagen, Inc.), and RNA was quantified from optical density and purity determined (Nanodrop, Thermo Scientific, Inc.). Total RNA (1 µg) was reverse transcribed using genomic DNA elimination and RT^2 First Strand kit (#C-03, SABiosciences Inc.). Comparison of the relative expression of cytokine genes were performed using the PCR array on an ABI 7300 Real-Time PCR System (Applied Biosystems, Foster City, CA). Lactate dehydrogenase A, Ribosomal genes *L13A*, hypoxanthine phosphoribosyltransferase 1 (*HP1*), and beta actin (*Actb*) were used as housekeeping genes and were all stable in retina from eyes with control and elevated IOP. Data were analyzed with the SABiosciences Web-Based PCR Array Data Analysis, where *p* values were calculated based on a Student's *t*-test of the replicate $2^{-\Delta\Delta Ct}$ values for each gene in the control group and experimental groups.

Quantitative PCR: RNA was processed as above. Quantitative PCR (qPCR) was carried out using Power SYBR Green master mix with primer pair sequences shown in Table 3-1, using the 7300 Real-Time PCR System. Data were analyzed using the delta-delta CT approach, with results expressed as fold change in gene expression in eyes with elevated IOP versus control samples ($2^{-\Delta\Delta Ct}$) using an unpaired t-test as described recently (Karmakar et al., 2015).

Intravitreous injection: Intravitreal injections were performed as described (Hu et al., 2010) under a dissecting microscope with a micropipette connected to a

microsyringe (Drummond Scientific Co., Broomall, PA). The glass pipette filled with drug was passed through the superior nasal region of sclera into the vitreous cavity at a point approximately 1 mm from the limbus. The total volume injected was 5 µl over a 30 sec time period. P2X7 receptor antagonist Brilliant Blue G (BBG, 0.8%) was dissolved in sterile saline and injected 1-3 days before IOP elevation. To examine the effects of P2X7 stimulation, Long Evans rats were injected with either 2 µl 250 µM P2X7 receptor agonist Bz-ATP or sterile saline. Rats were sacrificed and the retina dissected, with total RNA isolated from the retina and processed as described above.

Immunoblots: Immunoblots were processed as described (Guha et al., 2013). In brief, whole retinas were washed twice with cold PBS and lysed in RIPA buffer containing 50 mM Tris-HCl, 150 mM NaCl, protease inhibitor cocktail (Complete; Roche Diagnostics, Germany), 1% Triton X-100, 0.1% SDS, and 10% glycerol. Samples were sonicated and cleared by centrifugation (10,000g) for 10 min at 4°C, with protein concentrations determined using a BCA Protein Assay (Pierce/ThermoFisher). Protein was separated using conventional SDS-PAGE, and processed using standard immunoblot protocols (Karmakar et al., 2015). Blots were incubated with a monoclonal antibody to rat IL-6 overnight at 4°C (1:1000 R&D Systems, # MAB5061), followed by incubation with anti-mouse IgG conjugated to horseradish peroxidase (1:5000; Amersham Biosciences Corp., Arlington Heights, IL) at room temperature for 1 hr. and developed by chemiluminescence detection (ECL detection system; Amersham Biosciences

Corp.). The ImageQuant LAS 4100 imager and Image Quant software (Both GE Healthcare Lifesciences) were used to detect and quantify the intensity of the specific bands. Western blots were performed 3-4 times each.

Optic nerve head astrocytes: Primary rat optic nerve head astrocyte cultures were grown as described (Beckel et al., 2014) based upon a protocol modified from Mandal et. al. (Mandal et. al., 2009). The optic nerve head tissue proximal to the sclera in rat pups up to postnatal day 5 was digested for 1 hr in 0.25% trypsin. Cells were grown in medium comprised of Dulbecco's minimal essential medium/F12, 10% fetal bovine serum (FBS), 1% penicillin/streptomycin and 25ng/ml epidermal growth factor (EGF) and used up to passage 5. Cell identification was performed with GFAP immunostaining as described (Beckel et al., 2014). For stretch experiments, astrocytes were seeded on a silicon substrate (Silastic, Specialty Manufacturing, Saginaw, MI), bathed in isotonic solution (in mM; 105 NaCl, 5 KCl, 4 NaHEPES, 6 HEPES acid, 1.3 $CaCl_2$, 5 glucose, 5 $NaHCO_3$, 60 mannitol and 0.25 $MgCl_2$ pH 7.4). Cells were subjected to a 5% equibiaxial strain at 0.3 Hz for 2 min using a specially designed pneumatic piston as described (Beckel et al., 2014; Winston et al., 1989). Cells were exposed to 30% hypotonic solution (isotonic solution diluted with dH2O) for swelling experiments with Brilliant Blue G (BBG, Sigma Corp.), A839977 (Tocris/BioTechne) or BzATP (Sigma Corp.) for 4 hrs at 37°C before RNA was extracted as detailed above. Samples of the extracellular media were taken before and after stretch or BzATP and stored at -80°C. The release of IL-6 from

astrocytes was then measured by Rat IL-6 Quantikine@ ELISA kit (#R6000B, R&D systems) following manufacturer's instructions, with data acquired using a 96-well plate reader SpectraMax M5 (Molecular Devices).

IL-6 release from isolated retinal ganglion cells: Isolation of retinal ganglion cells was performed using the immunopanning procedure as described (Xia et al., 2012b; Zhang et al., 2010). Isolated RGCs were seeded onto 0.1% poly-L-lysine (Peptides International) and 1 µg/mL laminin coated coverslips or elastic silicone sheeting in stretch chambers and cultured at 37^{o}C with 5% CO_2. Attached cells were bathed in 750µl of isotonic solution including 100 µM of the ectoATPase inhibitor βγ methylene ATP, and stretched by application of 20 mmHg of pressure resulting in a 4.1% deformation strain (see (Xia et al., 2012a) for detail). Pressure inside the stretch chamber was increased to 20 mmHg for 4 min, returned to 0 mmHg for 1 min and the cycle repeated three times for a total duration of 15 min. Immediately following stretch, a 250 µL sample of the extracellular solution was collected from the center of the stretch chamber. Stretch did not induce release of lactose dehydrogenase. IL-6 levels were determined with the rat antibody cytokine array following manufacturer's instructions (R&D Systems), as described in detail in a recent publication (Lim et al., 2016). In brief, IL-6 levels were quantified by incubating the membrane in Streptavidin-HRP followed by chemiluminescent detection reagents (GE Healthcare). The production of light corresponding to levels of bound cytokine was determined with ImageQuant LAS4000 and the intensity of each spot was

measured using ImageQuant TL analysis software (all GE Healthcare). Results represent 4 independent trials of stretch or BzATP experiments, each performed in duplicate.

Data analysis and study design: Data are reported as mean ± standard error of the mean. Statistical analysis used a 1-way ANOVA with appropriate post-hoc test, or a paired Student's t- test when comparing eyes from the same animal. Results with $p<0.05$ were considered significant. When data were not distributed normally, analysis on ranks was performed. All statistical analysis was performed using SigmaStat software (Systat Software Inc.). The number of experimental repeats was determined in part by sample size calculations and power analysis. Data within two standard deviations of the mean was included unless accompanied by signs of animal distress or unexpected deviation. Analysis was performed in a masked fashion where appropriate.

Table 3-1 Primers used for qPCR of IL-6 study

Gene Name	GenBank Accession	Forward Primer (5' to 3')	Reverse Primer (5' to 3')	Size(bp)
Anxa3	NM_012823	ATCCGGAAAGCAATCAAAGG	CCATGACATGCTCAAAGTGG	174
Bax	NM_017059	TGCCAGCAAACTGGTGCT	ACCCAACCACCCTGGTCTT	129
Cfos	NM_022197	CCTGTGAGCAGTCAGAGAAGG	CGGAAGAGGTGAGGACTGG	194
CyclinD1	NM_171992	CCCACGATTTCATCGAACACT	GATCATCCGCAAACATGCA	77
ATF3	NM_012912	CGAAGACTGGAGCAAAATGATG	CAGGTTAGCAAAATCCTCAAACAC	123
IL-6	NM_012589	CTCCGCAAGAGACTTCCAG	GGTCTGTTGTGGGTGGTATC	119
P2X4R	NM_031594	GCAAGACGTTCTTCCACCCTATACA	TCCATACGCTCACACTGTATAAGCC	137
P2X5R	NM_080780	GACATCCAGGAGACACTTAGCTTCG	CAGCAAGAGCTGAACTGCACAAGTC	230
P2X7R	NM_019256	TAATGCCTCAGCCTAGTGCCTTTGG	CTGCTGCTCCAGAGGGCTCAAGTTC	107
P2Y1R	NM_012800	GCAGCTTCCACTGCCAAAGGCTAAT	ATTGTAAAGCTTCAAGATCTGGCAG	172
P2Y2R	NM_017255	AGCAGCTCAGTCAGGTGTCAGTTCA	TCAGGTGGCGTTGCCTTAGATACGA	214
P2Y4R	NM_031680	ATAGCTGTCTTGATCCAGTGCTCTA	AGCAGCAGGGTTACAATCGATCTCC	215
P2Y6R	NM_057124	TAGGTCCTGGAATAGCACTGCAAAT	AAAGTCTTGGCAAATGGATGGGAAT	171
A1AR	NM_017155	AGCCTGGATGTCTTCCTTGTATGGA	TAGACATAGGGACCTCCTTGAGAAC	121
A3AR	NM_012896	GAGCTTCTCTCATTCAATTCTGTGG	CCTAGGGATCCTTCAACGCAGGTTC	183
GAPDH	NM_017008	CCATGGAGAAGGCTGGGG	CAAAGTTGTCATGGATGACC	195

Results

Pressure-dependent elevation in message for IL-6

Initial experiments to screen for cytokine pathways activated *in vivo* by transient elevations in IOP were determined using a cytokine PCR Array. IOP in one eye of a rat was raised to 50 mmHg for 4 hrs. Although this is considerably above the baseline IOP levels of 12.8 mmHg in the conscious Sprague-Dawley rat (Cabrera et al., 1999), this increase did not prevent blood flow through the retinal vessels. Similar transient rises in IOP have been found to induce minimal permanent damage (Abbott et al., 2014; Crowston et al., 2015; Morrison et al., 2010; Zhi et al., 2012). qPCR analysis indicated no rise in pro-apoptotic genes, although expression of the early stress-response ATF3 was increased, consistent with findings in the hypertonic saline model (Guo et al., 2011) (Appendix. Fig S1).

To obtain an objective measure of the cytokine response to transient pressure elevation, retinal gene levels were examined 20 hrs after IOP returned to baseline using a cytokine PCR array. Analysis showed 9 genes with a >2-fold change in expression levels between the pressurized and control rat retina (Appendix. Fig 1A and B). *IL-6* showed the greatest rise, with a 29- fold increase. *IL1m*, *IL24*, *Tnf*, *Csf1* and *Lif* were also elevated more than two-fold. Three genes, *Tnfsf11*, *Gdf9* and *Tnfsf4*, were down-regulated more than two-fold.

Given that *IL-6* was the gene altered most using the cytokine gene array, results were confirmed using traditional qPCR. *IL-6* was elevated 16.9 fold in eyes with increased IOP as compared with contralateral eyes (Appendix. Fig 1C). This substantial increase measured using qPCR strongly supported the result from the PCR array suggesting that expression of *IL-6* was increased in retinas exposed to transient elevations in IOP.

Purines and IL-6 expression in vivo

As purinergic signaling has been repeatedly implicated in retinal cells exposed to elevated IOP (Reigada et al., 2008; Sanderson et al., 2014), expression of gene *ENTPD1* was examined. *ENTPD1* codes for the ectoATDPase NTPDase1, which was previously identified as a possible marker for a sustained rises in extracellular ATP, with increased levels of the gene *ENTPD1* and protein for NTPDase1 triggered by sustained exposure to ATP (Lu et al., 2007). Levels of NTPDase1 were elevated in parallel to extracellular ATP concentrations in rat, mouse and primate models of chronic IOP elevation (Karmakar et al., 2015). In material from rat retinas obtained both 1 and 5 days after transient IOP elevation, ENTPD1 was upregulated (Figure 3.1.A), suggesting levels of extracellular ATP were elevated. after moderate IOP elevation.

A considerable body of past work implicates autostimulation of the P2X7 receptor following the mechanosensitive release of ATP in the retina (Beckel et al., 2014; Reigada et al., 2008; Xia et al., 2012b; Zhang et al., 2006), and recent

work demonstrates P2X7 receptor stimulation leads to IL-3 responses in isolated retinal ganglion cells (Lim et al., 2016). As stimulation of P2X7 receptors by ATP has been associated with the upregulation of IL-6 in microglia cells (Shieh et al., 2014), the role of the P2X7 receptor in mediating the pressure-dependent rise in *IL-6* was examined.

Initial involvement of the P2X7 receptor as determined using antagonist Brilliant Blue G. While BBG can act at other P2X receptors (Bo et al. 2003), it is well tolerated in the eye (Totan et al., 2014). In addition, the blue color of the compound enabled the retinal distribution of the antagonist to be more accurately determined (Figure 3.1.B); material from the targeted retina was preferentially analyzed. The pressure-dependent increase in *IL-6* mRNA was blocked by intravitreal injection of 0.8% BBG 1-3 days before the IOP rise (Figure 3.1.C). Levels were compared to the rise seen in pressurized eyes injected with only saline, to control for any injection artifact. Immunoblots confirmed that IL-6 protein was also increased in the retina following a rise in pressure (Figure 3.1.D). Changes in protein level paralleled those of mRNA, with IOP rise leading to an increase in IL-6 protein that was prevented by BBG (Figure 3.1.E).

To determine whether stimulation of the P2X7 receptor was sufficient to trigger upregulation of *IL-6*, agonist BzATP was injected intravitreally (2 µl, 250 µM) with sterile saline injected into the contralateral eye and levels of *IL-6* mRNA present in the retina 24 hrs later were determined. Retinal *IL-6* expression was increased

4-fold by the P2X7 receptor agonist BzATP in the absence of any changes in IOP (Figure 3.1.F).

Involvement of purines in the response to elevated IOP was further probed by examining expression of certain receptors. Receptor genes *P2RX7* and *ADORA3,* coding for the adenosine A3 receptor, were elevated in many retinas examined after 1 day, but considerable variation meant the rises were not significant (Appendix. Fig S2). Genes *P2RX4* and *P2RY6* for purinergic receptors were increased 1 day, but not 5 days after IOP elevation. While the precise contribution of these receptors remains to be determined, their increased expression is consistent for mechanosensitive purinergic signaling.

Pressure-dependent upregulation of IL-6 absent in P2X7 knockout mice:

Further confirmation of the role of the P2X7 receptor in the pressure-dependent rise in *IL-6* was provided with P2X7 knockout mice. Elevating the IOP of wild-type C57Bl6J mouse eyes to 60 mmHg for 4 hrs led to a rise in *IL-6* levels analogous to that observed in the rat eye (Figure 3.1.G). In mice missing the P2X7 gene, however, this rise in IOP did not significantly change *IL-6* levels (Figure 3.1.H). This supported the pharmacological identification, while also demonstrating the response occurred in multiple species.

IL-6 upregulation and release from optic nerve head astrocytes:

In vitro experiments from isolated cells were pursued to enable identification of specific cell types and better control of pharmacological manipulation. Optic nerve head astrocytes undergo multiple changes in response to the mechanical strain in glaucoma (Hernandez, 2000). As we have previously found that stretch of these astrocytes leads to the release of ATP through pannexin hemichannels and subsequent autostimulation of P2X7 receptors (Beckel et al., 2014), the mechanosensitive response of *IL-6* in these astrocytes and the contribution of the P2X7 receptor was examined.

Isolated rat optic nerve head astrocytes expressed GFAP, confirming the identity of the cultured cells (Figure 3.2.A). Astrocytes were plated on a silicone substrate and subjected to a 5% equilateral strain at 0.3 Hz for 4 hrs, followed by a 20-hr break before RNA was extracted to increase parallels to *in vivo* experiments. Levels of *IL-6* mRNA were increased 2-fold in stretched astrocytes as compared to controls (Figure 3.2.B). Unstretched astrocytes exposed to 50 μM BzATP for 4 hrs also demonstrated a 2-fold rise in *IL-6*, suggesting the P2X7 receptor was sufficient to trigger the rise in *IL-6* mRNA expression (Figure 3.2.C) as found *in vivo*. An analogous rise in *IL-6* was produced by swelling astrocytes with a 30% hypotonic solution for 4 hrs (Figure 3.2.D); this rise in *IL-6* mRNA was prevented by P2X7 receptor antagonists BBG and A839977 (Figure 3.2D).

To confirm the contribution of the P2X7 receptor, the rise in *IL-6* expression in optic nerve head astrocytes isolated from C57Bl6J mice and P2X7 knockout

mice was compared. Swelling cells from wildtype mice induced a significant increase in *IL-6* expression (Figure 3.2.E). In contrast, astrocytes isolated from P2X7$^{-/-}$ mice showed a drop in the *IL-6* expression with swelling.

IL-6 released from optic nerve head astrocytes

While the ability of P2X7 receptors to trigger the upregulation of *IL-6* mRNA *in vivo* and *in vitro* implied an increased involvement of the cytokine, the ability of the receptor to trigger release of IL-6 was also tested. Measurement of IL-6 levels in the bath surrounding the astrocytes using an ELISA assay demonstrated that the cytokine was released into the bath after stretch (Figure 3.2.F). Exposure of astrocytes to agonist BzATP also led to a substantial release of IL-6 (Figure 3.2.G). Cytokine release in many cell types is mediated by increases in intracellular calcium; for example, the release of IL-6 from spinal cord astrocytes is calcium dependent (Codeluppi et al., 2014). To confirm optic nerve head astrocytes experience a rise in calcium upon swelling, levels were monitored with indicator Fura-2. The rise in calcium was rapid and reversible (Figure 3.2.H). To determine whether this response was dependent upon autostimulation of the P2X7 receptor, the ability of BBG to antagonize this rise was examined. Pretreatment of astrocytes with blocker BBG eliminated the rise in calcium, implicating autostimulation of the P2X7 receptor, and consistent with a role for calcium in the release.

IL-6 released from isolated retinal ganglion cells:

Although the above experiments clearly indicate that mechanical strain and stimulation of the P2X7 receptor can lead to release of IL-6 from optic nerve head astrocytes, immunostaining indicated that retinal ganglion cells expressed high levels of IL-6 (Appendix. Fig 4A). The staining pattern was particulate, consistent with IL-6 stored in vesicles. As such, the ability of retinal ganglion cells to release IL-6 was tested. As ganglion cells *in situ* are intertwined with various other cell types, a two-step immunopanning procedure was used to isolate retinal ganglion cells (Appendix. Fig 4B); previous analysis indicates that >98% of cells obtained in this way are ganglion cells (Zhang et al., 2006). The purified cells were plated on a silicone substrate and, once attached, a 4.1% deformation strain was applied to stretch the cells for 4 min. Cells were then returned to baseline for 1 min, with the stretch cycle repeated 2 more times. There was a significant increase in extracellular levels of IL-6 released into the bath after this stretch period (Appendix. Fig 4C). Analogous trials indicate that stimulation of the P2X7 receptor with BzATP also released IL-6 from isolated retinal ganglion cells (Appendix. Fig 4D). Attempts to process RNA from these isolated ganglion cells were unsuccessful, precluding examination of *IL-6* expression. However, application of BzATP led to a rapid increase in intracellular calcium in isolated retinal ganglion cells (Appendix. Fig 4E); the response was rapid, reversible and repeatable.

Discussion

The signaling pathways linking mechanical strain to inflammation play an important role in the cellular response to stress. The current study implicates the P2X7 receptor for extracellular ATP in the mechanosensitive upregulation of cytokine IL-6 in the retina. *In vivo* data demonstrate *IL-6* mRNA was substantially upregulated after a transient elevation of IOP in the rat retina, with the P2X7 receptor antagonist BBG preventing the upregulation of both *IL-6* mRNA and IL-6 protein in retinal tissue. The transient rise in IOP increased *IL-6* expression in the retina of wildtype mice but not in P2X7 knockout mice, further implicating the P2X7 receptor and demonstrating the effect was not species dependent. In isolated optic nerve head astrocytes, *IL-6* expression was increased by stretch, swelling and directly by the P2X7 agonist BzATP. The swelling- induced rise in *IL-6* in astrocytes was prevented by two different P2X7 antagonists. In addition, both astrocytes and retinal ganglion cell released IL-6 in response to agonist BzATP or to mild stretch. Together these data identify a role for the P2X7 receptor in the mechanosensitive IL-6 response of neurons and astrocytes in the retina.

Signaling pathways linking mechanical strain to IL-6

The intracellular signaling pathways linking mechanical strain to the IL-6 response can be at least partially described by integrating previous findings with the results of the current study. Increased pressure in the whole retina, or

mechanical strain to either optic nerve head astrocytes or retinal ganglion cells leads to ATP release through pannexin hemichannels (Beckel et al., 2014; Reigada et al., 2008; Xia et al., 2012b). Release from astrocytes is partially dependent on Rho kinase, consistent with a mechanosensor like TRPV4 as in other ocular cells (Jo et al., 2015; Shahidullah et al., 2012). In both astrocytes and retinal ganglion cells, the released ATP autostimulated P2X7 receptors on the same cell type.

The present study clearly implicates the P2X7 receptor in the IL-6 response to mechanical strain. The P2X7 antagonist BBG prevented the rise in *IL-6* expression *in vivo*, while BBG and a second antagonist A839977 prevented the rise in astrocytes. In addition, agonist BzATP emulated the effects of mechanical strain both *in vivo* and *in vitro*. Although BzATP and BBG can act at other P2 receptors (Bo et al., 2003; Wildman et al., 2003), A839977 is more selective (Honore et al., 2009). In addition, the reduced *IL-6* response in $P2X7^{-/-}$ mice *in vivo*, and in optic nerve head astrocytes isolated from the $P2X7^{-/-}$ mice, implicated the P2X7 receptor in linking the mechanical strain to the *IL-6* response. The retinal response resembles that in cultured microglia, where the P2X7 receptor triggers *IL-6* mRNA upregulation and release of the cytokine (Shieh et al., 2014).

While the use of agonists, antagonists and knockout mice together imply the P2X7 receptor makes a substantial contribution to the mechanosensitive IL-6

response, a contribution from other P2 receptors cannot be ruled out in the present study, and other P2 receptors have been linked to IL-6 (Inoue et al., 2007; Kawano et al., 2015; Shigemoto-Mogami et al., 2001). A study of the same $P2X7^{-/-}$ mice used here found that while most of the peritoneal rise in IL-6 accompanying ATP injection was eliminated in the knockout mice, the residual response may have reflected action of additional receptors, with P2Y receptors suggested as a possible source (Solle et al., 2001). The increased expression of the P2Y6 receptor in retinas exposed to transient pressure elevation is interesting, but as the agonist for this receptor is UDP, and ATP itself has little affinity, activation of this receptor by ATP released after elevated pressure is likely to be complex (Communi et al., 1996; Satrawaha et al., 2011). It is also not clear whether the response is direct or reflects a secondary response to IL-1β release, as IL-1β can lead to upregulation of *IL-6* expression (Cadman et al., 1994). Experiments are currently underway to determine whether stimulation of the P2X7 receptor leads to IL-1β release.

In addition to the upregulation of *IL-6* message and protein levels, mechanical strain and the P2X7 receptor also triggered a rapid release of IL-6 from astrocytes and retinal ganglion cells. The P2X7 receptor is a ligand gated non-selective cation channel, and its stimulation raises intracellular calcium in both astrocytes and retinal ganglion cells (Beckel et al., 2014; Xia et al., 2012b). The vesicular release of IL-6 from spinal cord is calcium-dependent (Codeluppi et al., 2014), and the time course of the IL-6 release above implies the signaling

mechanisms are distinct from those involved in transcriptional upregulation. While the increased expression of *IL-6* would provide more IL-6 for release upon later stimulation, this complex positive feedback pathway was not investigated in the present study.

Separating mechanical strain from cell death and the P2X7 receptor

The data here indicate that P2X7 receptor was involved in the increase in *IL-6* after a transient non-ischemic elevation in IOP. We used this model because it was reported to induce little cell death (Abbott et al., 2014; Crowston et al., 2015; Morrison et al., 2010; Morrison et al., 2014), and enabled us to distinguish between responses resulting from mechanical strain and those due to cell death; the lack of response in genes *ANAX3*, *BAX* or *CCND1,* associated with apoptosis or extreme stress, suggest this distinction was largely achieved. In a variant of the rat model in which IOP was raised to 50 mmHg for 8 h, there was no substantial RGC loss or decreases in axon transport (Abbott et al., 2014). Elevation of mouse IOP to 50 mmHg for 30 min led to a transient reduction in the photopic negative response (PhNR), attributed largely to retinal ganglion cell function, although the number of ganglion cells was not reduced when examined 7 days later (Chrysostomou and Crowston, 2013; Crowston et al., 2015). Presumably the maintenance of retinal blood flow prevents the retinal ganglion cells loss associated with more ischemic models (Zhi et al., 2012). Overall this suggests that the robust IL-6 response, and the stimulation of the P2X7 receptor which precedes it, are distinct from cell death.

Relevant cell types

Our *in vivo* experiments identified elevated *IL-6* mRNA and IL-6 protein using material from the entire retina. The optic nerve head is the focus of the mechanical forces induced upon elevation of IOP (Downs, 2015), and the *in vitro* experiments clearly demonstrate a rise in *IL-6* expression in optic nerve head astrocytes, consistent with previous findings of a large rise in optic nerve head *IL-6* in response to IOP elevation (Johnson et al., 2011). However, the optic nerve head tissue is a minor component of the retina and it is likely that other cell types contribute to the rise in *IL-6* expression found in the whole tissue. While the restricted levels of cell material in panned retinal ganglion cells precluded reliable molecular analysis of *IL-6* levels in this study, the cells are also likely to contribute. The increased expression of *IL-6* 1 day after IOP elevation using the laser photocoagulation model co-localized with amyloid precursor protein, a marker of fast axonal transport, and suggested the axonal transport of IL-6 synthesized in retinal ganglion cells was impeded with increased IOP (Chidlow et al., 2012). This may relate to a more recent study in which IL-6 increased with age in the proximal optic nerve of DBA mice, and correlated with the loss of axonal transport (Wilson et al., 2015). The predicted involvement of microglial cells here is complex; cultured retinal microglia released IL-6 when subjected to hydrostatic pressure increase (Sappington et al., 2006), while activated microglial cells were observed *in vivo* only one week after elevation of IOP but not at earlier time points (Kezic et al., 2013). Future experiments are needed to understand

the role of microglial cells given their responsiveness to extracellular ATP (Franke et al., 2007).

Physiological implications:

While the results from the present study clearly demonstrate a role for the P2X7 receptor in the upregulation and release of IL-6, the physiological implications will depend upon the cell types involved, the conditions that lead to the response, and whether the resulting IL-6 mediates protective or detrimental effects. IL-6 signaling is complex; although IL-6 is traditionally described as a "pro-inflammatory" cytokine, it can be both protective and pathological in neural tissues (Spooren et al., 2011). Expression of IL-6 in cortical astrocytes confers protection from focal injury in neural tissue (Penkowa et al., 2003). In the retina, several groups have identified protective actions by IL-6 and suggested it is an early protective response. The death of retinal ganglion cells following increased hydrostatic pressure was prevented by IL-6 (Sappington et al., 2006), and IL-6 enhanced neurogenesis in retinal ganglion cells (Chidlow et al., 2012). If IL-6 represents an early response to protect neurons, then the present study suggests that the mechanosensitive release of ATP through pannexin hemichannels and autostimulation of P2X7 receptors that lead to the increased IL-6 response may also be protective, at least in young healthy tissue. This would add to the increasing recognition of the P2X7 receptor as more than just a "death receptor" in neural tissues.

Acknowledgments:

We thank Wennan Lu for assistance with the *in vivo* experiments, and Jason Lim for the assistance with the ELISA measurements. This work is supported by grants from the NIH EY015537 and EY013434 and core grant EY001583 (CHM).

Figures

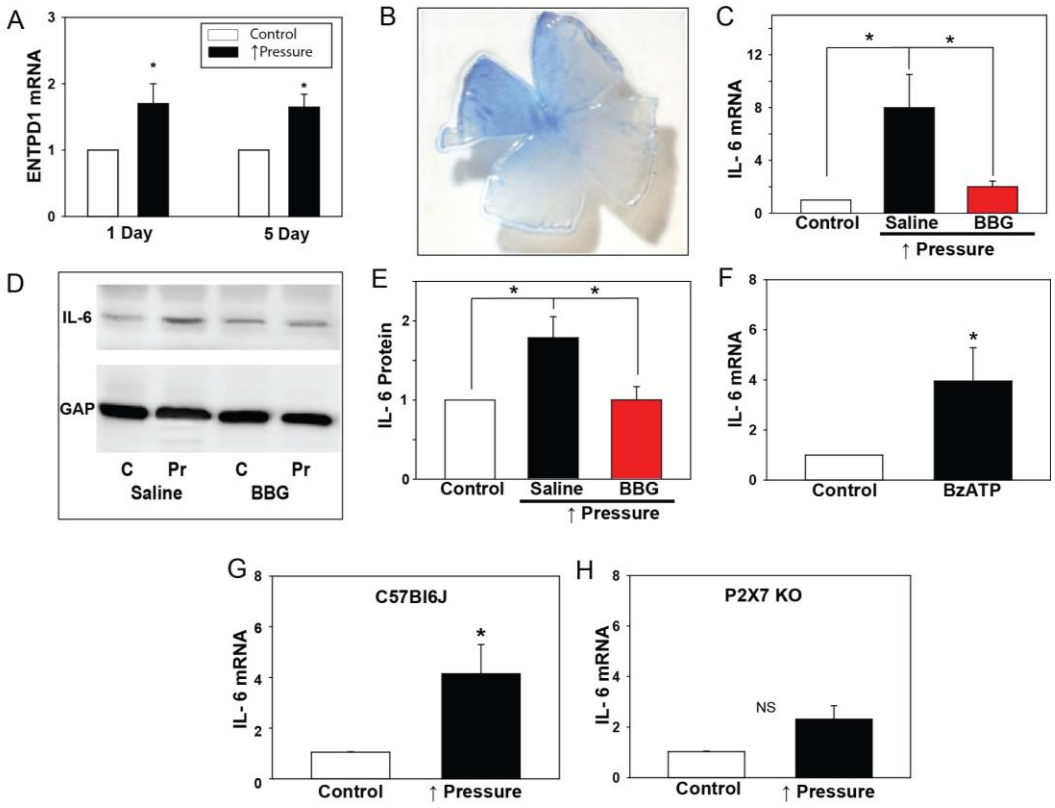

Figure 3.1 Involvement of ATP and P2X7 receptor in IL-6 elevation *in vivo*

A. Expression of ectoATPase gene *ENTPD1* was elevated 1 day after increase in IOP to 50 mmHg for 4 hrs (Pressure, *p=0.033, N=10). *ENTPD1* remained elevated 5 days after the procedure (*p=0.004, N=8).
B. The distribution of P2X7 antagonist Brilliant Blue G (BBG) in the retina 1 day after intravitreal injection. The staining pattern suggests distribution of BBG through the vitreal cavity to the retina was restricted. A similar staining pattern remained in retinas examined 6 days after injection.
C. The pressure-dependent rise in *IL-6* mRNA was substantially decreased following injection of BBG. Data are expressed as relative gene expression in the pressurized vs non-pressurized retina for eyes injected with 0.8% BBG or saline 1-3 days before the moderate elevation of IOP to 50 mmHg for 4 hrs. N=6-9. *p<0.004 saline pressurized vs. non-pressurized; *p<0.013 saline pressurized vs. BBG pressurized.

D. Representative immunoblots from whole retina lysates probed for IL-6 (22 kDa) and housekeeping protein GAPDH (GAP, 37 kDa). Expression of *IL-6* is greater in the eye subject to the moderate IOP increase (Pr) treated with saline as compared to the contralateral non-pressurized control eye, but this pressure-dependent increase is reduced after injection with BBG.
E. Summary of relative protein expression from experiments illustrated in C quantified with densitometry; N=4-5. * $p<0.001$ saline pressurized vs. non-pressurized; *$p<0.035$ saline pressurized vs. BBG pressurized
F. P2X7 receptor agonist BzATP was sufficient to increase levels of *IL-6* mRNA in the retina 1 day after intravitreally injection (250 μM, 2 μl per eye), N=5, *$p=0.021$.
G. In wildtype C57Bl6J mice, transient elevation of IOP to 60 mmHg for 4 hrs (Pressure) raised retina levels of *IL-6* mRNA. N=7, *$p<0.001$.
H. In P2X7 knockout mice, the same elevation in IOP did not significantly increase levels of *IL-6*. N=6.

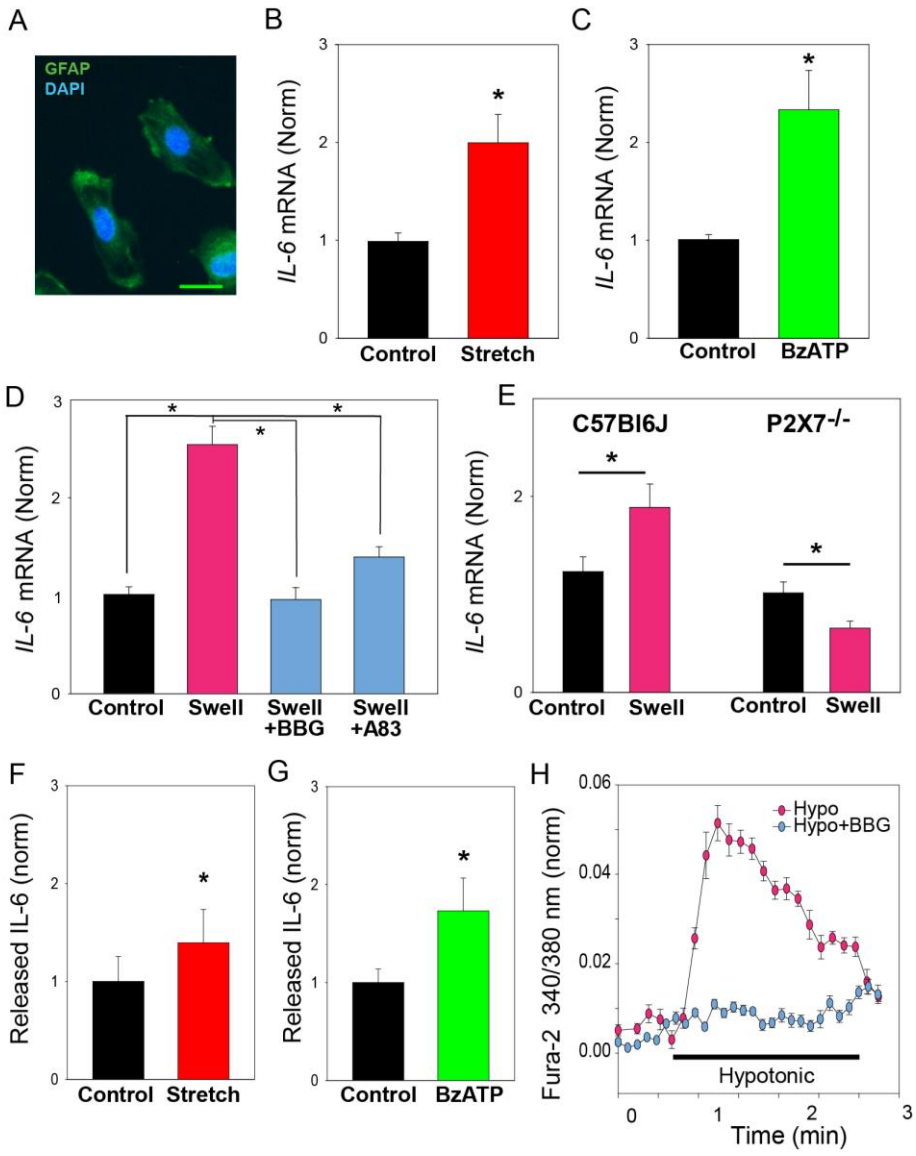

Figure 3.2 IL-6 response in astrocytes

A. Cultured rat optic nerve head astrocytes stained for GFAP (green) and DAPI (blue). Bar=20 μm.
B. Increased expression of *IL-6* mRNA in stretched astrocytes; cells were subject to a 5% equilateral strain at 0.3 Hz for 4 hrs, followed by a 20 hr break before extraction of RNA. N=8-9, *p=0.011.
C. *IL-6* expression was increased in astrocytes exposed to 50 μM BzATP for 4 hrs. N=5, *p=0.008.

D. Expression of *IL-6* was also increased in cells exposed to moderate swelling induced by 30% hypotonicity for 4 hrs. However, this rise in expression was inhibited by P2X7 receptor antagonists BBG (50 μM) or A839977 (A83; 10 μM). Cells were pretreated with antagonists in isotonic solution for 1 hr. before swelling. N=4 * $p<0.001$ Swell vs. Control, *$p<0.001$ Swell vs. swell+BBG, *$p<0.001$ Swell vs. swell+A839977.
E. Cell swelling in 30% hypotonic solution induced rise in *IL-6* mRNA was observed in optic nerve head astrocytes from C57Bl6J mice (N=6, * $p=0.006$), but swelling in astrocytes isolated from $P2X7^{-/-}$ mice actually reduced *IL-6* expression ($p=0.043$, N=6).
F. The concentration of IL-6 in the bath surrounding astrocytes was higher after exposing cells to stretch (* $p=0.036$, N=7).
G. Levels of IL-6 in the bath were also increased after exposure of astrocytes to 50 μM BzATP for 30 min (* $p=0.011$, N=6, paired t-test for F and G).
H. Swelling of astrocytes by hypotonic solution rapidly raised intracellular calcium, as indicated by the ratio of light excited at 340 nm vs 380 nm in cells loaded with indicator Fura-2. In the presence of 100μM BBG, no rise in cell calcium was observed. Symbols represent mean ±SEM, N=16.

Chapter 4 :

Discussion and Future Directions

The signaling pathways linking mechanical strain to inflammation play an important role in the cellular response to stress. In glaucoma, which is the second most common cause of blindness worldwide (Resnikoff et al., 2004), IOP elevation is one of the most common risk factors (Casson et al., 2012). IOP elevation causes mechanical strain with forces particularly focused on the optic nerve head (Bellezza et al., 2003; Burgoyne, 2011; Sigal and Ethier, 2009), where astrocytes reside and are affected by strain (Hernandez et al., 2008). Several studies have shown that IOP elevation in glaucoma models leads to morphological and structural changes to the ONH (Burgoyne, 2011; Burgoyne et al., 1995; Downs, 2015; Yang et al., 2009), along with signs of inflammation including upregulation of TNFα and activation of the complement system (Plantinga et al., 2013). However, the pathological changes in glaucoma and several other chronic inflammatory disorders are not well understood. In glaucoma, the pathological changes continue for years, eventually leading to neuronal death and blindness. The results of this study suggest a novel explanation to link mechanical strain with inflammatory signaling.

Understanding how mechanical strain in the optic nerve head is translated to pathological changes in retinal ganglion cells is a major challenge in glaucoma

research. The goal of this thesis was to identify a pathway for inflammasome priming and IL-6 in response to mechanical strain in the context of sterile inflammation. A better understanding of the cellular and molecular events involved in the process could lead to the development of more effective treatment options for glaucoma patients. Moreover, these findings could potentially be relevant to responses to mechanical in other tissue compartments including dentally-related structures.

The work presented in this thesis supports a critical role for purinergic signaling activated by mechanical strain in the inflammation accompanying glaucoma. We presented evidence that pro-IL-1β and IL-6 mRNA and protein are significantly upregulated in a non-ischemic glaucoma model with IOP elevation. In addition, this work demonstrated that mechanical strain leads to ATP release from pannexin hemichannels that autostimulate the P2X7 receptor, and the P2X7 receptor was found to be necessary and sufficient to upregulate *IL-1β* and *IL-6* expression. We also found that swelling astrocytes activated the transcription factor NFκB, which is known to upregulate expression of the genes encoding IL-6 and IL-1β (Cogswell et al., 1994; Korcok et al., 2004; Rego et al., 2011; Yu et al., 2009).

The function and the regulation of cytokines are complex. IL-1β is a pro-inflammatory cytokine and contributes to signaling pathways involved in cell death (Dinarello, 2002). IL-1β also contributes to retinal ganglion cell toxicity in

an ischemia model (Yoneda et al., 2001). IL-6 is traditionally described as a proinflammatory cytokine, but it can also be protective to neuronal tissue (Penkowa et al., 2003; Spooren et al., 2011). The presence of both neurotoxic and neuroprotective effects following cytokine responses by the P2X7 receptor stresses the complexity of the signaling system and emphasized the need for caution when interpreting ultimate outcomes of receptor stimulation. For example, ocular hypertension studies showed that the rise in IL-6 expression is transient, whereas IL-1β expression increases with sustained IOP elevation, suggesting that the IL-1β/IL-6 ratio influences RGC health in chronic glaucoma (Chidlow et al., 2012). Therefore, evaluating the effect of IL-1β and IL-6 on the health of RGC at different time points and at different concentrations is needed to properly understand their role in diseases.

Although the work reported in chapters 2 and 3 investigated the role of P2X7 receptor in priming IL-1β and IL-6 in parallel, both cytokines can produce a wide range of signaling that can positively or negatively affect the other. IL-1β mainly binds to the IL-1 receptor, which can activate NFκB, c-Jun N-terminal kinases (JNK) and MAPK pathways, resulting in changes in genes including IL-6, COX-2, IL-8 and MKP-1(Arulkumaran et al., 2011; Dinarello, 2002; Weber et al., 2010). In fact, IL-1β upregulates IL-6 in cultured cortical neurons and astrocytes (Benveniste et al., 1990; Ringheim et al., 1995; Tsakiri et al., 2008). IL-6 bound to its receptor can interact with Glycoprotein 130 (gp130), resulting in activation of the JAK/STAT signal transduction pathway and regulation of gene expression

(Ivashkiv and Hu, 2003; Leonard and O'Shea, 1998). It is thus possible that IL-1β and IL-6 can modulate the expression of each other after stretch; further investigation of their interactions in response to mechanical strain is needed. IL-1 receptor antagonists, IL-1β knockout mice, and IL-1β antibody can be tested to determine whether the release of IL-1β modulates IL-6. In addition, IL-6 knockout mice, which are commercially available, can be tested to identify the role of IL-6 in regulating inflammasome priming.

Glaucoma model:

Understanding the mechanisms that underlie glaucomatous changes in the optic nerve is essential for developing a treatment for glaucoma. This involves identifying how elevated IOP leads to axonal injury and retinal ganglion cell death. Because the ONH is a likely site of axonal injury (Burgoyne et al., 2005; Downs et al., 2008), an ideal animal model that separates the effect of cell death from the effect of elevated IOP is needed. The CEI model used here provides a high degree of control over IOP elevation over an extended period of time without major damage to the retina or the optic nerve. Although a small but significant reduction in ganglion cell activity occurred using a variant where IOP was elevated to 60mm Hg for 8 hr (Morrison et al., 2016), the loss of permanent damage after only 4 hr elevation (Crowston et al., 2015) supports our conclusion that there is little damage in our hands. As such, we feel this allow the effects of elevated IOP and cell death to be adequately separated. Our findings are supported by use of a genetically induced outflow obstruction model (Tg-

Myoc^{Y437H} mice), in addition to the CEI protocol used in two different species. This approach enabled us to explore specific mechanisms while also demonstrating that the response is not restricted to a single species. This is especially important, given the considerable differences in the P2X7 receptor sequence in mice and rats (Donnelly-Roberts et al., 2009a).

The role of purinergic signaling:

In Chapter 2 we showed the involvement of extracellular ATP in IL-1β priming, based on the ability of apyrase, which hydrolyzes ATP, to block gene upregulation. We think ATP release is unlikely to be due to cell lysis, since previous work in our lab confirmed the lack of cell death with swell and stretch using Lactose dehydrogenase (LDH) cytotoxicity assay (Beckel et al., 2014). As this reaction showed no sign of cellular rupture and release of the cytoplasmic enzyme into the bath, the mechanosensitive release of ATP was deemed to be physiological.

To confirm a role of pannexin hemichannels in the priming of cytokines that followed mechanosensitive activation of astrocytes, we used three different pannexin antagonists to enhance specificity. Carbenoxolone partially blocked the release of ATP with a consistent reduction of *IL-1β* mRNA after the swell. While the 10μM concentration produced only a partial block, specificity over other channels is higher at this concentration (Beckel et al., 2014; Xia et al., 2012b). Therefore, we also tested probenecid and ^{10}Panx1 peptide. Probenecid is known

to act on an organic anion transporter, and also has been shown to affect ATP release (van Aubel et al., 2002). Several pharmacological results suggest that it inhibits the nonvesicular release of ATP, with pannexin1 being a prominent target of the molecule (Dahl et al., 2013; Qiu et al., 2011). In addition, probenecid at 1mM inhibits currents mediated by pannexin1 channels but not connexins (Silverman et al., 2008). ^{10}Panx1 is a mimetic inhibitory peptide that blocks the first extracellular loop of pannexin1 and has been shown to significantly inhibit channel currents, dye uptake and ATP released by pannexin1 in multiple cell types (Pelegrin and Surprenant, 2007; Seminario-Vidal et al., 2011). However, this peptide also shows nonspecific targets such NMDA receptor and Cx46 hemichannels (Lohman and Isakson, 2014). Although none of the individual drugs are specific for pannexins, the inhibition we observed with all three compounds strongly implicates pannexins as the conduit for ATP release.

The Pannexin hemichannel family has three members designated pannexin 1, 2, and 3. Pannexin 2 can form functional homomeric pores at high voltage in Xenopus oocytes (Penuela et al., 2013). The ability of pannexin 3 to form a homomeric functional single membrane pore is still controversial and electrophysiological evidence has yet to be reported (Penuela et al., 2013). On the other hand, pannexin 1 channels can be activated to form pores by mechanical stimulation, caspase cleavage, cytoplasmic Ca^{2+}, membrane depolarization, extracellular ATP and K^+ (Bao et al., 2004; Silverman et al., 2009). In contrast to the situation with pannexin 2 and 3, the ability of pannexin 1

to act as a pathway for ATP release and enable communication with the extracellular environment is well established (Dahl, 2015; Pelegrin and Surprenant, 2006). Although we did not directly attempt to identify the specific member of the pannexin family involved in the phenomena described in this thesis, our data are consistent with a role of Pannexin 1 in ATP release after mechanical strain.

The reduction in IL-1β we found with pannexin 1 inhibitors is consistent with the altered ATP release from these cells with the inhibitors (Beckel et al., 2014), and the reduction of ATP in cortical astrocytes from pannexin 1 knockout mice (Suadicani et al., 2012). Determining whether the remaining ATP release in astrocytes in this study reflects a contribution from pannexin 2 or other channels will require more experiments. Previous attempts to silence pannexin 1 with siRNA led to the upregulation of other pannexins and connexin proteins in the Mitchell lab, so this approach was avoided. In addition, we attempted to investigate this issue in conditional GFAP-Cre: $Panx1^{f/f}$ mice but encountered technical difficulties. Additional methods such as using CRISPR/Cas 9 to knockout pannexin 1 could be used to confirm the mechanosensitive role of this channel specifically.

Evidence linking the P2X7 receptor with IL-6 and IL-1β priming comes from *in vivo* and *in vitro* assays of mRNA and protein. The small *in vitro* upregulation of IL-1β in astrocytes from $P2X7^{-/-}$ mice (Figure 2.9) may reflect the involvement of

other pathways; however, the presence of P2X7 splice variants provides an alternate explanation (Valentin et al., 2009). While the use of agonists, antagonists and knockout mice together imply the P2X7 receptor makes a substantial contribution to the mechanosensitive IL-1β and IL-6 responses, a contribution from other P2 receptors cannot be ruled out in the present study. However, the role of different splice variants could be investigated by developing a P2X7 receptor knock out mice utilizing CRISPR/Cas 9 to target multiple exons.

Contribution of astrocytes:

The involvement of the astrocytes in IL-6 upregulation and release and IL-1β priming was outlined in the experiments in Chapter 2 and 3. The immunostaining (Figure 2.5.C) does not exclude the possibility of the involvement of other cells, such as Muller glial cells, neurons and microglia. However, astrocytes are located at the optic nerve head, where the mechanical strain produced by IOP elevation is focused and showed morphological changes in patients with glaucoma (Burgoyne, 2011; Hernandez, 2000; Lye-Barthel et al., 2013; Sigal and Ethier, 2009). Furthermore, astrocytes are known to express mechanosensitive channels (Choi et al., 2015) and contribute to the inflammatory response in glaucomatous eyes (Johnson and Morrison, 2009). As such, the identification of the P2X7 receptor linking mechanical strain to inflammasome priming in optic nerve head astrocytes is particularly relevant.

In addition, astrocytes are in contact with neurons and provide both metabolic and structural support to neurons as part of normal physiology (Plantinga, Joosten et al. 2013). They can undergo morphological changes in response to mechanical stress, including redistribution of cytoskeletal proteins (Ho et al., 2014). Evaluating these changes in optic nerve head astrocytes can confirm their role in the pathological process in glaucoma. This can be achieved by: (1) measuring the length of filamentous actin (F-actin) after staining to determine whether or not there are changes in the cytoskeleton and (2) comparing the ratio of F-actin to the global actin (G-actin) on immunoblots of cell lysates.

To further confirm the role of the astrocyte P2X7 receptor in IL-1β changes, a cell-specific knockout is needed. Developing P2X7 receptor floxed mice then breeding them with the GFAP-Cre mice, to produce a conditional P2X7 receptor knockout in astrocytes will allow an extensive and accurate measurement of the role of P2X7 receptor astrocytes in glaucoma.

Microglial cells are present in the retina, where they are a potent source of IL-1β and have a crucial role in mediating inflammation. Therefore, in future studies it will be important to determine if the P2X7 receptor contributes to the inflammasome response in retinal microglia and whether the response is mechanosensitive. To directly address these possibilities, Cx3cr1CreER mice can be bred with floxed P2X7 receptor knock-out mice to generate microglial specific knockouts. Additionally, *in vitro* stretching experiments using retinal

microglial cells can be conducted to identify the pathways linking mechanical stretch to IL-6 and inflammasome priming and activation in this important cell type.

Gene expression:

Elevated IOP and mechanical strain differentially affected the expression of numerous genes. The increase in *IL-1β* and *IL-6* in response to mechanical strain was particularly consistent in contrast to the somewhat inconsistent enhanced expression observed for *NLRP3, CASP1,* ASC and *IL-18* The relative variability in gene expression may have been time-dependent, as the expression of most genes was substantially larger in the mouse retina 22 hrs after IOP elevation was returned to baseline. Interestingly, the magnitude of upregulation of these genes reflects the nature of their function. For example, when IL-1β is released it binds to the IL-1 receptor in a 1:1 ratio. Therefore, a significant upregulation of IL-1β production is needed to induce a vigorous inflammatory reaction. On the other hand, NLRP3 and caspase 1 are catalysts for the production of the mature cytokines such that relatively small increase in their production has a dramatic impact on the induction of an inflammatory response. Given that *IL-1β, IL-18, NLRP3, CASP1,* and *ASC* are all regulated by different combinations of transcription factors, the diverse responses to swelling and stretching were not unexpected. In addition, CASP1 and IL-18 are constitutively expressed in monocytes and epithelial cells (Dinarello, 2007; Thornberry et al., 1992), making a moderate increase in expression proportionally less impactful.

NLRP3 mRNA was upregulated *in vivo* after IOP elevation and, to a lesser extent, after BzATP injection. *In vitro* BzATP treatment also upregulated the expression of *NLRP3*. However, P2X7 receptor and pannexin 1 antagonists, as well as apyrase, were not able to block this upregulation. This indicates the presence of additional mechanisms, in addition to P2X7 receptor, and confirms the complexity of the priming regulation of the NLRP3 (Juliana et al., 2012; Schroder et al., 2012). Additional studies including a NLRP3-luciferase reporter assay and investigating additional factors, such as calcium signaling, would provide more information about NLRP3 priming.

Calcium can be involved in the signaling transduction that leads to transcriptional upregulation of IL-6 and the inflammasome genes. This upregulation could be relevant to the ability of calcium to activate the transcription factor NFκB (Lilienbaum and Israel, 2003). The P2X7 receptor is known to increase intracellular calcium in both astrocytes and retinal ganglion cells (Beckel et al., 2014; Xia et al., 2012b). In our work, swelling of astrocytes by hypotonic solution rapidly raised intracellular calcium, but in the presence of BBG no rise in cell calcium or cytokine increase was observed. Swelling and stretch experiments in calcium free solutions could shed light on the role of calcium influx through P2X7 receptor in inflammasome priming.

Sensing the stress:

Conversion ofmechanical stimuli into biological responses is involved in activity number of physiologic processes including blood flow, pain, touch, hearing and mastication (Chalfie, 2009). While our results showed a clear role for pannexin hemichannels in connecting mechanical strain to ATP release, they do not identify the first sensor of mechanical stress. Recent findings suggest that Piezo cation channels are likely sensors of mechanical strain in the cell membrane (Coste et al., 2010). The Piezo family consists of Piezo1 and 2 (also known as Fam38A and Fam38B, respectively), that are localized to the optic nerve head astrocytes (Choi et al., 2015). Our work focused on the signaling pathways downstream of these channels. Thus future studies investigating their role in priming the inflammasome might explain some of the variability in expression of certain genes in response to mechanical stretch.

In this work, we specifically focused on the role of the P2X7 receptor on the priming of IL-1β*,* as this was less well understood relative to receptor's role in activation of the inflammasome. Future studies focused on the contributions of the P2X7 receptor to inflammasome activation following its role in priming will clarify how the inflammasome with the double signals impacts the inflammatory state of the retina. Available assays can detect the activation of caspase 1 based on detection of cleavage of substrate such as YVAD-AFC by the active enzyme, which can be quantified using a fluorometer. Also, evaluation of the signaling transduction of P2X7 receptor activated by BzATP/mechanical strain may identify

a possible mechanism of regulating the inflammasome, and thus of treating glaucoma.

Finally, the findings of this thesis outlined a novel pathway, in which mechanical strain leads to extracellular ATP release through pannexin 1 hemichannels, which autostimulates the P2X7 receptors involved in the priming of the NLRP3 inflammasome and IL-6 mRNA and protein upregulation. These findings have a considerable relevance to our understanding of how mechanical strain leads to chronic inflammation throughout the body. In the dental field, TMJ disorders and orthodontic induced apical root resorption are inflammatory disorders in sterile conditions linked to mechanical strain, and thus are relevant to this work. In addition, occlusal trauma resulting from excessive forces being applied on the teeth can accelerate the progression of the bone loss in the presence of active periodontitis (Lindhe and Svanberg, 1974). This could be due to the inflammatory signals affecting the periodontal ligament in response to mechanical stimulation. A recent study conducted in human periodontal ligament cells has illustrated a contribution of Pannexin 1, ATP and P2X7 receptor in IL-1β production in response to compressive loading (Kanjanamekanant et al., 2014). These findings are consistent with our results and indicate a relevant pathway in the dental structures. Utilizing the knowledge and tools that I have learned during this work I hope to expand these findings to connect mechanical strain to inflammatory signaling in dental fields in the future.

Chapter 5 : Appendix

Effects of Lidocaine and Articaine on Neuronal Survival and Recovery

Farraj Albalawi BDS, [1,2], Jason C Lim BS[1], Kyle V DiRenzo[1], Elliot V. Hersh DMD, MS, PhD[3] and Claire H. Mitchell PhD[1,4,5]

Departments of [1]Anatomy and Cell Biology, [2]Orthodontics and [3]Oral & Maxillofacial Surgery/Pharmacology. University of Pennsylvania School of Dental Medicine, Philadelphia, PA, 19104 Departments of [4]Physiology and [5]Ophthalmology, Perelman School of Medicine, University of Pennsylvania, Philadelphia, PA 19104

As a dentist, I was interested in doing a side project directly related to the dental field. Therefore, I was involved in the work of this chapter in collaboration with Dr. Hersh as part of a project funded by the Rabinowitz award. In this chapter, we compared the SH-SY5Y (neuroblastoma cell line) survival and functional impairment after they were treated with the two most commonly used local dental anesthesia (Lidocaine and Articaine). Even though is chapter may be different from the main work, neuronal death with these drugs may involve pathways regulated by caspases.

This chapter has been accepted for publication in Anesthesia Progress Journal. *2017* June.

Abstract:

The local anesthetics lidocaine and articaine are among the most widely used drugs in the dentist's arsenal, relieving pain by blocking voltage dependent Na^+ channels and thus preventing transmission of the pain signal. Given reports of infrequent but prolonged paresthesias with 4% articaine, we compared their neurotoxicity and functional impairment by screening cultured neural SH-SY5Y cells with formulations used in patients (2% lidocaine + 1:100,000 epinephrine or 4% articaine + 1:100,000 epinephrine), and with pure formulations of the drugs. Voltage-dependent sodium channels Na(v)1.2 and Na(v)1.7 were expressed in SH-SY5Y cells. To test the effects on viability, cells were exposed to drugs for 5 min and, after washing, cells were treated with the ratiometric Live/Dead assay. Articaine had no effect on the survival of SH-SY5Y cells while lidocaine only produced a significant reduction when used as pure powder. To determine reversibility of blockage, wells were exposed to drugs for 5 min, returned for medium for 30 min, and the calcium elevation induced by depolarizing cells with a high potassium solution was measured using calcium indicator Fura-2. High potassium raised calcium in control SH-SY5Y cells and those treated with articaine, but lidocaine treatment significantly reduced the response. In conclusion, articaine does not damage neural cells more than lidocaine in this *in vitro* model. While this does not question the safety of lidocaine used clinically, it does suggest that articaine is no more neurotoxic, at least in the *in vitro* setting.

Introduction:

The development of safe and effective local anesthetic agents is possibly the most important advance in providing pain control in dental practice (Moore and Hersh, 2010). The agents currently available in dentistry are extremely safe and fulfill most of the characteristics of an ideal local anesthetic. These agents can be administered with minimal tissue irritation or likelihood of inducing allergic reactions. A variety of agents are available that provide rapid onset and adequate duration of surgical anesthesia that is completely reversible, and systemic toxicity is rarely reported; these events invariably being the result of overdoses in young children (Goodson and Moore, 1983; Hersh et al., 1991).

Two percent lidocaine with 1:100,000 epinephrine is the most widely used local anesthetic in the United States,(Moore and Hersh, 2010) while in Canada and several European countries articaine with 1:100,000 epinephrine has supplanted lidocaine as the most frequently employed local anesthetic agent (Haas and Lennon, 1995). 4% articaine with 1:100,000 epinephrine provides more profound infiltration anesthesia than does 2% lidocaine with 1:100,000 epinephrine;(Snoeck, 2012) while it is not as clear if 4% articaine with 1:100,000 epinephrine is superior in anesthetic efficacy compared to 2% lidocaine with 1:100,000 epinephrine with regards to mandibular block anesthesia, a recent meta-analysis revealed the superiority of the former when this injection technique is employed (Brandt et al., 2011). A large prospective safety study of 1325 individuals revealed no difference in systemic or local toxicity between 4%

articaine with 1:100,000 epinephrine and 2% lidocaine with 1:100,000 epinephrine (Malamed et al., 2001). However while relatively rare in occurrence, retrospective studies and case reports have associated the use of 4% articaine with 1:100,000 epinephrine with a higher incidences of paresthesia following mandibular block injections than 2% lidocaine with 1:100,000 epinephrine (Garisto et al., 2010; Haas and Lennon, 1995). An additional study reported that articaine was shown to contribute to more than a 20-fold increase in reported paresthesia compared with all other local anesthetics combined (Hillerup and Jensen, 2006). Nonsurgical cases of paresthesia in dentistry are almost exclusively related to inferior alveolar nerve block injection and appear to affect the lingual nerve more frequently than the inferior alveolar nerve.[4,9] Available data indicate that 85%–94% of such cases resolve spontaneously within 8 weeks; however, about two-thirds of those who do not recover quickly may never fully recover (Pogrel, 2007).

This study asked whether articaine was more neurotoxic than lidocaine at levels used clinically, and whether the channel block was more sustained with articaine than lidocaine. In contrast to our predictions, we found lidocaine both more toxic and with a greater residual block to cellular responsiveness.

Methods:

Drugs: Clinically relevant formulations of lidocaine (2% Xylocaine, Dentsply Pharmaceutical) and articaine (4% Septocaine, Septadont) were used (both with 1:100,000 epinephrine). Drugs were delivered from the cartridges at full strength or diluted 1:3 and 1:9. with DMEM/Ham F12 medium (1:1). According to the accompanying literature, each mL of the solution in the Xylocaine cartridge contained lidocaine hydrochloride (20mg), epinephrine bitartrate (as base, 0.01mg), NaCl (6.5mg), potassium metabisulfite (1.2mg), Edetate Disodium (EDTA) (0.25mg). Each mL of the solution in the Septocaine cartridge contained articaine hydrochloride (40mg), epinephrine tartrate (0.018mg) corresponding in epinephrine base to (0.01mg), NaCl (1.6mg), sodium metabisulfite (0.5mg). Additional experiments were performed with pure powdered lidocaine (RBI, #L-102) and articaine (obtained from Septodont Inc.) to test for the effects of these additional constituents, particularly EDTA. Drugs were dissolved in DMEM/Ham F12 medium and concentrations were chosen so that the maximum levels were approximately the same for drugs in powder and cartridge formulations.

Cell culture: The SH-SY5Y neuroblastoma cell line was used to examine the effects of the two drugs on cell survival. Cells were maintained in DMEM/Ham F12 medium (1:1), 10% fetal bovine serum (FBS), 1% penicillin /streptomycin and 1% amphotericin B (Fungizone®). In some experiments, wells were coated with poly-L-lysine (Peptides International, UKK-0356). Cells were grown for a minimum of 5 days. Initial experiments were performed on differentiated SH-

SY5Y cells induced by reducing FBS to 1%, adding 10 μM retinoic acid 1 and 3 days after plating, and then brain-derived neurotrophic factor (25ng/ml) in a serum-free medium 4-5 days later. While this led to a more neural phenotype and increased expression of sodium channels described below, the reduced cell attachment complicated their use in assays. Although the use of ratiometric assays enabled measurement of viability and calcium levels independent of cell number, experiments reported here were performed on undifferentiated cells to maximize accurate evaluation.

PCR: Confluent plates of SH-SY5Y cells were homogenized in 1 ml TRIzol (Invitrogen Corp.) and total RNA was purified using RNeasy mini kit (Qiagen, Inc. #79254, Gaithersburg, MD). cDNA was synthesized from 500ng of total RNA per reaction using the High Capacity cDNA Reverse Transcription Kit (Applied Biosystems #4368814). qPCR was performed using SYBR Green and the 7300 RealTimePCR system (Invitrogen Corp.) as described (Guha et al., 2013). Primers used were Na(v)1.2: F: TGATGGTGATGTGTTTGTG, R: TCTCTGTCTTGTTATAGGCACTG, 109 base pairs; Na(v)1.7: F:AGACCTCTCTTTCCATGTAGATTAC, R: TGTAACTGCCTTTCTGTATTGTTG, 129 base pairs. Primers were designed from published sequences (Vetter et al., 2012).

LiveDead Assay: The Live/Dead Assay (ThermoFisher #L3224) was used to determine cell viability. Cells grown in 96-well plates were washed and incubated with 10μl ethidium homodimer-1 (EthD-1) and 5 μl calcein–AM in 5 ml medium

for 30 min at 25 °C. A positive control was applied by adding 70% methanol for 5 min. After washing, cells were imaged with a microplate fluorometer (Fluoroskan Ascent; Labsystems, Franklin, MA). Calcein (Live) was excited at 488 nm and emitted at 560 nm to indicate healthy cells with functioning esterases to cleave the AM bond and render the dye fluorescent. EthD-1 was excited at 544nm (em 590nm) to quantify cells with compromised plasma membranes. The ratio of light excited at 488nm to 544nm provides an index of cell viability independent of cell number. For images, cells were exposed to full strength lidocaine or articaine for 5 min, washed with medium, then to 3µl of 1 mM Calcein AM (ThermoFisher Scientific #C31100MP) mixed with 2µl ethidium homodimer (ThermoFisher Scientific #L7013) for 20 min at room temperature before washing then imaged on a Nikon Eclipse E600 (Nikon USA, Melville, NY) at ex460-500 Chroma filter for live cells and ex530-550 Chroma filter for dead cells. Images were captured with a Nikon DS-Fi1 camera and processed with ImageJ software (Schindelin et al., 2015), with parallel modifications performed to all images.

Cytoplasmic Ca^{2+} measurement: Neuronal activity was determined by examining the influx of Ca^{2+} upon depolarization. The Goldman/Hodgkin/Katz equation predicts a shift in membrane potential from -71 mV to -20 mV when cells are exposed to the high-K solution; this is raised above the threshold for activation of the voltage-dependent Na^{+} channels, and thus an action potential is expected. This is predicted to induce an influx of Ca^{2+} through voltage-dependent channels, which was measured with the dye Fura-2. Calcium levels were measured from

SH-SY5Y cells grown in 96-well plates the dye Fura-2 as described (Reigada et al., 2005) Basically, Fura-2 AM (ThermoFisher Scientific, #F1201) was loaded by incubating wells for 30 min with 5 μM Fura-2 AM and 0.02% pluronic acid. After washing, 90 μl of isotonic control solution contain 5 mM KCl and 120 mM NaCl was added and the ratio of light excited at 340/380 nm emitted >510 nm was determined in the microplate fluorometer. A baseline reading was obtained for 5 min, after which a high K^+ solution was injected through the fluorimeter to give a final concentration of 50 mM KCl and 75 mM NaCl.

Statistical analysis: Data are reported as mean ± SEM. Analysis was performed in a masked fashion whenever possible. Statistical analysis on the Live/Dead assay was performed using a Kruskal-Wallis one-way analysis on ranks with Dunn's post-hoc test versus control. Analysis of the calcium response was performed using a Student's t-test. Both sets of analysis were performed using Systat Software Inc. (San Jose, CA). Results with $p<0.05$ were considered significant.

***Results**:*

The SH-SY5Y cells used in this study expressed the voltage-dependent sodium channels Na(v)1.2 and Na(v)1.7, predicted to be targeted by the drugs (Figure 5.1.A). To determine whether lidocaine or articaine were neurotoxic, SH-SY5Y cells were exposed to drugs for 5 min. Each drug was obtained directly from the cartridge used to treat patients and employed at full strength or diluted in cell medium 1:3 or 1:9. After washing, cells were exposed to the Live/Dead assay for 30 min, and the relative levels of green and red fluorescence were quantified (Figure 5.1.B). Neither articaine nor lidocaine had a significant effect on cell viability at any concentration when obtained from the cartridge (Figure 5.1.C), although 2% lidocaine increased the ratio of dead to live cells substantially.

As cells displayed some signs of detachment in preliminary trials, several steps were taken to minimize this effect. The use of ratiometric assays meant that cell survival measures were independent of cell numbers, and undifferentiated cells survived manipulations more robustly, with poly-L-lysine coating the substrate increasing this further. Of note was the presence of 0.7 mM of calcium/magnesium chelator EDTA. While this level of EDTA was less than that used experimentally to detach cells (1-10 mM) there was some concern that the presence of EDTA in the lidocaine but not articaine formulations could influence the outcome. To control for this, the effect of adding 0.7 mM EDTA on

cell adherence was examined directly; there was no increase in cell detachment with EDTA, however.

The cell viability experiments were confirmed with pure lidocaine and articaine from powder to avoid influence from secondary components like EDTA or epinephrine. Concentrations were chosen so that the highest level of lidocaine and articaine from powder equaled the full-strength drug from the cartridge. While there was no effect of purified articaine at any concentration, 74 mM of purified lidocaine significantly increased the percentage of dead cells to 55% (Figure 5.1.D).

Delayed neuronal recovery

Given reports of delayed local anesthetic recovery with articaine, experiments were designed to determine whether treatment with either anesthetic led to a delayed recovery from nerve block by examining the response to depolarization 30 min after treatment with drugs. Specifically, the Ca^{2+} influx to depolarizing cells with high (50 mM) K^+ solution was measured. Raising the level of extracellular K^+ from 5 mM to 50 mM was calculated to raise the membrane potential from -71 mV to -20mV, above the threshold to activation of the voltage-dependent Na(v)1.2 and Na(v)1.7 channels (Catterall et al., 2005). Cellular Ca^{2+} was used as a proxy for membrane potential as the ratiometric output of Ca^{2+}-sensor Fura-2 was very sensitive and provided reading independent of cell number.

Baseline levels of cytoplasmic Ca^{2+} were not affected by exposure to 2% lidocaine or 4% articaine 30 min previously (Figure 5.2.A). However, cells treated with lidocaine displayed a significantly reduced responsiveness to depolarization as compared with controls (Figure 5.2.B), while the effect of articaine was not significant.

Discussion:

In the current study, the use of the ratiometric Live/Dead assay to determine cell viability suggests that articaine was no more likely to kill cultured neuronal SY-SY5Y cells than lidocaine. However, solutions made with pure lidocaine from powder lead to a small but significant increase in neuronal death. In addition, results obtained with the ratiometric Ca^{2+} indicator Fura-2 imply that articaine does not produce a more sustained blockage of neural response *in vitro* than lidocaine. Lidocaine treatment led to a reduced cell responsiveness 30 min after drugs were washed off. While these findings are the opposite of what was predicted based upon the proposed enhancement of paresthesia by articaine in the clinical setting,(Haas and Lennon, 1995) data from the two different assays in the present study support the conclusion that articaine does not directly lead to neuronal damage *in vitro*. The findings agree with a report suggesting lidocaine had a lower LD_{50} than articaine (Malet et al., 2015). This published data was based on the production of glycolytic production of NADPH, and is thus a simplistic measure of total metabolic activity. The combined use of the Live/Dead and Fura-2 assays in the present study provide a more accurate measure of cell stress that is independent of the number of cells.

While the use of drugs directly from the injection cartridges provides relevance to the clinical condition, we felt it was important to verify the results using the purified forms of the drugs. This was particularly true of the lidocaine, as inclusion of EDTA may have interacted with cells and complicated interpretation.

While there was a trend towards decreased cell viability in experiments where lidocaine from the cartridge was used at full strength, cell death was only significant with the powder form. Given that lidocaine is considered a very safe drug clinically, it is likely that this level of significance in the powder form of the drug does not translate to the clinic.

While both lidocaine and articaine are thought to produce a reversible block of the voltage-dependent Na^+ channels associated with the transmission of dental pain, several reports link articaine with sustained paresthesia (Haas and Lennon, 1995; Pedlar, 2003). However, the current study found that neural responsiveness was reduced in SH-SY5Y cells 30 min after cells were exposed to lidocaine, but not articaine. Of course, the measure of cellular responsiveness used here, based on Ca^{2+} rise, provided an indirect measure of Na^+ channel activity, and may reflect effects of lidocaine downstream from the Na^+ channel. The similar baseline levels in cells pretreated with lidocaine, articaine and control solution suggests there is not an overall change in Ca^{2+} regulation in the cells. As exposure to high levels of KCl is expected to depolarize the cells similarly, the reduced rise in intracellular Ca^{2+} is predicted to reflect a difference in the activation of the voltage-dependent Na^+ channels needed to depolarize the cells into the range of Ca^{2+} channel activation. While precise site of action cannot be determined without direct inspection of the ionic currents, the parallel findings with the two assays imply articaine is not impacting the cells.

Although the results of the current study suggest articaine is no more disruptive than lidocaine to neural cells, there are several other mechanisms that could underlie differential rates of paresthesia reported in the literature. For example, the low overall occurrence suggests that genetic polymorphisms in the ionic channels may contribute, as polymorphisms in Na(v)1.7 result in a range of pain phenotypes (Drenth and Waxman, 2007). A cell culture model such as the one employed in these experiments does not account for rare genetic differences in sodium channel sensitivity to potential neurotoxic agents. The actual magnitude of the problem with articaine is also somewhat unclear, because unfortunately clinicians typically only file FDA Medwatch reports when there is a fear of litigation. In addition to genetic polymorphisms, local anesthetic neurotoxicity may also be concentration related. As neither articaine in the pure form, nor articaine from the clinical cartridge led to issues in the present study, it is unlikely that additives increase neurotoxicity.

In summary, articaine did not produce a prolonged block of neuronal responsiveness, or an increased toxicity, as compared to lidocaine in SH-SY5Y cells. The use of ratiometric assays to determine viability and Ca^{2+} levels strengthen the conclusions. It should be stressed that numerous studies have found lidocaine to be remarkably safe in a clinical setting (Moore and Hersh, 2010). The findings of the present refer specifically to SH-SY5Y cells in an *in vitro* setting and should not be taken to imply there is any additional concern with the use of lidocaine in patients. The corollary that articaine does not produce a

prolonged loss of responsiveness or cell death as compared to lidocaine under these reductionist conditions, is perhaps the most relevant conclusion.

Portions of this work were previously presented in abstract form.[19]

Acknowledgements

This work was supported by a grant from the Rabinowitz Foundation to Drs. Mitchell and Hersh. Dr. Albalawi is supported by King Saud bin Abdulaziz University for Health Sciences.

Disclosures

EVH representing the Trustees of the University of Pennsylvania received research grants from Septodont (the maker of articaine plus 1:100,000 and 1:200,000 epinephrine) for research he performed on the clinical development of articaine formulations between 2003 -2005. He has also received funding from Septodont for research performed on phentolamine mesylate (Oraverse®) in pediatric dental patients from 2011 – 2014.

Figures

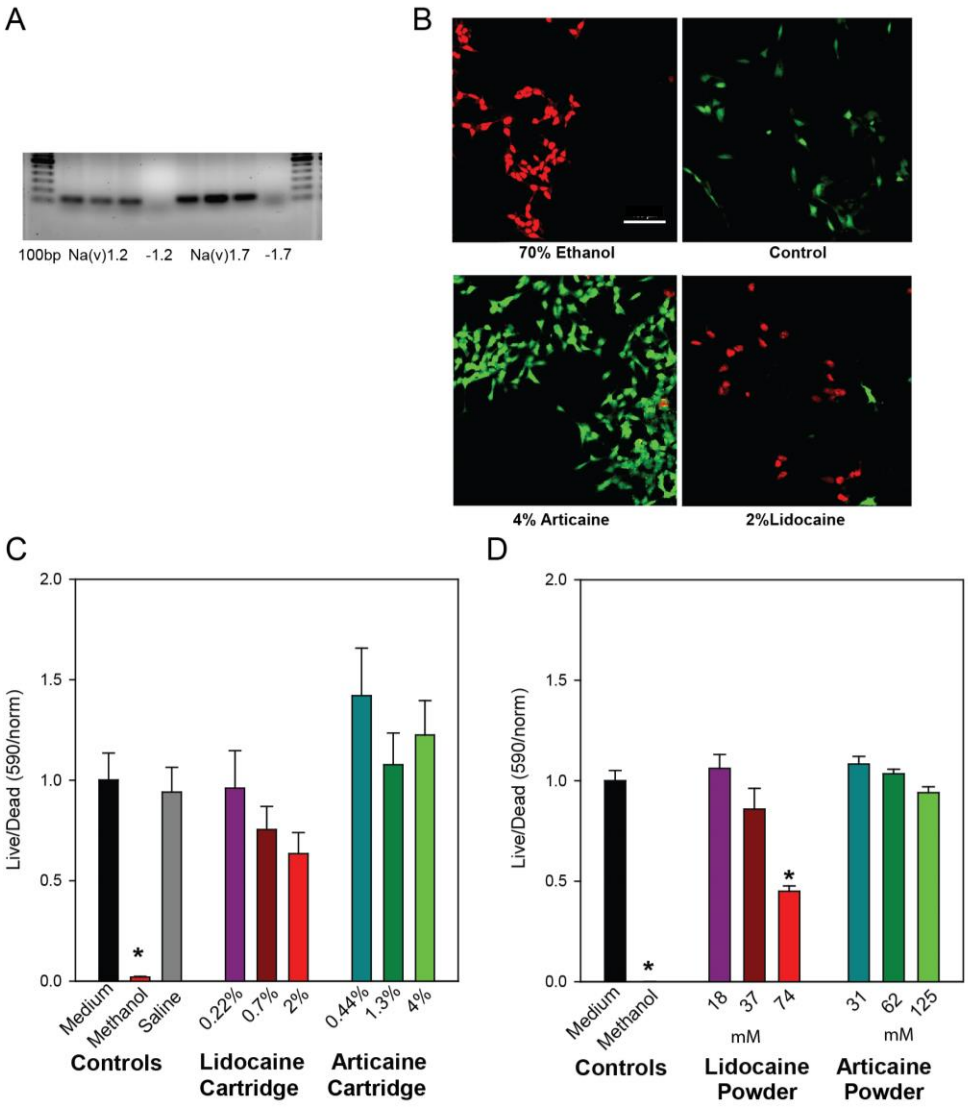

Figure 5.1 Effects of lidocaine and articaine on viability of SH-SY5Y cells

A. Expression of Na(V) in SH-SY5Y cells. PCR gel showing cells expressed mRNA for both Na(V)1.2 and Na(V)1.7. Gels show bands of expected size from three cell preparations. “-1.2” and “-1.7” indicate lanes where reverse transcriptase was omitted from the mix for Na(V)1.2 and Na(V)1.7, respectively. Bars are 100 base pairs.

B. Example of images of SH-SY5Y cells loaded with the Live/Dead assay in response to various conditions; Cells treated for 5 min with 4% articaine, or 2% lidocaine (both from the cartridge), washed, then loaded with the Live/Dead dye. Positive control of cells treated with 70% ethanol are shown on the top left, while untreated cells are shown on the right. Green – calcein indicating healthy cells, Red - ethidium homodimer indicating compromised cells. Bar = 100 μM.
C. Quantification of Live/Dead levels from SH-SY5Y cells treated with lidocaine + 1:100000 epinephrine or articaine + 1:100000 epinephrine from the cartridges used clinically. The reduced viability observed using lidocaine at full strength was not significant (Kruskal-Wallis one-way analysis on ranks with Dunn's post-hoc test). Articaine did not lead to cell death at any strength. Numbers along the abscissa axis indicate the % of drug, with 2% lidocaine and 4% articaine the full strength from the cartridge. Numbers along the ordinate represent the ratio of light excited at 488 nm vs 544 nm, normalized to the mean control for each set. * $p<0.001$ methanol vs. saline; n=10.
D. Quantification of the Live/Dead levels from SH-SY5Y cells treated with pure Lidocaine or Articaine. Lidocaine increased the number of dead cells when used in pure powdered form at the highest concentration, while pure articaine did not alter cell survival. Numbers along the abscissa indicate the concentration in mM, with the highest levels of both drugs equal to the maximum level with the cartridge. Numbers along the ordinate represent the Live/Dead ratio normalized as in C. * $p<0.001$ (methanol and 74 mM lidocaine), n=18.

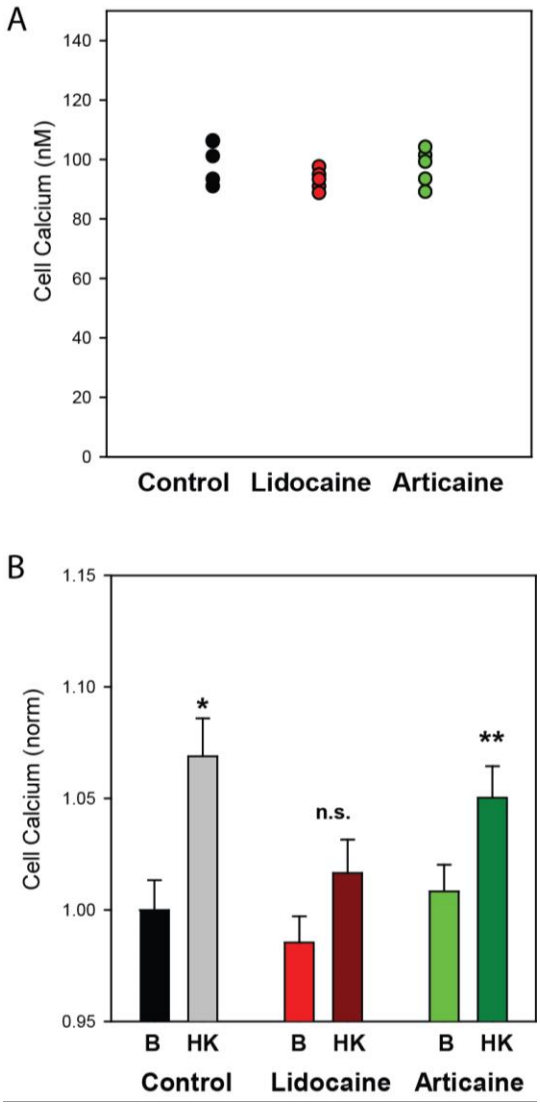

Figure 5.2 Neuronal responsiveness impaired by previous lidocaine treatment.

A. Typical baseline cytoplasmic Ca2+ levels in SH-SY5Y cells.

B. Mean levels of Ca2+ under baseline conditions (B, 5 mM K+) and after exposure to 50 mM K+ (HK) in cells exposed to 2% lidocaine, 4% articaine or control solution 30 min before measurements were made. Baseline Ca2+ levels show no significant difference between the three treatment groups. While depolarization with the high K+ solution significantly raised cellular Ca2+ levels in the control cells (* p=0.004) and those previously exposed to articaine (**p=0.031), the response in cells previously exposed to 2% lidocaine was not significant, Student's t-test, n=15.

The P2X7 receptor links mechanical strain to cytokine IL-6 upregulation and release in neurons and astrocytes

Wennan Lu[1], **Farraj Albalawi**[1,2] Jonathan M. Beckel[1,5], Jason C. Lim[1], Alan M. Laties[3], Claire H. Mitchell[1,3,4]

Author affiliation: Departments of [1]Anatomy and Cell Biology, [2]Orthodontics, [3]Ophthalmology and [4]Physiology, University of Pennsylvania, Philadelphia, PA 19104; [5]Department of Pharmacology and Chemical Biology, University of Pittsburgh, PA 15261

This is the published paper referred to in Chapter 3. Supplemental figures from the publication are included here.

Journal of Neurochemistry

JOURNAL OF NEUROCHEMISTRY | 2017 | 141 | 436–448 doi: 10.1111/jnc.13998

ORIGINAL ARTICLE

The P2X7 receptor links mechanical strain to cytokine IL-6 up-regulation and release in neurons and astrocytes

Wennan Lu,* Farraj Albalawi,*,† Jonathan M. Beckel,*,‡ Jason C. Lim,* Alan M. Laties§ and Claire H. Mitchell*,§,¶

*Department of Anatomy and Cell Biology, University of Pennsylvania, Philadelphia, Pennsylvania, USA

†Department of Orthodontics, University of Pennsylvania, Philadelphia, Pennsylvania, USA

‡Department of Pharmacology and Chemical Biology, University of Pittsburgh, Pennsylvania, USA

§Department of Ophthalmology, University of Pennsylvania, Philadelphia, Pennsylvania, USA

¶Department of Physiology, University of Pennsylvania, Philadelphia, Pennsylvania, USA

Abstract

Mechanical strain in neural tissues can lead to the up-regulation and release of multiple cytokines including interleukin 6 (IL-6). In the retina, the mechanosensitive release of ATP can autostimulate P2X7 receptors on both retinal ganglion cell neurons and optic nerve head astrocytes. Here, we asked whether the purinergic signaling contributed to the IL-6 response to increased intraocular pressure (IOP) *in vivo*, and stretch or swelling *in vitro*. Rat and mouse eyes were exposed to non-ischemic elevations in IOP to 50–60 mmHg for 4 h. A PCR array was used to screen cytokine changes, with quantitative (q)PCR used to confirm mRNA elevations and immunoblots used for protein levels. P2X7 antagonist Brilliant Blue G (BBG) and agonist (4-benzoyl-benzoyl)-ATP (BzATP) were injected intravitreally. ELISA was used to quantify IL-6 release from optic nerve head astrocytes or retinal ganglion cells. Receptor identity was confirmed pharmacologically and in P2X7$^{-/-}$ mice, acute elevation of IOP altered retinal expression of multiple cytokine genes. Elevation of *IL-6* was greatest, with expression of *IL1rn*, *IL24*, *Tnf*, *Csf1*, and *Lif* also increased more than twofold, while expression of *Tnfsf11*, *Gdf9*, and *Tnfsf4* were reduced. qPCR confirmed the rise in *IL-6* and extracellular ATP marker *ENTPD1,* but not pro-apoptotic genes. Intravitreal injection of P2X7 receptor antagonist BBG prevented the pressure-dependent rise in *IL-6* mRNA and protein in the rat retina, while injection of P2X7 receptor agonist BzATP was sufficient to elevate *IL-6* expression. IOP elevation increased *IL-6* in wild-type but not P2X7R knockout mice. Application of mechanical strain to isolated optic nerve head astrocytes increased *IL-6* levels. This response was mimicked by agonist BzATP, but blocked by antagonists BBG and A839977. Stretch or BzATP led to IL-6 release from both astrocytes and isolated retinal ganglion cells. The mechanosensitive up-regulation and release of cytokine IL-6 from the retina involves the P2X7 receptor, with both astrocytes and neurons contributing to the response.

Keywords: astrocytes, cytokines, IOP, mechanical strain, P2X7, retina.

J. Neurochem. (2017) **141**, 436–448.

Received August 5, 2016; revised manuscript received January 11, 2017; accepted February 9, 2017.

Address correspondence and reprint requests to Dr Claire H. Mitchell, Department of Anatomy and Cell Biology, University of Pennsylvania, 240 S. 40th St, Philadelphia, PA 19104-6030, USA. E-mail: chm@upenn.edu

Abbreviations used: ATP, adenosine triphosphate; BBG, Coomassie Brilliant Blue G; BzATP, (4-benzoyl-benzoyl)-ATP; ELISA, enzyme-linked immunosorbent assay; FBS, fetal bovine serum; GFAP, glial fibrillary acidic protein; HEPES, 4-(2-hydroxyethyl)-1-piperazineethanesulfonic acid; HP1, hypoxanthine phosphoribosyltransferase 1; HRP, horseradish peroxidase; IL-1β, interleukin 1 beta; IL-6, interleukin 6; IOP, intraocular pressure; NFκB, nuclear factor kappa-light-chain-enhancer of activated B cells; NTPDase1, ectonucleoside triphosphate diphosphohydrolase-1; PBS, phosphate-buffered saline; qPCR, quantitative PCR; RGC, retinal ganglion cell; RIPA, radioimmunoprecipitation assay buffer; SDS, sodium dodecyl sulfate polyacrylamide gel electrophoresis; SEM, standard error of the mean; TBI, traumatic brain injury.

Mechanical strain to neurological tissues frequently leads to both inflammatory and protective responses (Corps *et al.* 2015). The cytokine interleukin 6 (IL-6) is of particular relevance as it can mediate pathological or protective actions in neural systems depending on context (Erta *et al.* 2012). IL-6 can lead to neuroinflammation after traumatic brain injury (TBI) and cerebrospinal fluid levels of IL-6 correlate with pathological progression after TBI (Yang *et al.* 2013; Kumar *et al.* 2015). However, IL-6 can also induce neurogenesis and protect neural cells after damage (Penkowa *et al.* 2003; Erta *et al.* 2012). A better understanding of the pathways linking mechanical strain to IL-6 may help determine the mechanism for the shift of IL-6 from detrimental to protective actions.

The purinergic system has been implicated in regulation of IL-6 in several cell types including fibroblasts (Inoue *et al.* 2007), skeletal muscle cells (Bustamante *et al.* 2014), macrophages (Hanley *et al.* 2004), and microglia (Shieh *et al.* 2014). Purinergic signaling is particularly sensitive to mechanical strain, with ATP release accompanying increases in shear stress, stretch, and swelling (Praetorius and Leipziger 2009; Corriden and Insel 2010). In neural tissue, ATP can be released through pannexin hemichannels in response to mechanical strain (Iglesias *et al.* 2009; Xia *et al.* 2012). The release of ATP and stimulation of the P2X7 receptor is closely linked with inflammatory responses in non-neural cell types (Gombault *et al.* 2012), leading to inflammasome activation and IL-1β release (Ferrari *et al.* 2006; Franceschini *et al.* 2015). Of particular relevance is the priming and release of IL-6 in microglial cells in response to stimulation of the P2X7 receptor (Shieh *et al.* 2014).

The retina provides an ideal model with which to examine the relationship between strain, purines, and IL-6 in neural tissue. Mechanical strain is experienced by neurons and glial cells in the retina when the intraocular pressure (IOP) rises during glaucoma (Sigal and Ethier 2009; Downs 2015). Retinal ganglion cells are the most susceptible to neuropathological changes and death in response to elevated IOP, while the focal point for mechanical strain is the optic nerve head, with optic nerve head astrocytes identified as a critical intermediary (Hernandez 2000; Downs *et al.* 2008).

Perturbed purinergic signaling is implicated in response to glaucoma and elevated IOP. For example, human patients with both acute and chronic glaucoma have elevated levels of extracellular ATP in ocular fluids (Zhang *et al.* 2007; Li *et al.* 2011). Primate, rat and mouse models of sustained IOP elevation show elevated extracellular ATP (Lu *et al.* 2015). These models also demonstrated increased expression of the ectoATPase ectonucleoside triphosphate diphosphohydrolase-1 (NTPDase1), previously identified to act as a marker for sustained elevation of extracellular ATP (Lu *et al.* 2007). The pressure-dependent ATP release from retina is inhibited by blockers of pannexin hemichannels and not linked to lactase dehydrogenase, suggesting it is a physiological response (Reigada *et al.* 2008). Both optic nerve head astrocytes (Beckel *et al.* 2014) and retinal ganglion cells (Xia *et al.* 2012) release ATP through pannexin hemichannels when subjected to mechanical strain. This released ATP can autostimulate the P2X7 receptor in both cell types.

Alterations in cytokine IL-6 have also been recognized as an important response to elevated IOP. Levels of IL-6 have been detected in the aqueous humor of patients with chronic glaucoma (Chen *et al.* 1999; Zenkel *et al.* 2010). In the hypertonic saline model of chronic IOP elevation, *IL-6* was the most up-regulated gene in the optic nerve head tissue (Johnson *et al.* 2011), while *IL-6* was also elevated following transient elevation of IOP (Cepurna *et al.* 2008). Several observations suggest IL-6 confers protection to retinal ganglion cells; exposure of isolated ganglion cells to high hydrostatic pressure *in vitro* led to apoptotic death that was attenuated by addition of recombinant IL-6 (Sappington *et al.* 2006), and IL-6 increased both the number and the length of neurites sprouting from isolated retinal ganglion cells (Chidlow *et al.* 2012). While these observations suggest IL-6 has an important role in the response to increased pressure, the signaling mechanisms linking the mechanical strain to the IL-6 response are largely unknown.

Given the link between mechanical strain, ATP release, and P2X7 receptor autostimulation in the retina, the connection between the purinergic signaling and IL-6 activation, and evidence implicating IL-6 in glaucoma, this study was based on the hypothesis that mechanosensitive stimulation of the P2X7 receptor was involved in the IL-6 response to elevated IOP in the retina. To distinguish between responses as a result of elevated IOP and those because of cell death, an *in vivo* model of acute but non-ischemic IOP elevation was employed as studies indicate it is generally not lethal to retinal neurons (Abbott *et al.* 2014; Crowston *et al.* 2015). Isolated optic nerve head astrocytes and retinal ganglion cells were also utilized to investigate the response in more mechanistic detail *in vitro*.

Methods

Animals

All experimental protocols were approved by the Institutional Animal Care and Use Committee of the University of Pennsylvania. The P2X7 knockout ($P2X7^{-/-}$) mice originally generated from Pfizer (B6.129P2-P2rx7tm1Gab/J), along with age-matched 9-month-old C57Bl6J wild-type controls were obtained from Jackson Laboratories (Bar Harbor, ME USA). Sprague-Dawley and Long-Evans rats were obtained from Harlan Laboratories (Fredrick, MD, USA). Mice and rats of both sexes were utilized.

Model of moderate temporally controlled IOP elevation

Acute elevation of IOP experiments were performed using adult Sprague-Dawley rats based on the control elevation of IOP

protocol developed by John Morrison and colleagues (Morrison *et al.* 2010, 2014). Adult rats were given a prior dose of 2 mg/kg meloxicam and then deeply anesthetized with intraperitoneal injection of ketamine (80 mg/kg) and xylazine (10 mg/kg). Proparacaine (1%) was added to the ocular surface and one drop of Tropicamide (1%) was administered into each eye for pupil dilation. Once anesthesia had taken effect, one eye was cannulated with a 27 gauge shielded wing needle (Becton-Dickinson, Franklin Lakes, NJ, USA) inserted into the anterior chamber and connected to a 20 mL syringe filled with sterile phosphate-buffered saline. IOP was increased to 50 mmHg by positioning the syringe at the appropriate height (68 cm H_2O) while the contralateral eye without cannulation served as a normotensive control. During the initial development of the model, IOP was calibrated with a TonoLab tonometer (Colonial Medical Supply, Windham, NH, USA) at the beginning and end of the elevation of the reservoir. As IOP was found to be remarkably consistent both throughout the 4 h of elevation and between animals, it was usually just measured at the end of the 4 h period during experiments to avoid excessive force on the needle tip inside the eye. The retina was carefully observed under an operating microscope to ensure that blood flow through the retinal vessels was maintained. After 4 h IOP elevation, pressure was returned to normal, the needle was removed and 0.3–1% gentamycin ointment or erythromycin (0.5%) was applied to the cornea. Animals were killed 20 h (i.e., 1 day) or 5 days later and the retina, including the optic nerve head material, was dissected.

Experiments were also performed on mice using procedures similar to those used for rat with parallels to those described by Crowston and colleagues (Crowston *et al.* 2015). Mice were given a prior dose of meloxicam and then anesthetized with 1.5% isoflurane. IOP was increased to 50–60 mmHg for 4 h. Mice were killed immediately after the pressure was returned to baseline, or 20 h later. The contralateral eye without cannulation served as a normotensive control.

PCR array

Expression of mRNA for 84 rat interferons, cytokines, and interleukins in the retina was determined using the Rat Common Cytokine RT2 Profiler™ PCR Array (#PARN-021A; SABiosciences Corp., Frederick, MD, USA). Samples were processed according to the manufacturer's protocol. In brief, total RNA was isolated from the control and pressurized retinas using Trizol and RNeasy mini kit (Qiagen, Valencia, CA, USA), and RNA was quantified from optical density and purity determined (Nanodrop; Thermo Scientific, Inc., Wilmington, DE, USA). Total RNA (1 μg) was reverse transcribed using genomic DNA elimination and RT^2 First Strand kit (#C-03; SABiosciences Inc.). Comparison of the relative expression of cytokine genes were performed using the PCR array on an ABI 7300 Real-Time PCR System (Applied Biosystems, Foster City, CA, USA). Lactate dehydrogenase A, Ribosomal genes *L13A*, hypoxanthine phosphoribosyltransferase 1, and beta actin (*Actb*) were used as housekeeping genes and were all stable in retina from eyes with control and elevated IOP. Data were analyzed with the SABiosciences Web-Based PCR Array Data Analysis, where *p* values were calculated based on a Student's *t*-test of the replicate $2^{-\Delta\Delta Ct}$ values for each gene in the control group and experimental groups.

Quantitative PCR

RNA was processed as above. Quantitative PCR (qPCR) was carried out using Power SYBR Green master mix with primer pair sequences shown in Table 1, using the 7300 Real-Time PCR System. Data were analyzed using the delta-delta CT approach, with results expressed as fold change in gene expression in eyes with elevated IOP versus control samples ($2^{-\Delta\Delta Ct}$) using an unpaired *t*-test as described recently (Lu *et al.* 2015).

Intravitreous injection

Intravitreal injections were performed as described (Hu *et al.* 2010) under a dissecting microscope with a micropipette connected to a

Table 1 Primers used for quantitative real time PCR

Gene Name	GenBank Accession	Forward Primer (5' to 3')	Reverse Primer (5' to 3')	Size (bp)
Anxa3	NM_012823	ATCCGGAAAGCAATCAAAGG	CCATGACATGCTCAAAGTGG	174
Bax	NM_017059	TGCCAGCAAACTGGTGCT	ACCCAACCACCCTGGTCTT	129
Cfos	NM_022197	CCTGTGAGCAGTCAGAGAAGG	CGGAAGAGGTGAGGACTGG	194
CyclinD1	NM_171992	CCCACGATTTCATCGAACACT	GATCATCCGCAAACATGCA	77
ATF3	NM_012912	CGAAGACTGGAGCAAAATGATG	CAGGTTAGCAAAATCCTCAAACAC	123
IL-6	NM_012589	CTCCGCAAGAGACTTCCAG	GGTCTGTTGTGGGTGGTATC	119
P2X4R	NM_031594	GCAAGACGTTCTTCCACCCTATACA	TCCATACGCTCACACTGTATAAGCC	137
P2X5R	NM_080780	GACATCCAGGAGACACTTAGCTTCG	CAGCAAGAGCTGAACTGCACAAGTC	230
P2X7R	NM_019256	TAATGCCTCAGCCTAGTGCCTTTGG	CTGCTGCTCCAGAGGGCTCAAGTTC	107
P2Y1R	NM_012800	GCAGCTTCCACTGCCAAAGGCTAAT	ATTGTAAAGCTTCAAGATCTGGCAG	172
P2Y2R	NM_017255	AGCAGCTCAGTCAGGTGTCAGTTCA	TCAGGTGGCGTTGCCTTAGATACGA	214
P2Y4R	NM_031680	ATAGCTGTCTTGATCCAGTGCTCTA	AGCAGCAGGGTTACAATCGATCTCC	215
P2Y6R	NM_057124	TAGGTCCTGGAATAGCACTGCAAAT	AAAGTCTTGGCAAATGGATGGGAAT	171
A1AR	NM_017155	AGCCTGGATGTCTTCCTTGTATGGA	TAGACATAGGGACCTCCTTGAGAAC	121
A3AR	NM_012896	GAGCTTCTCTCATTCAATTCTGTGG	CCTAGGGATCCTTCAACGCAGGTTC	183
GAPDH	NM_017008	CCATGGAGAAGGCTGGGG	CAAAGTTGTCATGGATGACC	195

microsyringe (Drummond Scientific Co., Broomall, PA, USA). The glass pipette filled with drug was passed through the superior nasal region of sclera into the vitreous cavity at a point approximately 1 mm from the limbus. The total volume injected was 5 μL over a 30 s time period. P2X7 receptor antagonist Brilliant Blue G (BBG, 0.8%) was dissolved in sterile saline and injected 1–3 days before IOP elevation. To examine the effects of P2X7 stimulation, Long-Evans rats were injected with either 2 μL of 250 μM P2X7 receptor agonist BzATP or sterile saline. Rats were killed and the retina dissected, with total RNA isolated from the retina and processed as described above.

Immunoblots

Immunoblots were processed as described (Guha *et al.* 2013). In brief, whole retinas were washed twice with cold phosphate-buffered saline and lysed in radioimmunoprecipitation assay buffer containing 50 mM Tris-HCl, 150 mM NaCl, protease inhibitor cocktail (Complete; Roche Diagnostics, Mannheim, Germany), 1% Triton X-100, 0.1% sodium dodecyl sulfate, and 10% glycerol. Samples were sonicated and cleared by centrifugation (10 000 g) for 10 min at 4°C, with protein concentrations determined using a bicinchoninic acid Protein Assay (Pierce, Rockford, IL, USA/ThermoFisher). Protein was separated using conventional sodium dodecyl sulfate–polyacrylamide gel electrophoresis, and processed using standard immunoblot protocols (Lu *et al.* 2015). Blots were incubated with a monoclonal antibody to rat IL-6 overnight at 4°C (1 : 1000; R & D Systems, Minneapolis, MN, USA, # MAB5061), followed by incubation with anti-mouse IgG conjugated to horseradish peroxidase (1 : 5000; Amersham Biosciences Corp., Arlington Heights, IL, USA) at 23°C for 1 h and developed by chemiluminescence detection (ECL detection system; Amersham Biosciences Corp.). The ImageQuant LAS 4100 imager and Image Quant software (Both GE Healthcare Lifesciences, Pittsburgh, PA, USA) were used to detect and quantify the intensity of the specific bands. Western blots were performed 3–4 times each.

Optic nerve head astrocytes

Primary rat optic nerve head astrocyte cultures were grown as described (Beckel *et al.* 2014) based upon a protocol modified from Mandal *et al.* (2009). The optic nerve head tissue proximal to the sclera in rat pups up to post-natal day 5 was digested for 1 h in 0.25% trypsin. Cells were grown in medium comprised of Dulbecco's minimal essential medium/F12, 10% fetal bovine serum, 1% penicillin/streptomycin, and 25 ng/mL epidermal growth factor and used up to passage 5. Cell identification was performed with glial fibrillary acidic protein immunostaining as described (Beckel *et al.* 2014). For stretch experiments, astrocytes were seeded on a silicon substrate (Silastic; Specialty Manufacturing, Saginaw, MI, USA), bathed in isotonic solution (in mM; 105 NaCl, 5 KCl, 4 NaHEPES, 6 HEPES acid, 1.3 $CaCl_2$, 5 glucose, 5 $NaHCO_3$, 60 mannitol, and 0.25 $MgCl_2$ pH 7.4). Cells were subjected to a 5% equibiaxial strain at 0.3 Hz for 2 min using a specially designed pneumatic piston as described (Winston *et al.* 1989; Beckel *et al.* 2014). Cells were exposed to 30% hypotonic solution (isotonic solution diluted with dH2O) for swelling experiments with BBG (Sigma, St Louis, MO, USA), A839977 (Tocris/BioTechne) or (4-benzoyl-benzoyl)-ATP (BzATP) (Sigma Corp.) for 4 h at 37°C before RNA was extracted as detailed above. Samples of the extracellular media were taken before and after stretch or BzATP and stored at −80°C. The release of IL-6 from astrocytes was then measured by Rat IL-6 Quantikine® ELISA kit (#R6000B; R & D Systems) following manufacturer's instructions, with data acquired using a 96-well plate reader SpectraMax M5 (Molecular Devices, Palo Alto, CA, USA).

IL-6 release from isolated retinal ganglion cells

Isolation of retinal ganglion cells was performed using the immunopanning procedure as described (Zhang *et al.* 2010; Xia *et al.* 2012). Isolated retinal ganglion cells were seeded onto 0.1% poly-L-lysine (Peptides International, Louisville, Kentucky, USA) and 1 μg/mL laminin coated coverslips or elastic silicone sheeting in stretch chambers and cultured at 37°C with 5% CO_2. Attached cells were bathed in 750 μL of isotonic solution including 100 μM of the ectoATPase inhibitor βγ methylene ATP, and stretched by application of 20 mmHg of pressure resulting in a 4.1% deformation strain (see Xia *et al.* 2012 for detail). Pressure inside the stretch chamber was increased to 20 mmHg for 4 min, returned to 0 mmHg for 1 min and the cycle repeated three times for a total duration of 15 min. Immediately following stretch, a 250 μL sample of the extracellular solution was collected from the center of the stretch chamber. Stretch did not induce release of lactose dehydrogenase. IL-6 levels were determined with the rat antibody cytokine array following manufacturer's instructions (R & D Systems), as described in detail in a recent publication (Lim *et al.* 2016). In brief, IL-6 levels were quantified by incubating the membrane in Streptavidin-horseradish peroxidase followed by chemiluminescent detection reagents (GE Healthcare). The production of light corresponding to levels of bound cytokine was determined with ImageQuant LAS4000 and the intensity of each spot was measured using ImageQuant TL analysis software (all GE Healthcare). Results represent four independent trials of stretch or BzATP experiments, each performed in duplicate.

Data analysis and study design

Data are reported as mean ± standard error of the mean. Statistical analysis used a one-way ANOVA with appropriate *post hoc* test, or a paired Student's *t*-test when comparing eyes from the same animal. Results with $p < 0.05$ were considered significant. When data were not distributed normally, analysis on ranks was performed. All statistical analysis was performed using SigmaStat software (Systat Software Inc., San Jose, CA, USA). The number of experimental repeats was determined in part by sample size calculations and power analysis. Data within two standard deviations of the mean were included unless accompanied by signs of animal distress or unexpected deviation. Analysis was performed in a masked fashion where appropriate.

Results

Pressure-dependent elevation in message for IL-6

Initial experiments to screen for cytokine pathways activated *in vivo* by transient elevations in IOP were determined using a cytokine PCR Array. IOP in one eye of a rat was raised to 50 mmHg for 4 h. Although this is considerably above the baseline IOP levels of 12.8 mmHg in the conscious Sprague–Dawley rat (Cabrera *et al.* 1999),

this increase did not prevent blood flow through the retinal vessels. Similar transient rises in IOP have been found to induce minimal permanent damage (Zhi *et al.* 2012; Abbott *et al.* 2014; Crowston *et al.* 2015). qPCR analysis indicated no rise in pro-apoptotic genes, although expression of the early stress-response ATF3 was increased, consistent with findings in the hypertonic saline model (Guo *et al.* 2011) (Figure S1).

To obtain an objective measure of the cytokine response to transient pressure elevation, retinal gene levels were examined 20 h after IOP returned to baseline using a cytokine PCR array. Analysis showed nine genes with a > 2-fold change in expression levels between the pressurized and control rat retina (Fig. 1a and b). *IL-6* showed the greatest rise, with a 29-fold increase. *IL1rn*, *IL24*, *Tnf*, *Csf1*, and *Lif* were also elevated more than twofold. Three genes, *Tnfsf11*, *Gdf9*, and *Tnfsf4*, were down-regulated more than twofold.

Given that *IL-6* was the gene altered most using the cytokine gene array, results were confirmed using traditional qPCR. *IL-6* was elevated 16.9-fold in eyes with increased IOP as compared with contralateral eyes (Fig. 1c). This substantial increase measured using qPCR strongly supported the result from the PCR array suggesting that expression of *IL-6* was increased in retinas exposed to transient elevations in IOP.

Purines and IL-6 expression *in vivo*

As purinergic signaling has been repeatedly implicated in retinal cells exposed to elevated IOP (Reigada *et al.* 2008; Sanderson *et al.* 2014), expression of gene *ENTPD1* was examined. *ENTPD1* codes for the ectoATDPase NTPDase1, which was previously identified as a possible marker for sustained rises in extracellular ATP (Lu *et al.* 2007). Increased levels of the gene *ENTPD1* and protein for NTPDase1 were triggered by sustained exposure to ATP. Levels of NTPDase1 protein were elevated in parallel to extracellular ATP concentrations in rat, mouse, and primate models of chronic IOP elevation (Lu *et al.* 2015). In material from rat retinas obtained both 1 and 5 days after transient IOP elevation, ENTPD1 was up-regulated (Fig. 2a), suggesting levels of extracellular ATP were elevated after moderate IOP elevation.

A considerable body of past work implicates autostimulation of the P2X7 receptor following the mechanosensitive release of ATP in the retina (Zhang *et al.* 2006; Reigada *et al.* 2008; Xia *et al.* 2012; Beckel *et al.* 2014), and recent work demonstrates P2X7 receptor stimulation leads to IL-3 responses in isolated retinal ganglion cells (Lim *et al.* 2016). As stimulation of P2X7 receptors by ATP has been associated with the up-regulation of IL-6 in microglia cells (Shieh *et al.* 2014), the role of the P2X7 receptor in mediating the pressure-dependent rise in *IL-6* was examined.

Initial involvement of the P2X7 receptor was determined using antagonist BBG. While BBG can act at other P2X receptors (Bo *et al.* 2003), it is well tolerated in the eye (Totan *et al.* 2014). In addition, the blue color of the compound enabled the retinal distribution of the antagonist to be more accurately determined (Fig. 2b); material from the targeted retina was preferentially analyzed. The pressure-dependent increase in *IL-6* mRNA was blocked by intravitreal injection of 0.8% BBG 1–3 days before the IOP rise (Fig. 2c). Levels were compared to the rise seen in pressurized eyes injected with only saline, to control for any injection artifact. Immunoblots confirmed that IL-6 protein was also increased in the retina following a rise in pressure (Fig. 2d). Changes in protein level paralleled those of mRNA, with IOP rise leading to an increase in IL-6 protein that was prevented by BBG (Fig. 2e).

To determine whether stimulation of the P2X7 receptor was sufficient to trigger up-regulation of *IL-6*, agonist BzATP was injected intravitreally (2 μL, 250 μM) with sterile saline injected into the contralateral eye and levels of *IL-6* mRNA present in the retina 24 h later were determined.

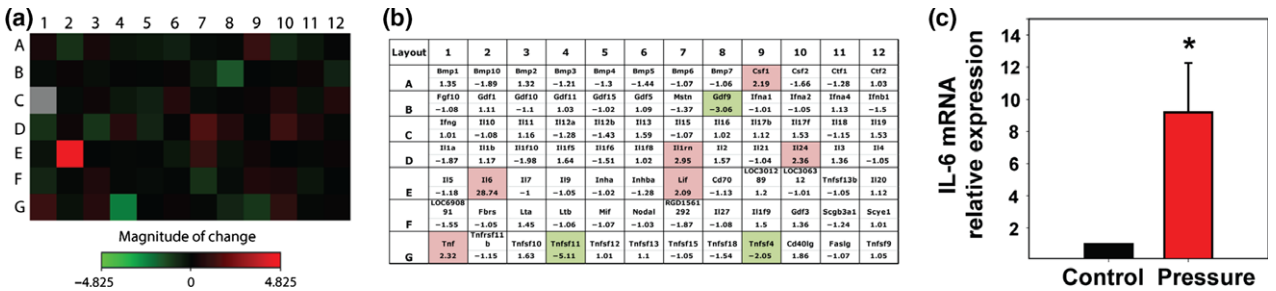

Layout	1	2	3	4	5	6	7	8	9	10	11	12
A	Bmp1 1.35	Bmp10 −1.89	Bmp2 1.32	Bmp3 −1.21	Bmp4 −1.3	Bmp5 −1.44	Bmp6 −1.07	Bmp7 −1.06	Csf1 2.19	Csf2 −1.66	Ctf1 −1.28	Ctf2 1.03
B	Fgf10 −1.08	Gdf1 1.11	Gdf10 −1.1	Gdf11 1.03	Gdf15 −1.02	Gdf5 1.09	Mstn −1.37	Gdf9 −3.06	Ifna1 −1.01	Ifna2 −1.05	Ifna4 1.13	Ifnb1 −1.5
C	Ifng 1.01	Il10 −1.08	Il11 1.16	Il12a −1.28	Il12b −1.43	Il13 1.59	Il15 −1.07	Il16 1.02	Il17b 1.12	Il17f 1.53	Il18 −1.15	Il19 1.53
D	Il1a −1.87	Il1b 1.17	Il1f10 −1.98	Il1f5 1.64	Il1f6 −1.51	Il1f8 1.02	Il1rn 2.95	Il2 1.57	Il21 −1.04	Il24 2.36	Il3 1.36	Il4 −1.05
E	Il5 −1.18	Il6 28.74	Il7 −1	Il9 −1.05	Inha −1.02	Inhba −1.28	Lif 2.09	Cd70 −1.13	LOC3012 89 1.2	LOC3063 12 −1.01	Tnfsf13b −1.05	Il20 1.12
F	LOC6908 91 −1.55	Fbrs −1.05	Lta 1.45	Ltb −1.06	Mif −1.07	Nodal −1.03	RGD1561 292 −1.87	Il27 −1.08	Il1f9 1.5	Gdf3 1.36	Scgb3a1 −1.24	Scye1 1.01
G	Tnf 2.32	Tnfrsf11b −1.15	Tnfsf10 1.63	Tnfsf11 −5.11	Tnfsf12 1.01	Tnfsf13 1.1	Tnfsf15 −1.05	Tnfsf18 −1.54	Tnfsf4 −2.05	Cd40lg 1.86	Faslg −1.07	Tnfsf9 1.05

Fig. 1 Changes in expression of cytokine genes 24 h after moderate intraocular pressure (IOP) elevation. Changes in cytokine gene expression 24 h after IOP was elevated to 50 mm Hg for 4 h (20 h after pressure returned to baseline). (a) Heat map of fold changes in gene expression in pressurized eye compared to control. Red indicates up-regulation, while green symbolizes down-regulation (b) Layout of 84 genes shown in heat map and fold changes relative to the control retina. Numbers are mean change in pressurized eye compared to control in two pairs. Genes were evaluated based on the criteria of at least a twofold up- or down-regulation compared to control. (c) Increased expression of *IL-6* in pressurized retinas confirmed using qPCR. $N = 9$, $*p < 0.001$.

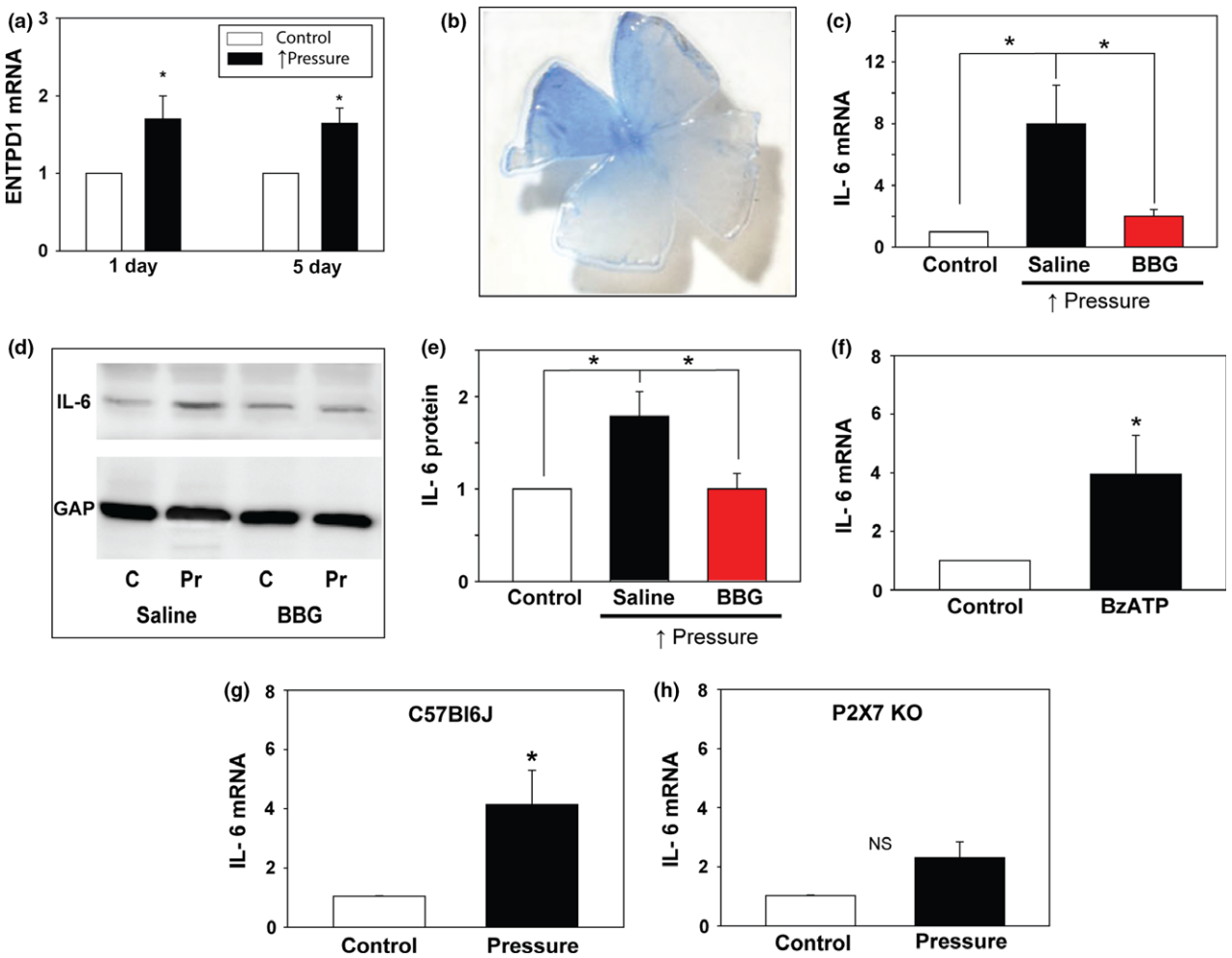

Fig. 2 Involvement of ATP and P2X7 receptor in *IL-6* elevation *in vivo*. (a) Expression of ectoATPase gene *ENTPD1* was elevated 1 day after increase in intraocular pressure (IOP) to 50 mmHg for 4 h (Pressure, $*p = 0.033$, $N = 10$). *ENTPD1* remained elevated 5 days after the procedure ($*p = 0.004$, $N = 8$). (b) The distribution of P2X7 antagonist Brilliant Blue G (BBG) in the retina 1 day after intravitreal injection. The staining pattern suggests distribution of BBG through the vitreal cavity to the retina was restricted. A similar staining pattern remained in retinas examined 6 days after injection. (c) The pressure-dependent rise in *IL-6* mRNA was substantially decreased following injection of BBG. Data are expressed as relative gene expression in the pressurized versus non-pressurized retina for eyes injected with 0.8% BBG or saline 1–3 days before the moderate elevation of IOP to 50 mmHg for 4 h. $N = 6$–9. $*p < 0.004$ saline pressurized versus non-pressurized; $*p < 0.013$ saline pressurized versus BBG pressurized. (d) Representative immunoblots from whole retina lysates probed for IL-6 (22 kDa) and housekeeping protein GAPDH (GAP, 37 kDa). Expression of *IL-6* is greater in the eye subject to the moderate IOP increase (Pr) treated with saline as compared to the contralateral non-pressurized control eye, but this pressure-dependent increase is reduced after injection with BBG. (e) Summary of relative protein expression from experiments illustrated in C quantified with densitometry; $N = 4$–5. $*p < 0.001$ saline pressurized versus non-pressurized; $*p < 0.035$ saline pressurized versus BBG pressurized. (f) P2X7R agonist BzATP was sufficient to increase levels of *IL-6* mRNA in the retina 1 day after intravitreally injection (250 μM, 2 μL per eye), $N = 5$, $*p = 0.021$. (g) In wild-type C57Bl6J mice, transient elevation of IOP to 60 mmHg for 4 h (Pressure) raised retina levels of *IL-6* mRNA. $N = 7$, $*p < 0.001$. (h) In P2X7 knockout mice, the same elevation in IOP did not significantly increase levels of *IL-6*. $N = 6$.

Retinal *IL-6* expression was increased fourfold by the P2X7 receptor agonist BzATP in the absence of any changes in IOP (Fig. 2f).

Involvement of purines in the response to elevated IOP was further probed by examining expression of certain receptors. Receptor genes *P2RX7* and *ADORA3,* coding for the adenosine A3 receptor, were elevated in many retinas examined after 1 day, but considerable variation meant the rises were not significant (Figure S2). Genes *P2RX4* and *P2RY6* for purinergic receptors were increased 1 day, but not 5 days after IOP elevation. While the precise contribution of these receptors remains to be determined, their increased expression is consistent for mechanosensitive purinergic signaling.

Pressure-dependent up-regulation of IL-6 absent in P2X7 knockout mice

Further confirmation of the role of the P2X7 receptor in the pressure-dependent rise in *IL-6* was provided with P2X7 knockout mice. Elevating the IOP of wild-type C57Bl6J mouse eyes to 60 mmHg for 4 h led to a rise in *IL-6* levels analogous to that observed in the rat eye (Fig. 2g). In mice missing the P2X7 gene, however, this rise in IOP did not significantly change *IL-6* levels (Fig. 2h). This supported the pharmacological identification, while also demonstrating the response occurred in multiple species.

IL-6 up-regulation and release from optic nerve head astrocytes

In vitro experiments from isolated cells were pursued to enable identification of specific cell types and better control of pharmacological manipulation. Optic nerve head astrocytes undergo multiple changes in response to the mechanical strain in glaucoma (Hernandez 2000). As we have previously found that stretch of these astrocytes leads to the release of ATP through pannexin hemichannels and subsequent autostimulation of P2X7 receptors (Beckel *et al.* 2014), the mechanosensitive response of *IL-6* in these astrocytes and the contribution of the P2X7 receptor was examined.

Isolated rat optic nerve head astrocytes expressed glial fibrillary acidic protein, confirming the identity of the cultured cells (Fig. 3a). Astrocytes were plated on a silicone substrate and subjected to a 5% equilateral strain at 0.3 Hz for 4 h, followed by a 20 h break before RNA was extracted to increase parallels to *in vivo* experiments. Levels of *IL-6* mRNA were increased twofold in stretched astrocytes as compared to controls (Fig. 3b). Unstretched astrocytes exposed to 50 μM BzATP for 4 h also demonstrated a twofold rise in *IL-6*, suggesting the P2X7 receptor was sufficient to trigger the rise in *IL-6* mRNA expression (Fig. 3c) as found *in vivo*. An analogous rise in *IL-6* was produced by swelling astrocytes with a 30% hypotonic solution for 4 h (Fig. 3d); this rise in *IL-6* mRNA was prevented by P2X7 receptor antagonists BBG and A839977 (Fig. 3d).

To confirm the contribution of the P2X7 receptor, the rise in *IL-6* expression in optic nerve head astrocytes isolated from C57Bl6J mice and P2X7 knockout mice was compared. Swelling cells from wild-type mice induced a significant increase in *IL-6* expression (Fig. 3e). In contrast, astrocytes isolated from $P2X7^{-/-}$ mice showed a drop in the *IL-6* expression with swelling.

IL-6 released from optic nerve head astrocytes

While the ability of P2X7 receptors to trigger the up-regulation of *IL-6* mRNA *in vivo* and *in vitro* implied an increased involvement of the cytokine, the ability of the receptor to trigger release of IL-6 was also tested. Measurement of IL-6 levels in the bath surrounding the astrocytes using an ELISA assay demonstrated that the cytokine was released into the bath after stretch (Fig. 3f). Exposure of astrocytes to agonist BzATP also led to a substantial release of IL-6 (Fig. 3g). Cytokine release in many cell types is mediated by increases in intracellular calcium; for example, the release of IL-6 from spinal cord astrocytes is calcium dependent (Codeluppi *et al.* 2014). To confirm optic nerve head astrocytes experience a rise in calcium upon swelling, levels were monitored with indicator Fura-2. The rise in calcium was rapid and reversible (Fig. 3h). To determine whether this response was dependent upon autostimulation of the P2X7 receptor, the ability of BBG to antagonize this rise was examined. Pretreatment of astrocytes with blocker BBG eliminated the rise in calcium, implicating autostimulation of the P2X7 receptor, and consistent with a role for calcium in the release.

IL-6 released from isolated retinal ganglion cells

Although the above experiments clearly indicate that mechanical strain and stimulation of the P2X7 receptor can lead to release of IL-6 from optic nerve head astrocytes, immunostaining indicated that retinal ganglion cells expressed high levels of IL-6 (Fig. 4a). The staining pattern was particulate, consistent with IL-6 stored in vesicles. As such, the ability of retinal ganglion cells to release IL-6 was tested. As ganglion cells *in situ* are intertwined with various other cell types, a two-step immunopanning procedure was used to isolate retinal ganglion cells (Fig. 4b); previous analysis indicates that > 98% of cells obtained in this way are ganglion cells (Zhang *et al.* 2006). The purified cells were plated on a silicone substrate and, once attached, a 4.1% deformation strain was applied to stretch the cells for 4 min. Cells were then returned to baseline for 1 min, with the stretch cycle repeated two more times. There was a significant increase in extracellular levels of IL-6 released into the bath after this stretch period (Fig. 4c). Analogous trials indicate that stimulation of the P2X7 receptor with BzATP also released IL-6 from isolated retinal ganglion cells (Fig. 4d). Attempts to process RNA from these isolated ganglion cells were unsuccessful, precluding examination of *IL-6* expression. However, application of BzATP led to a rapid increase in intracellular calcium in isolated retinal ganglion cells (Fig. 4e); the response was rapid, reversible, and repeatable.

Discussion

The signaling pathways linking mechanical strain to inflammation play an important role in the cellular response to stress. This study implicates the P2X7 receptor for extracellular ATP in the mechanosensitive up-regulation of cytokine IL-6 in the retina. *In vivo* data demonstrate *IL-6* mRNA was

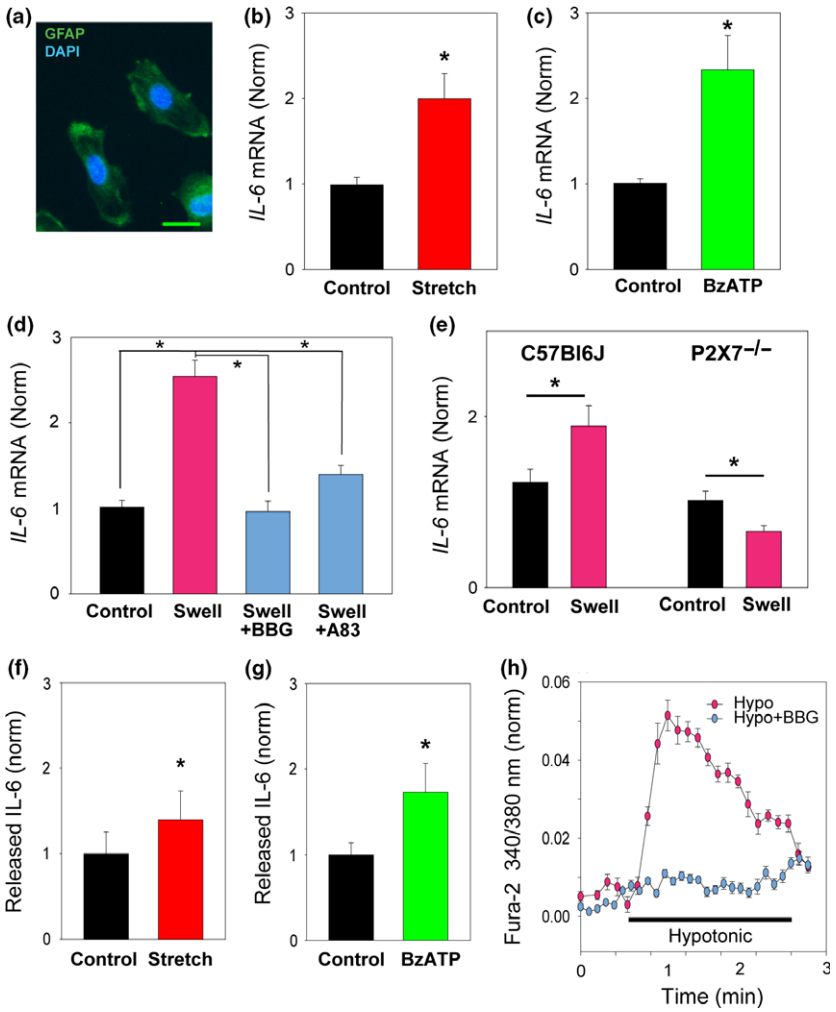

Fig. 3 *IL-6* response in astrocytes. (a) Cultured rat optic nerve head astrocytes stained for glial fibrillary acidic protein (green) and DAPI (blue). Bar = 20 μm. (b) Increased expression of *IL-6* mRNA in stretched astrocytes; cells were subject to a 5% equilateral strain at 0.3 Hz for 4 h, followed by a 20 h break before extraction of RNA. $N = 8–9$, $*p = 0.011$. (c) *IL-6* expression was increased in astrocytes exposed to 50 μM BzATP for 4 h. $N = 5$, $*p = 0.008$. (d) Expression of *IL-6* was also increased in cells exposed to moderate swelling induced by 30% hypotonicity for 4 h. However, this rise in expression was inhibited by P2X7R antagonists Coomassie Brilliant Blue G (BBG) (50 μM) or A839977 (A83; 10 μM). Cells were pre-treated with antagonists in isotonic solution for 1 h before swelling. $N = 4$ $*p < 0.001$ Swell versus Control, $*p < 0.001$ Swell versus swell+BBG, $*p < 0.001$ Swell versus swell+A839977. (e) Cell swelling in 30% hypotonic solution-induced rise in *IL-6* mRNA was observed in optic nerve head astrocytes from C57Bl6J mice ($N = 6$, $*p = 0.006$), but swelling in astrocytes isolated from P2X7$^{-/-}$ mice actually reduced *IL-6* expression ($*p = 0.043$, $N = 6$). (f) The concentration of IL-6 in the bath surrounding astrocytes was higher after exposing cells to stretch ($*p = 0.036$, $N = 7$). (g) Levels of IL-6 in the bath were also increased after exposure of astrocytes to 50 μM BzATP for 30 min ($*p = 0.011$, $N = 6$, paired *t*-test for f and g). (h) Swelling of astrocytes by hypotonic solution rapidly raised intracellular calcium, as indicated by the ratio of light excited at 340 nm versus 380 nm in cells loaded with indicator Fura-2. In the presence of 100 μM BBG, no rise in cell calcium was observed. Symbols represent mean ± SEM, $N = 16$.

substantially up-regulated after a transient elevation of IOP in the rat retina, with the P2X7 receptor antagonist BBG preventing the up-regulation of both *IL-6* mRNA and IL-6 protein in retinal tissue. The transient rise in IOP increased *IL-6* expression in the retina of wild-type mice but not in P2X7 knockout mice, further implicating the P2X7 receptor and demonstrating the effect was not species dependent. In isolated optic nerve head astrocytes, *IL-6* expression was increased by stretch, swelling, and directly by the P2X7 agonist BzATP. The swelling induced rise in *IL-6* in astrocytes was prevented by two different P2X7 antagonists. In addition, both astrocytes and retinal ganglion cell released IL-6 in response to agonist BzATP or to mild stretch. Together, these data identify a role for the P2X7 receptor in the mechanosensitive IL-6 response of neurons and astrocytes in the retina.

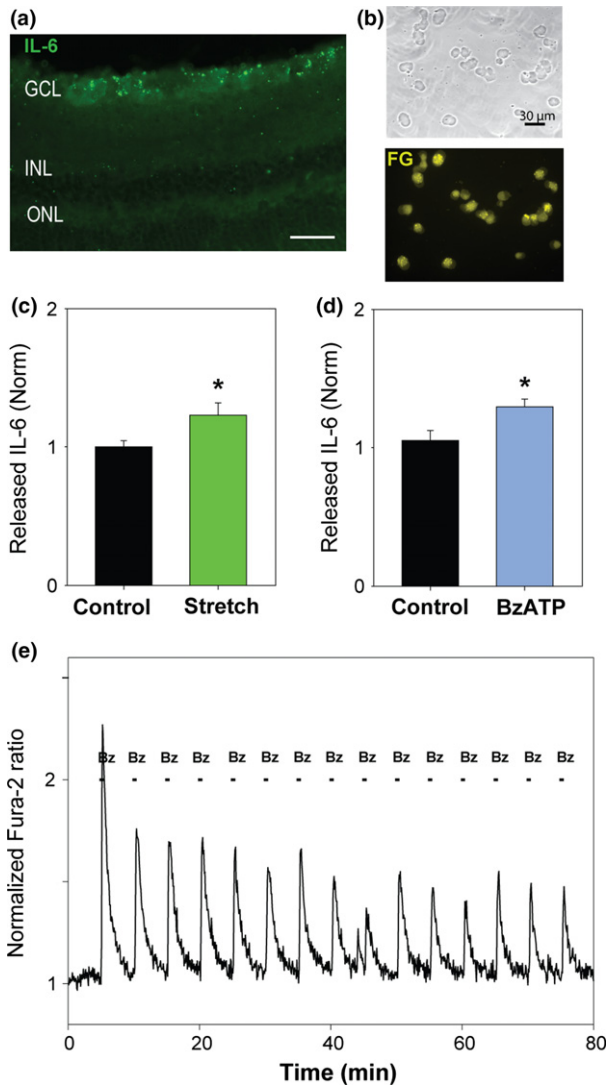

Fig. 4 IL-6 release from isolated retinal ganglion cells. (a) Retinal section stained for IL-6 indicating expression of the cytokine in the ganglion cell layer (GCL). IPL: inner plexiform layer, OPL: outer plexiform layer. Bar = 50 μm. (b) Retinal ganglion cells isolated with the two-step immunopanning procedure. The comparison of the phase contrast image (top) with the fluorescence image (ex 360 nM) indicates that the cells are labeled with Fluorogold (FG) transported from the superior colliculus, confirming their ganglion cell identity. Cells used for cytokine measurements were unlabeled and plated at a much higher density. (c) Application of a 4.1% deformation strain to stretch isolated RGCs attached to a silicone substrate increased the level of IL-6 detected in the bath. $N = 8$, $^*p = 0.022$. (d) Levels of IL-6 in the bath surrounding isolated RGCs increased in cells exposed to 50 μM of P2X7R agonist BzATP. $N = 8$, $^*p = 0.006$ paired *t*-test for (c) and (d). (e) Application of 50 μM BzATP for 15 s led to a repeatable and reversible rise in intracellular calcium in isolated retinal ganglion cells. Each bar represents the time of BzATP application.

Signaling pathways linking mechanical strain to IL-6

The intracellular signaling pathways linking mechanical strain to the IL-6 response can be at least partially described by integrating previous findings with the results of this study (see also the Graphical Abstract). Increased pressure in the whole retina, or mechanical strain to either optic nerve head astrocytes or retinal ganglion cells leads to ATP release through pannexin hemi-channels (Reigada *et al.* 2008; Xia *et al.* 2012; Beckel *et al.* 2014). Release from astrocytes is partially dependent on Rho kinase, consistent with a mechanosensor-like TRPV4 as in other ocular cells (Shahidullah *et al.* 2012; Jo *et al.* 2015). In both astrocytes and retinal ganglion cells, the released ATP autostimulated P2X7 receptors on the same cell type.

This study clearly implicates the P2X7 receptor in the IL-6 response to mechanical strain. The P2X7 antagonist BBG prevented the rise in *IL-6* expression *in vivo*, while BBG and a second antagonist A839977 prevented the rise in astrocytes. In addition, agonist BzATP emulated the effects of mechanical strain both *in vivo* and *in vitro*. Although BzATP and BBG can act at other P2 receptors (Bo *et al.* 2003; Wildman *et al.* 2003), A839977 is more selective (Honore *et al.* 2009). In addition, the reduced *IL-6* response in P2X7$^{-/-}$ mice *in vivo*, and in optic nerve head astrocytes isolated from the P2X7$^{-/-}$ mice, implicated the P2X7 receptor in linking the mechanical strain to the *IL-6* response. The retinal response resembles that in cultured microglia, where the P2X7 receptor triggers *IL-6* mRNA up-regulation and release of the cytokine (Shieh *et al.* 2014).

While the use of agonists, antagonists, and knockout mice together imply the P2X7 receptor makes a substantial contribution to the mechanosensitive IL-6 response, a contribution from other P2 receptors cannot be ruled out in this study, and other P2 receptors have been linked to IL-6 (Shigemoto-Mogami *et al.* 2001; Inoue *et al.* 2007; Kawano *et al.* 2015). A study of the same P2X7$^{-/-}$ mice used here found that while most of the peritoneal rise in IL-6 accompanying ATP injection was eliminated in the knockout mice, the residual response may have reflected action of additional receptors, with P2Y receptors suggested as a possible source (Solle *et al.* 2001). The increased expression of the P2Y6 receptor in retinas exposed to transient pressure elevation in Figure S2 is interesting, but as the agonist for this receptor is UDP, and ATP itself has little affinity, activation of this receptor by ATP released after elevated pressure is likely to be complex (Communi *et al.* 1996; Satrawaha *et al.* 2011). It is also not clear whether the response is direct or reflects a secondary response to IL-1β release, as IL-1β can lead to up-regulation of *IL-6* expression (Cadman *et al.* 1994). Experiments are currently underway to determine whether stimulation of the P2X7 receptor leads to IL-1β release.

In addition to the up-regulation of *IL-6* message and protein levels, mechanical strain and the P2X7 receptor also triggered a rapid release of IL-6 from astrocytes and retinal ganglion cells. The P2X7 receptor is a ligand gated non-selective cation channel, and its stimulation raises

intracellular calcium in both astrocytes and retinal ganglion cells (Xia *et al.* 2012; Beckel *et al.* 2014). The vesicular release of IL-6 from spinal cord is calcium dependent (Codeluppi *et al.* 2014), and the time course of the IL-6 release above implies the signaling mechanisms are distinct from those involved in transcriptional up-regulation. While the increased expression of *IL-6* would provide more IL-6 for release upon later stimulation, this complex positive feedback pathway was not investigated in this study.

Separating mechanical strain from cell death and the P2X7 receptor

The data here indicate that P2X7 receptor was involved in the increase in *IL-6* after a transient non-ischemic elevation in IOP. We used this model because it was reported to induce little cell death (Morrison *et al.* 2010, 2014; Abbott *et al.* 2014; Crowston *et al.* 2015). This enabled us to distinguish between responses resulting from mechanical strain and those because of cell death; the lack of response in genes *ANAX3*, *BAX* or *CCND1,* associated with apoptosis or extreme stress, suggest this distinction was largely achieved. In a variant of the rat model in which IOP was raised to 50 mmHg for 8 h, there was no substantial retinal ganglion cell loss or decreases in axon transport (Abbott *et al.* 2014). Elevation of mouse IOP to 50 mmHg for 30 min led to a transient reduction in the photopic negative response (PhNR), attributed largely to retinal ganglion cell function, although the number of ganglion cells was not reduced when examined 7 days later (Chrysostomou and Crowston 2013; Crowston *et al.* 2015). Presumably, the maintenance of retinal blood flow prevents the retinal ganglion cells loss associated with more ischemic models (Zhi *et al.* 2012). Overall this suggests that the robust IL-6 response, and the stimulation of the P2X7 receptor which precedes it, are distinct from cell death.

Relevant cell types

Our *in vivo* experiments identified elevated *IL-6* mRNA and IL-6 protein using material from the entire retina. The optic nerve head is the focus of the mechanical forces induced upon elevation of IOP (Downs 2015), and the *in vitro* experiments clearly demonstrate a rise in *IL-6* expression in optic nerve head astrocytes, consistent with previous findings of a large rise in optic nerve head *IL-6* in response to IOP elevation (Johnson *et al.* 2011). However, the optic nerve head tissue is a minor component of the retina and it is likely that other cell types contribute to the rise in *IL-6* expression found in the whole tissue. While the restricted levels of cell material in panned retinal ganglion cells precluded reliable molecular analysis of *IL-6* levels in this study, the cells are also likely to contribute. The increased expression of *IL-6* 1 day after IOP elevation using the laser photocoagulation model co-localized with amyloid precursor protein, a marker of fast axonal transport, and suggested the axonal transport of IL-6 synthesized in retinal ganglion cells was impeded with increased IOP (Chidlow *et al.* 2012). This may relate to a more recent study in which IL-6 increased with age in the proximal optic nerve of DBA mice, and correlated with the loss of axonal transport (Wilson *et al.* 2015). The predicted involvement of microglial cells here is complex; cultured retinal microglia released IL-6 when subjected to hydrostatic pressure increase (Sappington *et al.* 2006), while activated microglial cells were observed *in vivo* only 1 week after elevation of IOP but not at earlier time points (Kezic *et al.* 2013). Future experiments are needed to understand the role of microglial cells given their responsiveness to extracellular ATP (Franke *et al.* 2007).

Physiological implications

While the results from this study clearly demonstrate a role for the P2X7 receptor in the up-regulation and release of IL-6, the physiological implications will depend upon the cell types involved, the conditions that lead to the response, and whether the resulting IL-6 mediates protective or detrimental effects. IL-6 signaling is complex; although IL-6 is traditionally described as a 'pro-inflammatory' cytokine, it can be both protective and pathological in neural tissues (Spooren *et al.* 2011). Expression of IL-6 in cortical astrocytes confers protection from focal injury in neural tissue (Penkowa *et al.* 2003). In the retina, several groups have identified protective actions by IL-6 and suggested it is an early protective response. The death of retinal ganglion cells following increased hydrostatic pressure was prevented by IL-6 (Sappington *et al.* 2006), and IL-6 enhanced neurogenesis in retinal ganglion cells (Chidlow *et al.* 2012). If IL-6 represents an early response to protect neurons, then this study suggests that the mechanosensitive release of ATP through pannexin hemichannels and autostimulation of P2X7 receptors that lead to the increased IL-6 response may also be protective, at least in young healthy tissue. This would add to the increasing recognition of the P2X7 receptor as more than just a 'death receptor' in neural tissues.

Conclusion

In conclusion, this study demonstrates a role for the P2X7 receptor in linking mechanical strain to up-regulation and release of cytokine IL-6 in the retina. Involvement of the P2X7 receptor was demonstrated both *in vivo* and *in vitro* in astrocytes and neurons. As IL-6 has many protective effects in the retina, this study may consequently identify a beneficial role of the P2X7 receptor in neural tissues. Given the emerging relationship between cytokines and mechanical strain in TBI, this study suggests further investigation of the P2X7 receptor in TBI is warranted.

Portions of this work have appeared in abstract form (Lim *et al.* 2011; Lu *et al.* 2011, 2013).

Declarations

Ethics Approval and Consent to Participate: All experimental approaches on rats and mice were approved by the Animal Care and Use Committee of the University of Pennsylvania protocol #803584.

Availability of data and materials: All readily reproducible materials described in the manuscript, including new software, databases, and all relevant raw data will be freely available to any scientist wishing to use them.

Author contributions

WL helped design the study, carried out most of the rat IOP experiments, performed analysis of molecular and protein data and immunohistochemistry. FA carried out experiments on elevation of IOP in mice and analyzed associated data. JMB was responsible for many of the *in vitro* experiments on rat optic nerve head astrocytes. JCL carried out experiments on isolated ganglion cells. CHM conceived of the study, and participated in its design and coordination and helped to draft the manuscript. All authors read and approved the final manuscript.

Acknowledgments and conflict of interest disclosure

The authors thank Jonathan Huwe for help with qPCR experiments. The authors declare that they have no competing interests. This work is supported by grants from the NIH EY015537 and EY013434 and core grant EY001583 (CHM). NIH DK106115 (JMB), Jody Sack Fund (WL). These funding bodies had no direct role in the design of the study and collection, analysis, and interpretation of data or and in writing the manuscript. The authors have no conflict of interest to declare.

All experiments were conducted in compliance with the ARRIVE guidelines.

Supporting information

Additional Supporting Information may be found online in the supporting information tab for this article:

Figure S1. Changes in gene expression 1 and 5 days after CEI to 50 mmHg for 4 h.

Figure S2. Changes in expression of purine genes 1 and 5 days after CEI to 50 mmHg for 4 h.

References

Abbott C. J., Choe T. E., Lusardi T. A., Burgoyne C. F., Wang L. and Fortune B. (2014) Evaluation of retinal nerve fiber layer thickness and axonal transport 1 and 2 weeks after 8 hours of acute intraocular pressure elevation in rats. *Invest. Ophthalmol. Vis. Sci.* **55**, 674–687.

Beckel J. M., Argall A. J., Lim J. C. *et al.* (2014) Mechanosensitive release of ATP through pannexin channels and mechanosensitive upregulation of pannexin channels in optic nerve head astrocytes: a mechanism for purinergic involvement in chronic strain. *Glia* **62**, 1486–1501.

Bo X., Jiang L. H., Wilson H. L., Kim M., Burnstock G., Surprenant A. and North R. A. (2003) Pharmacological and biophysical properties of the human P2X5 receptor. *Mol. Pharmacol.* **63**, 1407–1416.

Bustamante M., Fernandez-Verdejo R., Jaimovich E. and Buvinic S. (2014) Electrical stimulation induces IL-6 in skeletal muscle through extracellular ATP by activating Ca(2+) signals and an IL-6 autocrine loop. *Am. J. Physiol. Endocrinol. Metab.* **306**, E869–E882.

Cabrera C. L., Wagner L. A., Schork M. A., Bohr D. F. and Cohan B. E. (1999) Intraocular pressure measurement in the conscious rat. *Acta Ophthalmol. Scand.* **77**, 33–36.

Cadman E. D., Naugles D. D. and Lee C. M. (1994) cAMP is not involved in interleukin-1-induced interleukin-6 release from human astrocytoma cells. *Neurosci. Lett.* **178**, 251–254.

Cepurna W. O., Guo Y., Doser T. A., Dyck J. A., Johnson E. C. and Morrison J. C. (2008) An interval of controlled intraocular pressure elevation alters optic nerve head gene expression without compromising retinal perfusion. *Invest. Ophthalmol. Vis. Sci.* **49**, 3695. ARVO E-Abstract.

Chen K. H., Wu C. C., Roy S., Lee S. M. and Liu J. H. (1999) Increased interleukin-6 in aqueous humor of neovascular glaucoma. *Invest. Ophthalmol. Vis. Sci.* **40**, 2627–2632.

Chidlow G., Wood J. P., Ebneter A. and Casson R. J. (2012) Interleukin-6 is an efficacious marker of axonal transport disruption during experimental glaucoma and stimulates neuritogenesis in cultured retinal ganglion cells. *Neurobiol. Dis.* **48**, 568–581.

Chrysostomou V. and Crowston J. G. (2013) The photopic negative response of the mouse electroretinogram: reduction by acute elevation of intraocular pressure. *Invest. Ophthalmol. Vis. Sci.* **54**, 4691–4697.

Codeluppi S., Fernandez-Zafra T., Sandor K. *et al.* (2014) Interleukin-6 secretion by astrocytes is dynamically regulated by PI3K-mTOR-calcium signaling. *PLoS ONE* **9**, e92649.

Communi D., Parmentier M. and Boeynaems J. M. (1996) Cloning, functional expression and tissue distribution of the human P2Y6 receptor. *Biochem. Biophys. Res. Commun.* **222**, 303–308.

Corps K. N., Roth T. L. and McGavern D. B. (2015) Inflammation and neuroprotection in traumatic brain injury. *JAMA Neurol.* **72**, 355–362.

Corriden R. and Insel P. A. (2010) Basal release of ATP: an autocrine-paracrine mechanism for cell regulation. *Sci. Signal.* **3**, 104, re1.

Crowston J. G., Kong Y. X., Trounce I. A., Dang T. M., Fahy E. T., Bui B. V., Morrison J. C. and Chrysostomou V. (2015) An acute intraocular pressure challenge to assess retinal ganglion cell injury and recovery in the mouse. *Exp. Eye Res.* **141**, 3–8.

Downs J. C. (2015) Optic nerve head biomechanics in aging and disease. *Exp. Eye Res.* **133**, 19–29.

Downs J. C., Roberts M. D. and Burgoyne C. F. (2008) Mechanical environment of the optic nerve head in glaucoma. *Optom. Vis. Sci.* **85**, 425–435.

Erta M., Quintana A. and Hidalgo J. (2012) Interleukin-6, a major cytokine in the central nervous system. *Int. J. Biol. Sci.* **8**, 1254–1266.

Ferrari D., Pizzirani C., Adinolfi E., Lemoli R. M., Curti A., Idzko M., Panther E. and Di Virgilio F. (2006) The P2X7 receptor: a key player in IL-1 processing and release. *J. Immunol.* **176**, 3877–3883.

Franceschini A., Capece M., Chiozzi P., Falzoni S., Sanz J. M., Sarti A. C., Bonora M., Pinton P. and Di Virgilio F. (2015) The P2X7 receptor directly interacts with the NLRP3 inflammasome scaffold protein. *FASEB J.* **29**, 2450–2461.

Franke H., Schepper C., Illes P. and Krügel U. (2007) Involvement of P2X and P2Y receptors in microglial activation in vivo. *Purinergic Signal* **3**, 435–445.

Gombault A., Baron L. and Couillin I. (2012) ATP release and purinergic signaling in NLRP3 inflammasome activation. *Front Immunol.* **3**, 414.

Guha S., Baltazar G. C., Coffey E. E. *et al.* (2013) Lysosomal alkalinization, lipid oxidation, impaired autophagy and reduced phagosome clearance triggered by P2X7 receptor activation in retinal pigmented epithelial cells. *FASEB J.* **27**, 4500–4509.

Guo Y., Johnson E. C., Cepurna W. O., Dyck J. A., Doser T. and Morrison J. C. (2011) Early gene expression changes in the retinal ganglion cell layer of a rat glaucoma model. *Invest. Ophthalmol. Vis. Sci.* **52**, 1460–1473.

Hanley P. J., Musset B., Renigunta V., Limberg S. H., Dalpke A. H., Sus R., Heeg K. M., Preisig-Muller R. and Daut J. (2004) Extracellular ATP induces oscillations of intracellular Ca^{2+} and membrane potential and promotes transcription of IL-6 in macrophages. *Proc. Natl Acad. Sci. USA* **101**, 9479–9484.

Hernandez M. R. (2000) The optic nerve head in glaucoma: role of astrocytes in tissue remodeling. *Prog. Retin. Eye Res.* **19**, 297–321.

Honore P., Donnelly-Roberts D., Namovic M. *et al.* (2009) The antihyperalgesic activity of a selective P2X7 receptor antagonist, A-839977, is lost in IL-1alphabeta knockout mice. *Behav. Brain Res.* **204**, 77–81.

Hu H., Lu W., Zhang M. *et al.* (2010) Stimulation of the P2X7 receptor kills rat retinal ganglion cells in vivo. *Exp. Eye Res.* **91**, 425–432.

Iglesias R., Dahl G., Qiu F., Spray D. C. and Scemes E. (2009) Pannexin 1: the molecular substrate of astrocyte "hemichannels". *J. Neurosci.* **29**, 7092–7097.

Inoue K., Hosoi J. and Denda M. (2007) Extracellular ATP has stimulatory effects on the expression and release of IL-6 via purinergic receptors in normal human epidermal keratinocytes. *J. Invest. Dermatol.* **127**, 362–371.

Jo A. O., Ryskamp D. A., Phuong T. T., Verkman A. S., Yarishkin O., MacAulay N. and Krizaj D. (2015) TRPV4 and AQP4 channels synergistically regulate cell volume and calcium homeostasis in retinal Muller glia. *J. Neurosci.* **35**, 13525–13537.

Johnson E. C., Doser T. A., Cepurna W. O., Dyck J. A., Jia L., Guo Y., Lambert W. S. and Morrison J. C. (2011) Cell proliferation and interleukin-6-type cytokine signaling are implicated by gene expression responses in early optic nerve head injury in rat glaucoma. *Invest. Ophthalmol. Vis. Sci.* **52**, 504–518.

Kawano A., Kadomatsu R., Ono M., Kojima S., Tsukimoto M. and Sakamoto H. (2015) Autocrine regulation of UVA-induced IL-6 production via release of ATP and activation of P2Y receptors. *PLoS ONE* **10**, e0127919.

Kezic J. M., Chrysostomou V., Trounce I. A., McMenamin P. G. and Crowston J. G. (2013) Effect of anterior chamber cannulation and acute IOP elevation on retinal macrophages in the adult mouse. *Invest. Ophthalmol. Vis. Sci.* **54**, 3028–3036.

Kumar R. G., Diamond M. L., Boles J. A., Berger R. P., Tisherman S. A., Kochanek P. M. and Wagner A. K. (2015) Acute CSF interleukin-6 trajectories after TBI: associations with neuroinflammation, polytrauma, and outcome. *Brain Behav. Immun.* **45**, 253–262.

Li A., Zhang X., Zheng D., Ge J., Laties A. M. and Mitchell C. H. (2011) Sustained elevation of extracellular ATP in aqueous humor from humans with primary chronic angle-closure glaucoma. *Exp. Eye Res.* **93**, 528–533.

Lim J. C., Lu W., Beckel J. M., Macarak E. J., Laties A. M. and Mitchell C. H. (2011) Mechanosensitive release of cytokines and chemokines from isolated retinal ganglion cells. *Invest. Ophthalmol. Vis. Sci.* **52**, 5458. ARVO-E-Abstract.

Lim J. C., Lu W., Beckel J. M. and Mitchell C. H. (2016) Neuronal release of cytokine IL-3 triggered by mechanosensitive autostimulation of the P2X7 receptor is neuroprotective. *Front. Cell. Neurosci.* **10**, 270.

Lu W., Reigada D., Sevigny J. and Mitchell C. H. (2007) Stimulation of the P2Y1 receptor up-regulates nucleoside-triphosphate diphosphohydrolase-1 in human retinal pigment epithelial cells. *J. Pharmacol. Exp. Ther.* **323**, 157–164.

Lu W., Guo Y., Huwe J., Laties A. M. and Mitchell C. H. (2011) Pressure, purines and cytokines; early response genes upregulated by short term IOP elevation. *Invest. Ophthalmol. Vis. Sci.* **52**, 5345. ARVO E-Abstract.

Lu W., Beckel J., Lim J., Zode G., Sheffield V., Laties A. and Mitchell C. (2013) Elevation of IOP triggers responses from cytokines IL-6 and IL-1β; involvement of both optic nerve head astrocytes and retinal ganglion cells. *Invest. Ophthalmol. Vis. Sci.* **54**, 784. ARVO E-Abstract.

Lu W., Hu H., Sevigny J. *et al.* (2015) Rat, mouse, and primate models of chronic glaucoma show sustained elevation of extracellular ATP and altered purinergic signaling in the posterior eye. *Invest. Ophthalmol. Vis. Sci.* **56**, 3075–3083.

Mandal A., Shahidullah M., Delamere N. A. and Teran M. A. (2009) Elevated hydrostatic pressure activates sodium/hydrogen exchanger-1 in rat optic nerve head astrocytes. *Am J Physiol Cell Physiol.* **297**, C111–120.

Morrison J. C., Cepurna W. O., Doser T. A., Dyck J. A. and Johnson E. C. (2010) A short interval of controlled elevation of IOP (CEI) reproduces early chronic glaucoma model optic nerve head (ONH) gene expression responses. *Invest. Ophthalmol. Vis. Sci.* **51**, 5216. ARVO E-Abstract.

Morrison J. C., Choe T. E., Cepurna W. O. and Johnson E. C. (2014) Optic nerve head (ONH) gene expression responses to elevated intraocular pressure (IOP), anesthesia and anterior chamber cannulation in the CEI (Controlled Elevation of IOP) model of IOP-induced optic nerve injury. *Invest. Ophthalmol. Vis. Sci.* **55**, 2402. ARVO E-Abstract.

Penkowa M., Giralt M., Lago N., Camats J., Carrasco J., Hernandez J., Molinero A., Campbell I. L. and Hidalgo J. (2003) Astrocyte-targeted expression of IL-6 protects the CNS against a focal brain injury. *Exp. Neurol.* **181**, 130–148.

Praetorius H. A. and Leipziger J. (2009) ATP release from non-excitable cells. *Purinergic Signal* **5**, 433–446.

Reigada D., Lu W., Zhang M. and Mitchell C. H. (2008) Elevated pressure triggers a physiological release of ATP from the retina: possible role for pannexin hemichannels. *Neuroscience* **157**, 396–404.

Sanderson J., Dartt D. A., Trinkaus-Randall V. *et al.* (2014) Purines in the eye: recent evidence for the physiological and pathological role of purines in the RPE, retinal neurons, astrocytes, Muller cells, lens, trabecular meshwork, cornea and lacrimal gland. *Exp. Eye Res.* **127**, 270–279.

Sappington R. M., Chan M. and Calkins D. J. (2006) Interleukin-6 protects retinal ganglion cells from pressure-induced death. *Invest. Ophthalmol. Vis. Sci.* **47**, 2932–2942.

Satrawaha S., Wongkhantee S., Pavasant P. and Sumrejkanchanakij P. (2011) Pressure induces interleukin-6 expression via the P2Y6 receptor in human dental pulp cells. *Arch. Oral Biol.* **56**, 1230–1237.

Shahidullah M., Mandal A. and Delamere N. A. (2012) TRPV4 in porcine lens epithelium regulates hemichannel-mediated ATP release and Na-K-ATPase activity. *Am. J. Physiol. Cell Physiol.* **302**, C1751–C1761.

Shieh C. H., Heinrich A., Serchov T., van Calker D. and Biber K. (2014) P2X7-dependent, but differentially regulated release of IL-6, CCL2, and TNF-alpha in cultured mouse microglia. *Glia* **62**, 592–607.

Shigemoto-Mogami Y., Koizumi S., Tsuda M., Ohsawa K., Kohsaka S. and Inoue K. (2001) Mechanisms underlying extracellular ATP-evoked interleukin-6 release in mouse microglial cell line, MG-5. *J. Neurochem.* **78**, 1339–1349.

Sigal I. A. and Ethier C. R. (2009) Biomechanics of the optic nerve head. *Exp. Eye Res.* **88**, 799–807.

Solle M., Labasi J., Perregaux D. G., Stam E., Petrushova N., Koller B. H., Griffiths R. J. and Gabel C. A. (2001) Altered cytokine production in mice lacking P2X(7) receptors. *J. Biol. Chem.* **276**, 125–132.

Spooren A., Kolmus K., Laureys G., Clinckers R., De Keyser J., Haegeman G. and Gerlo S. (2011) Interleukin-6, a mental cytokine. *Brain Res. Rev.* **67**, 157–183.

Totan Y., Guler E. and Dervisogullari M. S. (2014) Brilliant Blue G assisted epiretinal membrane surgery. *Sci. Rep.* **4**, 3956.

Wildman S. S., Unwin R. J. and King B. F. (2003) Extended pharmacological profiles of rat P2Y2 and rat P2Y4 receptors and their sensitivity to extracellular H^+ and Zn^{2+} ions. *Br. J. Pharmacol.* **140**, 1177–1186.

Wilson G. N., Inman D. M., Dengler Crish C. M., Smith M. A. and Crish S. D. (2015) Early pro-inflammatory cytokine elevations in the DBA/2J mouse model of glaucoma. *J. Neuroinflammation* **12**, 176.

Winston F. K., Macarak E. J., Gorfien S. F. and Thibault L. E. (1989) A system to reproduce and quantify the biomechanical environment of the cell. *J. Appl. Physiol.* **67**, 397–405.

Xia J., Lim J. C., Lu W., Beckel J. M., Macarak E. J., Laties A. M. and Mitchell C. H. (2012) Neurons respond directly to mechanical deformation with pannexin-mediated ATP release and autostimulation of P2X7 receptors. *J. Physiol.* **590**, 2285–2304.

Yang S. H., Gangidine M., Pritts T. A., Goodman M. D. and Lentsch A. B. (2013) Interleukin 6 mediates neuroinflammation and motor coordination deficits after mild traumatic brain injury and brief hypoxia in mice. *Shock* **40**, 471–475.

Zenkel M., Lewczuk P., Junemann A., Kruse F. E., Naumann G. O. and Schlotzer-Schrehardt U. (2010) Proinflammatory cytokines are involved in the initiation of the abnormal matrix process in pseudoexfoliation syndrome/glaucoma. *Am. J. Pathol.* **176**, 2868–2879.

Zhang X., Zhang M., Laties A. M. and Mitchell C. H. (2006) Balance of purines may determine life or death of retinal ganglion cells as A3 adenosine receptors prevent loss following P2X7 receptor stimulation. *J. Neurochem.* **98**, 566–575.

Zhang X., Li A., Ge J., Reigada D., Laties A. M. and Mitchell C. H. (2007) Acute increase of intraocular pressure releases ATP into the anterior chamber. *Exp. Eye Res.* **85**, 637–643.

Zhang M., Hu H., Zhang X., Lu W., Lim J., Eysteinsson T., Jacobson K. A., Laties A. M. and Mitchell C. H. (2010) The A3 adenosine receptor attenuates the calcium rise triggered by NMDA receptors in retinal ganglion cells. *Neurochem. Int.* **56**, 35–41.

Zhi Z., Cepurna W. O., Johnson E. C., Morrison J. C. and Wang R. K. (2012) Impact of intraocular pressure on changes of blood flow in the retina, choroid, and optic nerve head in rats investigated by optical microangiography. *Biomed. Opt. Express* **3**, 2220–2233.

The P2X7 receptor links mechanical strain to cytokine IL-6 upregulation and release in neurons and astrocytes

Authors: Wennan Lu[1], Farraj Albalawi[1,2] Jonathan M. Beckel[1,5], Jason C. Lim[1], Alan M. Laties[3], Claire H. Mitchell[1,3,4]

Author affiliation: Departments of [1]Anatomy and Cell Biology, [2]Orthodontics, [3]Ophthalmology and [4]Physiology, University of Pennsylvania, Philadelphia, PA 19104; [5]Department of Pharmacology and Chemical Biology, University of Pittsburgh, PA 15261

E-mail addresses: wennan@upenn.edu; farrajsaad@gmail.com; JMBECKEL@pitt.edu; jclim23@hotmail.com; chm@upenn.edu

Contact information: Dr. Claire H. Mitchell, Department of Anatomy and Cell Biology, University of Pennsylvania, 240 S. 40th St, Philadelphia, PA 19104-6030

Tel: 215-898-8994 FAX: 215-573-2324 e-mail:chm@upenn.edu

Figure S1

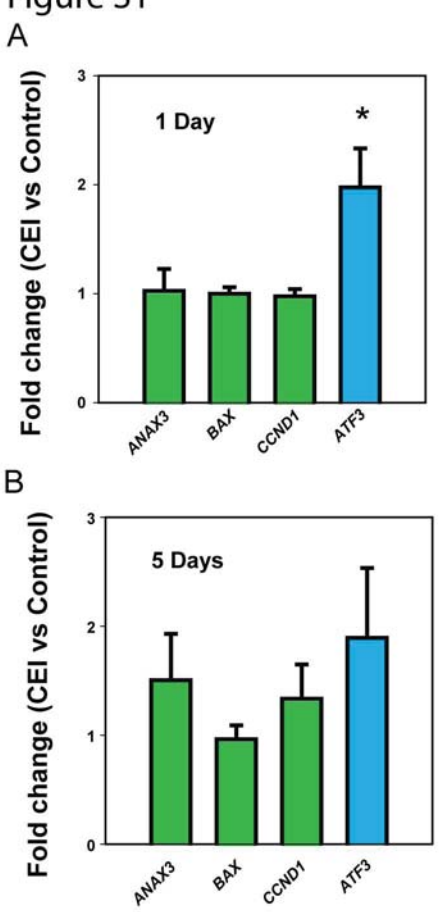

Figure S1. Changes in gene expression 1 day and 5 days after CEI to 50 mm Hg for 4 hours.

Summary of qPCR results from retinas exposed to moderate non-ischemic Controlled elevation of IOP (CEI) to 50 mmHg for 4 hrs (A). One day after the CEI procedure, significant increases were found in expression of early response transcription factor ATF3 (p=0.031), but not pre-apoptosis genes ANAX3, BAX or CCND1. (B). ATF3 was not significantly elevated 5 days after the procedure.

Figure S2

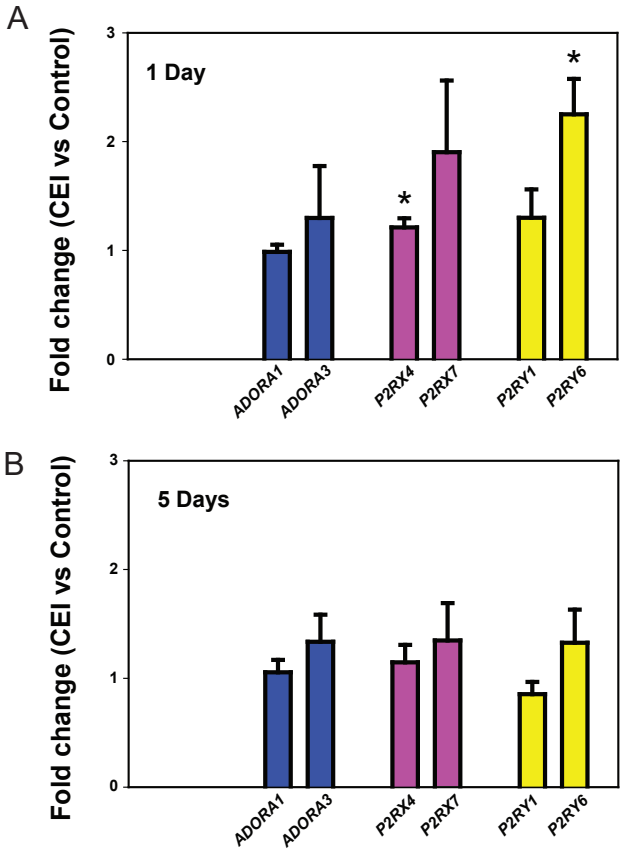

Figure S2. Changes in expression of purine genes 1 day and 5 days after CEI to 50 mm Hg for 4 hours.

A. Levels of purinergic genes P2RX4 (p=0.017) and P2RY6 (p=0.001) were elevated 1 day after the moderate elevation of IOP
B. Neither remained elevated 5 days after the procedure .
N=9-10 for retinas examined 1 day after IOP elevation and 6-8 for 5 days.
It should ne noted that the response of the P2Y6 receptor may be complicated by the presence of multiple transcription sites.

REFERENCES

Abbott, C.J., Choe, T.E., Lusardi, T.A., Burgoyne, C.F., Wang, L., and Fortune, B. (2014). Evaluation of retinal nerve fiber layer thickness and axonal transport 1 and 2 weeks after 8 hours of acute intraocular pressure elevation in rats. Invest Ophthalmol Vis Sci *55*, 674-687.

Agostini, L., Martinon, F., Burns, K., McDermott, M.F., Hawkins, P.N., and Tschopp, J. (2004). NALP3 forms an IL-1beta-processing inflammasome with increased activity in Muckle-Wells autoinflammatory disorder. Immunity *20*, 319-325.

Albalawi, F., Lu, W., Lim, J., and Mitchell, C.H. (2016). The Role of P2X7R in Priming the NLRP3 Inflammasome after Mechanical Strain. The FASEB Journal *30*, 745.744.

Arulkumaran, N., Unwin, R.J., and Tam, F.W. (2011). A potential therapeutic role for P2X7 receptor (P2X7R) antagonists in the treatment of inflammatory diseases. Expert Opin Investig Drugs *20*, 897-915.

Balaratnasingam, C., Morgan, W.H., Bass, L., Matich, G., Cringle, S.J., and Yu, D.Y. (2007). Axonal transport and cytoskeletal changes in the laminar regions after elevated intraocular pressure. Invest Ophthalmol Vis Sci *48*, 3632-3644.

Bao, L., Locovei, S., and Dahl, G. (2004). Pannexin membrane channels are mechanosensitive conduits for ATP. FEBS Lett *572*, 65-68.

Bauernfeind, F.G., Horvath, G., Stutz, A., Alnemri, E.S., MacDonald, K., Speert, D., Fernandes-Alnemri, T., Wu, J., Monks, B.G., Fitzgerald, K.A.*, et al.* (2009). Cutting edge: NF-kappaB activating pattern recognition and cytokine receptors license NLRP3 inflammasome activation by regulating NLRP3 expression. Journal of immunology (Baltimore, Md: 1950) *183*, 787-791.

Beckel, J.M., Argall, A.J., Lim, J.C., Xia, J., Lu, W., Coffey, E.E., Macarak, E.J., Shahidullah, M., Delamere, N.A., Zode, G.S.*, et al.* (2014). Mechanosensitive release of adenosine 5'-triphosphate through pannexin channels and mechanosensitive upregulation of pannexin channels in optic nerve head

astrocytes: a mechanism for purinergic involvement in chronic strain. Glia *62*, 1486-1501.

Bellezza, A.J., Rintalan, C.J., Thompson, H.W., Downs, J.C., Hart, R.T., and Burgoyne, C.F. (2003). Anterior scleral canal geometry in pressurised (IOP 10) and non-pressurised (IOP 0) normal monkey eyes. The British journal of ophthalmology *87*, 1284-1290.

Benveniste, E.N., Sparacio, S.M., Norris, J.G., Grenett, H.E., and Fuller, G.M. (1990). Induction and regulation of interleukin-6 gene expression in rat astrocytes. J Neuroimmunol *30*, 201-212.

Bernier, L.P. (2012). Purinergic regulation of inflammasome activation after central nervous system injury. J Gen Physiol *140*, 571-575.

Bezbradica, J.S., Coll, R.C., and Schroder, K. (2017). Sterile signals generate weaker and delayed macrophage NLRP3 inflammasome responses relative to microbial signals. Cell Mol Immunol *14*, 118-126.

Bo, X., Jiang, L.H., Wilson, H.L., Kim, M., Burnstock, G., Surprenant, A., and North, R.A. (2003). Pharmacological and biophysical properties of the human P2X5 receptor. Molecular pharmacology *63*, 1407-1416.

Boaru, S.G., Borkham-Kamphorst, E., Van de Leur, E., Lehnen, E., Liedtke, C., and Weiskirchen, R. (2015). NLRP3 inflammasome expression is driven by NF-kappaB in cultured hepatocytes. Biochem Biophys Res Commun *458*, 700-706.

Boassa, D., Ambrosi, C., Qiu, F., Dahl, G., Gaietta, G., and Sosinsky, G. (2007). Pannexin1 channels contain a glycosylation site that targets the hexamer to the plasma membrane. J Biol Chem *282*, 31733-31743.

Boassa, D., Qiu, F., Dahl, G., and Sosinsky, G. (2008). Trafficking dynamics of glycosylated pannexin 1 proteins. Cell communication & adhesion *15*, 119-132.

Brandt, R.G., Anderson, P.F., McDonald, N.J., Sohn, W., and Peters, M.C. (2011). The pulpal anesthetic efficacy of articaine versus lidocaine in dentistry: a meta-analysis. J Am Dent Assoc *142*, 493-504.

Broz, P. (2015). Inflammasome assembly: The wheels are turning. Cell Res *25*, 1277-1278.

Broz, P., Newton, K., Lamkanfi, M., Mariathasan, S., Dixit, V.M., and Monack, D.M. (2010). Redundant roles for inflammasome receptors NLRP3 and NLRC4 in host defense against Salmonella. J Exp Med *207*, 1745-1755.

Bruzzone, R., Barbe, M.T., Jakob, N.J., and Monyer, H. (2005). Pharmacological properties of homomeric and heteromeric pannexin hemichannels expressed in Xenopus oocytes. J Neurochem *92*, 1033-1043.

Burgoyne, C.F. (2011). A biomechanical paradigm for axonal insult within the optic nerve head in aging and glaucoma. Experimental eye research *93*, 120-132.

Burgoyne, C.F., Downs, J.C., Bellezza, A.J., Suh, J.K., and Hart, R.T. (2005). The optic nerve head as a biomechanical structure: a new paradigm for understanding the role of IOP-related stress and strain in the pathophysiology of glaucomatous optic nerve head damage. Prog Retin Eye Res *24*, 39-73.

Burgoyne, C.F., Quigley, H.A., Thompson, H.W., Vitale, S., and Varma, R. (1995). Early changes in optic disc compliance and surface position in experimental glaucoma. Ophthalmology *102*, 1800-1809.

Burnstock, G. (1972). Purinergic nerves. Pharmacol Rev *24*, 509-581.

Burnstock, G. (1980). Purinergic nerves and receptors. Prog Biochem Pharmacol *16*, 141-154.

Burnstock, G. (1999). Release of vasoactive substances from endothelial cells by shear stress and purinergic mechanosensory transduction. J Anat *194 (Pt 3)*, 335-342.

Burnstock, G. (2004). Introduction: P2 receptors. Current topics in medicinal chemistry *4*, 793-803.

Burnstock, G. (2009). Purinergic cotransmission. Exp Physiol *94*, 20-24.

Burnstock, G. (2012). Discovery of purinergic signalling, the initial resistance and current explosion of interest. Br J Pharmacol *167*, 238-255.

Burnstock, G. (2014). Purinergic signalling: from discovery to current developments. Exp Physiol *99*, 16-34.

Burnstock, G., and Kennedy, C. (2011). P2X receptors in health and disease. Adv Pharmacol *61*, 333-372.

Bustamante, M., Fernandez-Verdejo, R., Jaimovich, E., and Buvinic, S. (2014). Electrical stimulation induces IL-6 in skeletal muscle through extracellular ATP by activating Ca(2+) signals and an IL-6 autocrine loop. American journal of physiology Endocrinology and metabolism *306*, E869-882.

Cabrera, C.L., Wagner, L.A., Schork, M.A., Bohr, D.F., and Cohan, B.E. (1999). Intraocular pressure measurement in the conscious rat. Acta Ophthalmol Scand *77*, 33-36.

Cadman, E.D., Naugles, D.D., and Lee, C.M. (1994). cAMP is not involved in interleukin-1-induced interleukin-6 release from human astrocytoma cells. Neurosci Lett *178*, 251-254.

Casson, R.J., Chidlow, G., Wood, J.P., Crowston, J.G., and Goldberg, I. (2012). Definition of glaucoma: clinical and experimental concepts. Clinical & experimental ophthalmology *40*, 341-349.

Catterall, W.A., Goldin, A.L., and Waxman, S.G. (2005). International Union of Pharmacology. XLVII. Nomenclature and structure-function relationships of voltage-gated sodium channels. Pharmacol Rev *57*, 397-409.

Cepurna, W.O., Guo, Y., Doser, T.A., Dyck, J.A., Johnson, E.C., and Morrison, J.C. (2008). An interval of controlled intraocular pressure elevation alters optic nerve head gene expression without compromising retinal perfusion. Invest Ophthalmol Vis Sci *49*, ARVO E-Abstract 3695.

Chalaris, A., Rabe, B., Paliga, K., Lange, H., Laskay, T., Fielding, C.A., Jones, S.A., Rose-John, S., and Scheller, J. (2007). Apoptosis is a natural stimulus of IL6R shedding and contributes to the proinflammatory trans-signaling function of neutrophils. Blood *110*, 1748-1755.

Chalfie, M. (2009). Neurosensory mechanotransduction. Nat Rev Mol Cell Biol *10*, 44-52.

Chekeni, F.B., Elliott, M.R., Sandilos, J.K., Walk, S.F., Kinchen, J.M., Lazarowski, E.R., Armstrong, A.J., Penuela, S., Laird, D.W., Salvesen, G.S.*, et al.* (2010). Pannexin 1 channels mediate 'find-me' signal release and membrane permeability during apoptosis. Nature *467*, 863-867.

Chen, K.H., Wu, C.C., Roy, S., Lee, S.M., and Liu, J.H. (1999). Increased interleukin-6 in aqueous humor of neovascular glaucoma. Investigative ophthalmology & visual science *40*, 2627-2632.

Chi, W., Chen, H., Li, F., Zhu, Y., Yin, W., and Zhuo, Y. (2015). HMGB1 promotes the activation of NLRP3 and caspase-8 inflammasomes via NF-kappaB pathway in acute glaucoma. J Neuroinflammation *12*, 137.

Chi, W., Li, F., Chen, H., Wang, Y., Zhu, Y., Yang, X., Zhu, J., Wu, F., Ouyang, H., Ge, J.*, et al.* (2014). Caspase-8 promotes NLRP1/NLRP3 inflammasome

activation and IL-1beta production in acute glaucoma. Proceedings of the National Academy of Sciences of the United States of America *111*, 11181-11186.

Chidlow, G., Wood, J.P., Ebneter, A., and Casson, R.J. (2012). Interleukin-6 is an efficacious marker of axonal transport disruption during experimental glaucoma and stimulates neuritogenesis in cultured retinal ganglion cells. Neurobiology of disease *48*, 568-581.

Choi, A.J., and Ryter, S.W. (2014). Inflammasomes: molecular regulation and implications for metabolic and cognitive diseases. Mol Cells *37*, 441-448.

Choi, H.J., Sun, D., and Jakobs, T.C. (2015). Astrocytes in the optic nerve head express putative mechanosensitive channels. Mol Vis *21*, 749-766.

Choi, S.S., Lee, H.J., Lim, I., Satoh, J., and Kim, S.U. (2014). Human astrocytes: secretome profiles of cytokines and chemokines. PLoS One *9*, e92325.

Chrysostomou, V., and Crowston, J.G. (2013). The photopic negative response of the mouse electroretinogram: reduction by acute elevation of intraocular pressure. Investigative ophthalmology & visual science *54*, 4691-4697.

Codeluppi, S., Fernandez-Zafra, T., Sandor, K., Kjell, J., Liu, Q., Abrams, M., Olson, L., Gray, N.S., Svensson, C.I., and Uhlen, P. (2014). Interleukin-6 secretion by astrocytes is dynamically regulated by PI3K-mTOR-calcium signaling. PloS one *9*, e92649.

Cogswell, J.P., Godlevski, M.M., Wisely, G.B., Clay, W.C., Leesnitzer, L.M., Ways, J.P., and Gray, J.G. (1994). NF-kappa B regulates IL-1 beta transcription through a consensus NF-kappa B binding site and a nonconsensus CRE-like site. Journal of immunology *153*, 712-723.

Communi, D., Parmentier, M., and Boeynaems, J.M. (1996). Cloning, functional expression and tissue distribution of the human P2Y6 receptor. Biochem Biophys Res Commun *222*, 303-308.

Corps, K.N., Roth, T.L., and McGavern, D.B. (2015). Inflammation and neuroprotection in traumatic brain injury. JAMA Neurol *72*, 355-362.

Corriden, R., and Insel, P.A. (2010). Basal release of ATP: an autocrine-paracrine mechanism for cell regulation. Science signaling *3*, re1.

Coste, B., Mathur, J., Schmidt, M., Earley, T.J., Ranade, S., Petrus, M.J., Dubin, A.E., and Patapoutian, A. (2010). Piezo1 and Piezo2 are essential components of distinct mechanically activated cation channels. Science *330*, 55-60.

Cotrina, M.L., Lin, J.H., Alves-Rodrigues, A., Liu, S., Li, J., Azmi-Ghadimi, H., Kang, J., Naus, C.C., and Nedergaard, M. (1998). Connexins regulate calcium signaling by controlling ATP release. Proceedings of the National Academy of Sciences of the United States of America *95*, 15735-15740.

Crowston, J.G., Kong, Y.X., Trounce, I.A., Dang, T.M., Fahy, E.T., Bui, B.V., Morrison, J.C., and Chrysostomou, V. (2015). An acute intraocular pressure challenge to assess retinal ganglion cell injury and recovery in the mouse. Experimental eye research *141*, 3-8.

Dahl, G. (2015). ATP release through pannexon channels. Philos Trans R Soc Lond B Biol Sci *370*.

Dahl, G., Qiu, F., and Wang, J. (2013). The bizarre pharmacology of the ATP release channel pannexin1. Neuropharmacology *75*, 583-593.

Deguine, J., and Barton, G.M. (2014). MyD88: a central player in innate immune signaling. F1000Prime Rep *6*, 97.

Dinarello, C.A. (2002). The IL-1 family and inflammatory diseases. Clin Exp Rheumatol *20*, S1-13.

Dinarello, C.A. (2007). Interleukin-18 and the pathogenesis of inflammatory diseases. Seminars in nephrology *27*, 98-114.

Dinarello, C.A. (2011). A clinical perspective of IL-1beta as the gatekeeper of inflammation. European journal of immunology *41*, 1203-1217.

Donnelly-Roberts, D.L., Namovic, M.T., Han, P., and Jarvis, M.F. (2009a). Mammalian P2X7 receptor pharmacology: comparison of recombinant mouse, rat and human P2X7 receptors. Br J Pharmacol *157*, 1203-1214.

Donnelly-Roberts, D.L., Namovic, M.T., Han, P., and Jarvis, M.F. (2009b). Mammalian P2X7 receptor pharmacology: comparison of recombinant mouse, rat and human P2X7 receptors. British Journal of Pharmacology *157*, 1203-1214.

Downs, J.C. (2015). Optic nerve head biomechanics in aging and disease. Experimental eye research *133*, 19-29.

Downs, J.C., Roberts, M.D., and Burgoyne, C.F. (2008). Mechanical environment of the optic nerve head in glaucoma. Optom Vis Sci *85*, 425-435.

Drenth, J.P., and Waxman, S.G. (2007). Mutations in sodium-channel gene SCN9A cause a spectrum of human genetic pain disorders. J Clin Invest *117*, 3603-3609.

Erta, M., Quintana, A., and Hidalgo, J. (2012). Interleukin-6, a major cytokine in the central nervous system. International journal of biological sciences *8*, 1254-1266.

Ferrari, D., Pizzirani, C., Adinolfi, E., Lemoli, R.M., Curti, A., Idzko, M., Panther, E., and Di Virgilio, F. (2006). The P2X7 receptor: a key player in IL-1 processing and release. J Immunol *176*, 3877-3883.

Finco, T.S., and Baldwin, A.S. (1995). Mechanistic aspects of NF-κB regulation: The emerging role of phosphorylation and proteolysis. Immunity *3*, 263-272.

Flexcell (2011). BioFlex Culture Plate.

Franceschini, A., Capece, M., Chiozzi, P., Falzoni, S., Sanz, J.M., Sarti, A.C., Bonora, M., Pinton, P., and Di Virgilio, F. (2015). The P2X7 receptor directly interacts with the NLRP3 inflammasome scaffold protein. FASEB journal : official publication of the Federation of American Societies for Experimental Biology *29*, 2450-2461.

Franke, H., Schepper, C., Illes, P., and Krügel, U. (2007). Involvement of P2X and P2Y receptors in microglial activation in vivo. Purinergic signalling *3*, 435-445.

Freeman, L.C., and Ting, J.P. (2016). The pathogenic role of the inflammasome in neurodegenerative diseases. J Neurochem *136 Suppl 1*, 29-38.

Garisto, G.A., Gaffen, A.S., Lawrence, H.P., Tenenbaum, H.C., and Haas, D.A. (2010). Occurrence of paresthesia after dental local anesthetic administration in the United States. J Am Dent Assoc *141*, 836-844.

Gianchecchi, E., and Fierabracci, A. (2015). Gene/environment interactions in the pathogenesis of autoimmunity: new insights on the role of Toll-like receptors. Autoimmun Rev *14*, 971-983.

Gombault, A., Baron, L., and Couillin, I. (2012). ATP release and purinergic signaling in NLRP3 inflammasome activation. Frontiers in immunology *3*, 414.

Goodson, J.M., and Moore, P.A. (1983). Life-threatening reactions after pedodontic sedation: an assessment of narcotic, local anesthetic, and antiemetic drug interaction. J Am Dent Assoc *107*, 239-245.

Grygorczyk, R., Furuya, K., and Sokabe, M. (2013). Imaging and characterization of stretch-induced ATP release from alveolar A549 cells. The Journal of physiology *591*, 1195-1215.

Guha, S., Baltazar, G.C., Coffey, E.E., Tu, L.A., Lim, J.C., Beckel, J.M., Patel, S., Eysteinsson, T., Lu, W., O'Brien-Jenkins, A.*, et al.* (2013). Lysosomal alkalinization, lipid oxidation, and reduced phagosome clearance triggered by activation of the P2X7 receptor. FASEB journal : official publication of the Federation of American Societies for Experimental Biology *27*, 4500-4509

Guo, H., Callaway, J.B., and Ting, J.P. (2015). Inflammasomes: mechanism of action, role in disease, and therapeutics. Nat Med *21*, 677-687.

Guo, Y., Johnson, E.C., Cepurna, W.O., Dyck, J.A., Doser, T., and Morrison, J.C. (2011). Early gene expression changes in the retinal ganglion cell layer of a rat glaucoma model. Investigative ophthalmology & visual science *52*, 1460-1473.

Guptarak, J., Wanchoo, S., Durham-Lee, J., Wu, Y., Zivadinovic, D., Paulucci-Holthauzen, A., and Nesic, O. (2013). Inhibition of IL-6 signaling: A novel therapeutic approach to treating spinal cord injury pain. Pain *154*, 1115-1128.

Haas, D.A., and Lennon, D. (1995). A 21 year retrospective study of reports of paresthesia following local anesthetic administration. J Can Dent Assoc *61*, 319-320, 323-316, 329-330.

Halle, A., Hornung, V., Petzold, G.C., Stewart, C.R., Monks, B.G., Reinheckel, T., Fitzgerald, K.A., Latz, E., Moore, K.J., and Golenbock, D.T. (2008). The NALP3 inflammasome is involved in the innate immune response to amyloid-beta. Nature immunology *9*, 857-865.

Hamilton, N.B., and Attwell, D. (2010). Do astrocytes really exocytose neurotransmitters? Nat Rev Neurosci *11*, 227-238.

Hanley, P.J., Musset, B., Renigunta, V., Limberg, S.H., Dalpke, A.H., Sus, R., Heeg, K.M., Preisig-Muller, R., and Daut, J. (2004). Extracellular ATP induces oscillations of intracellular Ca2+ and membrane potential and promotes transcription of IL-6 in macrophages. Proc Natl Acad Sci U S A *101*, 9479-9484.

Hansson, G.K., and Klareskog, L. (2011). Pulling down the plug on atherosclerosis: cooling down the inflammasome. Nat Med *17*, 790-791.

Hattori, M., and Gouaux, E. (2012). Molecular mechanism of ATP binding and ion channel activation in P2X receptors. Nature *485*, 207-212.

Heinrich, P.C., Behrmann, I., Haan, S., Hermanns, H.M., Muller-Newen, G., and Schaper, F. (2003). Principles of interleukin (IL)-6-type cytokine signalling and its regulation. Biochem J *374*, 1-20.

Heppner, F.L., Ransohoff, R.M., and Becher, B. (2015). Immune attack: the role of inflammation in Alzheimer disease. Nat Rev Neurosci *16*, 358-372.

Hernandez, M.R. (2000). The optic nerve head in glaucoma: role of astrocytes in tissue remodeling. Prog Retin Eye Res *19*, 297-321.

Hernandez, M.R., Miao, H., and Lukas, T. (2008). Astrocytes in glaucomatous optic neuropathy. Progress in brain research *173*, 353-373.

Hersh, E.V., Helpin, M.L., and Evans, O.B. (1991). Local anesthetic mortality: report of case. ASDC journal of dentistry for children *58*, 489-491.

Hillerup, S., and Jensen, R. (2006). Nerve injury caused by mandibular block analgesia. International journal of oral and maxillofacial surgery *35*, 437-443.

Ho, K.W., Lambert, W.S., and Calkins, D.J. (2014). Activation of the TRPV1 cation channel contributes to stress-induced astrocyte migration. Glia *62*, 1435-1451.

Honore, P., Donnelly-Roberts, D., Namovic, M., Zhong, C., Wade, C., Chandran, P., Zhu, C., Carroll, W., Perez-Medrano, A., Iwakura, Y.*, et al.* (2009). The antihyperalgesic activity of a selective P2X7 receptor antagonist, A-839977, is lost in IL-1alphabeta knockout mice. Behav Brain Res *204*, 77-81.

Honore, P., Donnelly-Roberts, D., Namovic, M.T., Hsieh, G., Zhu, C.Z., Mikusa, J.P., Hernandez, G., Zhong, C., Gauvin, D.M., Chandran, P.*, et al.* (2006). A-740003 [N-(1-{[(cyanoimino)(5-quinolinylamino) methyl]amino}-2,2-dimethylpropyl)-2-(3,4-dimethoxyphenyl)acetamide], a novel and selective P2X7 receptor antagonist, dose-dependently reduces neuropathic pain in the rat. J Pharmacol Exp Ther *319*, 1376-1385.

Hu, H., Lu, W., Zhang, M., Zhang, X., Argall, A.J., Patel, S., Lee, G.E., Kim, Y.C., Jacobson, K.A., Laties, A.M.*, et al.* (2010). Stimulation of the P2X7 receptor kills rat retinal ganglion cells in vivo. Experimental eye research *91*, 425-432 PMCID 2941978.

Iglesias, R., Dahl, G., Qiu, F., Spray, D.C., and Scemes, E. (2009). Pannexin 1: the molecular substrate of astrocyte "hemichannels". J Neurosci *29*, 7092-7097.

Inoue, K., Hosoi, J., and Denda, M. (2007). Extracellular ATP has stimulatory effects on the expression and release of IL-6 via purinergic receptors in normal human epidermal keratinocytes. The Journal of investigative dermatology *127*, 362-371.

Ivashkiv, L.B., and Hu, X. (2003). The JAK/STAT pathway in rheumatoid arthritis: pathogenic or protective? Arthritis Rheum *48*, 2092-2096.

Jiang, L.H., Baldwin, J.M., Roger, S., and Baldwin, S.A. (2013). Insights into the Molecular Mechanisms Underlying Mammalian P2X7 Receptor Functions and Contributions in Diseases, Revealed by Structural Modeling and Single Nucleotide Polymorphisms. Front Pharmacol *4*, 55.

Jimenez-Dalmaroni, M.J., Gerswhin, M.E., and Adamopoulos, I.E. (2016). The critical role of toll-like receptors--From microbial recognition to autoimmunity: A comprehensive review. Autoimmun Rev *15*, 1-8.

Jo, A.O., Ryskamp, D.A., Phuong, T.T., Verkman, A.S., Yarishkin, O., MacAulay, N., and Krizaj, D. (2015). TRPV4 and AQP4 Channels Synergistically Regulate Cell Volume and Calcium Homeostasis in Retinal Muller Glia. The Journal of neuroscience : the official journal of the Society for Neuroscience *35*, 13525-13537.

Johansson, J.O. (1988). Inhibition and recovery of retrograde axoplasmic transport in rat optic nerve during and after elevated IOP in vivo. Experimental eye research *46*, 223-227.

Johnson, E.C., Doser, T.A., Cepurna, W.O., Dyck, J.A., Jia, L., Guo, Y., Lambert, W.S., and Morrison, J.C. (2011). Cell proliferation and interleukin-6-type cytokine signaling are implicated by gene expression responses in early optic nerve head injury in rat glaucoma. Invest Ophthalmol Vis Sci *52*, 504-518.

Johnson, E.C., and Morrison, J.C. (2009). Friend or foe? Resolving the impact of glial responses in glaucoma. J Glaucoma *18*, 341-353.

Juliana, C., Fernandes-Alnemri, T., Kang, S., Farias, A., Qin, F., and Alnemri, E.S. (2012). Non-transcriptional priming and deubiquitination regulate NLRP3 inflammasome activation. J Biol Chem *287*, 36617-36622.

Kanjanamekanant, K., Luckprom, P., and Pavasant, P. (2014). P2X7 receptor-Pannexin1 interaction mediates stress-induced interleukin-1 beta expression in human periodontal ligament cells. J Periodontal Res *49*, 595-602.

Karmakar, M., Katsnelson, M., Malak, H.A., Greene, N.G., Howell, S.J., Hise, A.G., Camilli, A., Kadioglu, A., Dubyak, G.R., and Pearlman, E. (2015). Neutrophil IL-1beta processing induced by pneumolysin is mediated by the NLRP3/ASC inflammasome and caspase-1 activation and is dependent on K+ efflux. In Journal of immunology, pp. 1763-1775.

Karmakar, M., Katsnelson, M.A., Dubyak, G.R., and Pearlman, E. (2016). Neutrophil P2X7 receptors mediate NLRP3 inflammasome-dependent IL-1beta secretion in response to ATP. Nature communications *7*, 10555.

Katsnelson, M.A., Rucker, L.G., Russo, H.M., and Dubyak, G.R. (2015). K+ efflux agonists induce NLRP3 inflammasome activation independently of Ca2+ signaling. Journal of immunology *194*, 3937-3952.

Kaushik, D.K., Gupta, M., Kumawat, K.L., and Basu, A. (2012). NLRP3 inflammasome: key mediator of neuroinflammation in murine Japanese encephalitis. PLoS One *7*, e32270.

Kawano, A., Kadomatsu, R., Ono, M., Kojima, S., Tsukimoto, M., and Sakamoto, H. (2015). Autocrine Regulation of UVA-Induced IL-6 Production via Release of ATP and Activation of P2Y Receptors. PloS one *10*, e0127919.

Kezic, J.M., Chrysostomou, V., Trounce, I.A., McMenamin, P.G., and Crowston, J.G. (2013). Effect of anterior chamber cannulation and acute IOP elevation on retinal macrophages in the adult mouse. Investigative ophthalmology & visual science *54*, 3028-3036.

Korcok, J., Raimundo, L.N., Ke, H.Z., Sims, S.M., and Dixon, S.J. (2004). Extracellular nucleotides act through P2X7 receptors to activate NF-kappa B in osteoclasts. J Bone Min Res *19*, 642-651.

Kumar, G., Kalita, J., and Misra, U.K. (2009). Raised intracranial pressure in acute viral encephalitis. Clin Neurol Neurosurg *111*, 399-406.

Kumar, R.G., Diamond, M.L., Boles, J.A., Berger, R.P., Tisherman, S.A., Kochanek, P.M., and Wagner, A.K. (2015). Acute CSF interleukin-6 trajectories after TBI: associations with neuroinflammation, polytrauma, and outcome. Brain, behavior, and immunity *45*, 253-262.

Lamkanfi, M., and Dixit, V.M. (2012). Inflammasomes and their roles in health and disease. Annu Rev Cell Dev Biol *28*, 137-161.

Lau, A., Arundine, M., Sun, H.S., Jones, M., and Tymianski, M. (2006). Inhibition of caspase-mediated apoptosis by peroxynitrite in traumatic brain injury. J Neurosci *26*, 11540-11553.

Lawrence, T. (2009). The nuclear factor NF-kappaB pathway in inflammation. Cold Spring Harb Perspect Biol *1*, a001651.

Lazarowski, E.R., Boucher, R.C., and Harden, T.K. (2003). Mechanisms of release of nucleotides and integration of their action as P2X- and P2Y-receptor activating molecules. Mol Pharmacol *64*, 785-795.

Le Guen, M., Grassin-Delyle, S., Naline, E., Buenestado, A., Brollo, M., Longchampt, E., Kleinmann, P., Devillier, P., and Faisy, C. (2016). The impact of low-frequency, low-force cyclic stretching of human bronchi on airway responsiveness. Respir Res *17*, 151.

Lee, J.K., Kim, S.H., Lewis, E.C., Azam, T., Reznikov, L.L., and Dinarello, C.A. (2004). Differences in signaling pathways by IL-1beta and IL-18. Proceedings of the National Academy of Sciences of the United States of America *101*, 8815-8820.

Leonard, W.J., and O'Shea, J.J. (1998). Jaks and STATs: biological implications. Annu Rev Immunol *16*, 293-322.

Li, A., Zhang, X., Zheng, D., Ge, J., Laties, A.M., and Mitchell, C.H. (2011). Sustained elevation of extracellular ATP in aqueous humor from humans with primary chronic angle-closure glaucoma. Experimental eye research *93*, 528-533 PMID:21745471 PMC23374644.

Liddelow, S.A., and Barres, B.A. (2017). Reactive Astrocytes: Production, Function, and Therapeutic Potential. Immunity *46*, 957-967.

Lilienbaum, A., and Israel, A. (2003). From calcium to NF-kappa B signaling pathways in neurons. Mol Cell Biol *23*, 2680-2698.

Lim, J.C., Lu, W., Beckel, J.M., and Mitchell, C.H. (2016). Neuronal Release of Cytokine IL-3 Triggered by Mechanosensitive Autostimulation of the P2X7 Receptor Is Neuroprotective. Front Cell Neurosci *10*, 270.

Lindhe, J., and Svanberg, G. (1974). Influence of trauma from occlusion on progression of experimental periodontitis in the beagle dog. J Clin Periodontol *1*, 3-14.

Liu, H.D., Li, W., Chen, Z.R., Hu, Y.C., Zhang, D.D., Shen, W., Zhou, M.L., Zhu, L., and Hang, C.H. (2013). Expression of the NLRP3 inflammasome in cerebral cortex after traumatic brain injury in a rat model. Neurochemical research *38*, 2072-2083.

Liu, H.T., Toychiev, A.H., Takahashi, N., Sabirov, R.Z., and Okada, Y. (2008). Maxi-anion channel as a candidate pathway for osmosensitive ATP release from mouse astrocytes in primary culture. Cell Res *18*, 558-565.

Liu, J., Li, Q., Liu, S., Gao, J., Qin, W., Song, Y., and Jin, Z. (2017). Periodontal Ligament Stem Cells in the Periodontitis Microenvironment Are Sensitive to Static Mechanical Strain. Stem Cells Int *2017*, 1380851.

Liu, Y., Xiao, Y., and Li, Z. (2011). P2X7 receptor positively regulates MyD88-dependent NF-kappaB activation. Cytokine *55*, 229-236.

Lohman, A.W., and Isakson, B.E. (2014). Differentiating connexin hemichannels and pannexin channels in cellular ATP release. FEBS Lett *588*, 1379-1388.

Lu, W., Albalawi, F., Lim, J.C., Beckel, J.M., and Mitchell, C.H. (2017). The P2X7 receptor links mechanical strain to cytokine IL-6 upregulation and release in neurons and astrocytes. J Neurochem.

Lu, W., Beckel, J., Lim, J., Zode, G., Sheffield, V., Laties, A., and Mitchell, C. (2013). Elevation of IOP triggers responses from cytokines IL-6 and IL-1{beta}; involvement of both optic nerve head astrocytes and retinal ganglion cells. Invest Ophthalmol Vis Sci *54*, 784-.

Lu, W., Hu, H., Sevigny, J., Gabelt, B.T., Kaufman, P.L., Johnson, E.C., Morrison, J.C., Zode, G.S., Sheffield, V.C., Zhang, X.*, et al.* (2015). Rat, mouse, and primate models of chronic glaucoma show sustained elevation of extracellular ATP and altered purinergic signaling in the posterior eye. Invest Ophthalmol Vis Sci *56*, 3075-3083.

Lu, W., Reigada, D., Sevigny, J., and Mitchell, C.H. (2007). Stimulation of the P2Y1 receptor up-regulates nucleoside-triphosphate diphosphohydrolase-1 in human retinal pigment epithelial cells. The Journal of pharmacology and experimental therapeutics *323*, 157-164.

Lye-Barthel, M., Sun, D., and Jakobs, T.C. (2013). Morphology of astrocytes in a glaucomatous optic nerve. Invest Ophthalmol Vis Sci *54*, 909-917.

Malamed, S.F., Gagnon, S., and Leblanc, D. (2001). Articaine hydrochloride: a study of the safety of a new amide local anesthetic. J Am Dent Assoc *132*, 177-185.

Malet, A., Faure, M.O., Deletage, N., Pereira, B., Haas, J., and Lambert, G. (2015). The comparative cytotoxic effects of different local anesthetics on a human neuroblastoma cell line. Anesthesia and analgesia *120*, 589-596.

Man, S.M., and Kanneganti, T.D. (2015). Regulation of inflammasome activation. Immunol Rev *265*, 6-21.

Mandal, A., Shahidullah, M., Delamere, N.A., and Teran, M.A. (2009). Elevated hydrostatic pressure activates sodium/hydrogen exchanger-1 in rat optic nerve head astrocytes. American journal of physiologyCell physiology *297*, C111-120.

Mariathasan, S., Weiss, D.S., Newton, K., McBride, J., O'Rourke, K., Roose-Girma, M., Lee, W.P., Weinrauch, Y., Monack, D.M., and Dixit, V.M. (2006). Cryopyrin activates the inflammasome in response to toxins and ATP. Nature *440*, 228-232.

Martinon, F. (2008). Detection of immune danger signals by NALP3. J Leukoc Biol *83*, 507-511.

Martinon, F., Burns, K., and Tschopp, J. (2002). The inflammasome: a molecular platform triggering activation of inflammatory caspases and processing of proIL-beta. Molecular cell *10*, 417-426.

Martinon, F., Holler, N., Richard, C., and Tschopp, J. (2000). Activation of a pro-apoptotic amplification loop through inhibition of NF-kappaB-dependent survival signals by caspase-mediated inactivation of RIP. FEBS Lett *468*, 134-136.

Medzhitov, R. (2008). Origin and physiological roles of inflammation. Nature *454*, 428-435.

Mitchell, C.H. (2001). Release of ATP by a human retinal pigment epithelial cell line: potential for autocrine stimulation through subretinal space. J Physiol *534*, 193-202.

Mitchell, C.H., Albalawi, F., Lim, J., and Lu, W.N. (2016). Priming of the NLRP3 inflammasome in optic nerve head astrocytes by mechanical strain and

stimulation of the P2X7 receptor. Investigative Ophthalmology & Visual Science *57*, 2.

Mitchell, C.H., Albalawi, F., and Lu, W. (2017). Increased IOP primes the NLRP3 inflammasome and increases IL-1β levels. Investigative Ophthalmology & Visual Science *58*, 851 Abstract.

Mitchell, C.H., Lu, W., Hu, H., Zhang, X., Reigada, D., and Zhang, M. (2009). The P2X(7) receptor in retinal ganglion cells: A neuronal model of pressure-induced damage and protection by a shifting purinergic balance. Purinergic Signal *5*, 241-249

Moore, P.A., and Hersh, E.V. (2010). Local anesthetics: pharmacology and toxicity. Dental clinics of North America *54*, 587-599.

Morgan, J.E. (2000). Optic nerve head structure in glaucoma: astrocytes as mediators of axonal damage. Eye (Lond) *14 (Pt 3B)*, 437-444.

Morrison, J.C., Cepurna, W.O., Doser, T.A., Dyck, J.A., and Johnson, E.C. (2010). A short interval of controlled elevation of IOP (CEI) reproduces early chronic glaucoma model optic nerve head (ONH) gene expression responses. Investigative ophthalmology & visual science *51*, 5216. ARVO E-Abstract.

Morrison, J.C., Cepurna, W.O., Tehrani, S., Choe, T.E., Jayaram, H., Lozano, D.C., Fortune, B., and Johnson, E.C. (2016). A Period of Controlled Elevation of IOP (CEI) Produces the Specific Gene Expression Responses and Focal Injury Pattern of Experimental Rat Glaucoma. Invest Ophthalmol Vis Sci *57*, 6700-6711.

Morrison, J.C., Cepurna Ying Guo, W.O., and Johnson, E.C. (2011). Pathophysiology of human glaucomatous optic nerve damage: insights from rodent models of glaucoma. Experimental eye research *93*, 156-164.

Morrison, J.C., Choe, T.E., Cepurna, W.O., and Johnson, E.C. (2014). Optic nerve head (ONH) gene expression responses to elevated intraocular pressure (IOP), anesthesia and anterior chamber cannulation in the CEI (Controlled Elevation of IOP) model of IOP-induced optic nerve injury. Investigative ophthalmology & visual science *55*, 2402. ARVO E-Abstract.

Nedergaard, M., Ransom, B., and Goldman, S.A. (2003). New roles for astrocytes: redefining the functional architecture of the brain. Trends in neurosciences *26*, 523-530.

Panchin, Y., Kelmanson, I., Matz, M., Lukyanov, K., Usman, N., and Lukyanov, S. (2000). A ubiquitous family of putative gap junction molecules. Current biology : CB *10*, R473-474.

Patel, M.N., Carroll, R.G., Galvan-Pena, S., Mills, E.L., Olden, R., Triantafilou, M., Wolf, A.I., Bryant, C.E., Triantafilou, K., and Masters, S.L. (2017). Inflammasome Priming in Sterile Inflammatory Disease. Trends Mol Med *23*, 165-180.

Pedlar, J. (2003). Prolonged paraesthesia. Br Dent J *195*, 119.

Pelegrin, P., and Surprenant, A. (2006). Pannexin-1 mediates large pore formation and interleukin-1beta release by the ATP-gated P2X7 receptor. The EMBO journal *25*, 5071-5082.

Pelegrin, P., and Surprenant, A. (2007). Pannexin-1 couples to maitotoxin- and nigericin-induced interleukin-1beta release through a dye uptake-independent pathway. J Biol Chem *282*, 2386-2394.

Penkowa, M., Giralt, M., Lago, N., Camats, J., Carrasco, J., Hernandez, J., Molinero, A., Campbell, I.L., and Hidalgo, J. (2003). Astrocyte-targeted expression of IL-6 protects the CNS against a focal brain injury. Exp Neurol *181*, 130-148.

Penuela, S., Gehi, R., and Laird, D.W. (2013). The biochemistry and function of pannexin channels. Biochim Biophys Acta *1828*, 15-22.

Perregaux, D., and Gabel, C.A. (1994). Interleukin-1 beta maturation and release in response to ATP and nigericin. Evidence that potassium depletion mediated by these agents is a necessary and common feature of their activity. J Biol Chem *269*, 15195-15203.

Petrilli, V., Papin, S., Dostert, C., Mayor, A., Martinon, F., and Tschopp, J. (2007). Activation of the NALP3 inflammasome is triggered by low intracellular potassium concentration. Cell death and differentiation *14*, 1583-1589.

Plantinga, T.S., Joosten, L.A., and Netea, M.G. (2013). Assessment of inflammasome activation in primary human immune cells. Methods in molecular biology *1040*, 29-39.

Pogrel, M.A. (2007). Permanent nerve damage from inferior alveolar nerve blocks--an update to include articaine. Journal of the California Dental Association *35*, 271-273.

Poornima, V., Madhupriya, M., Kootar, S., Sujatha, G., Kumar, A., and Bera, A.K. (2012). P2X7 receptor-pannexin 1 hemichannel association: effect of extracellular calcium on membrane permeabilization. J Mol Neurosci *46*, 585-594.

Praetorius, H.A., and Leipziger, J. (2009). ATP release from non-excitable cells. Purinergic signalling *5*, 433-446.

Qiu, F., Wang, J., Spray, D.C., Scemes, E., and Dahl, G. (2011). Two non-vesicular ATP release pathways in the mouse erythrocyte membrane. FEBS Lett *585*, 3430-3435.

Quigley, H.A., and Addicks, E.M. (1980). Chronic experimental glaucoma in primates. I. Production of elevated intraocular pressure by anterior chamber injection of autologous ghost red blood cells. Invest Ophthalmol Vis Sci *19*, 126-136.

Ransford, G.A., Fregien, N., Qiu, F., Dahl, G., Conner, G.E., and Salathe, M. (2009). Pannexin 1 contributes to ATP release in airway epithelia. Am J Respir Cell Mol Biol *41*, 525-534.

Rathinam, V.A., Vanaja, S.K., and Fitzgerald, K.A. (2012). Regulation of inflammasome signaling. Nature immunology *13*, 333-342.

Rego, D., Kumar, A., Nilchi, L., Wright, K., Huang, S., and Kozlowski, M. (2011). IL-6 production is positively regulated by two distinct Src homology domain 2-containing tyrosine phosphatase-1 (SHP-1)-dependent CCAAT/enhancer-binding protein beta and NF-kappa B Pathways J Immunol *186*, 5443-5456.

Reigada, D., Lu, W., Zhang, M., and Mitchell, C.H. (2008). Elevated pressure triggers a physiological release of ATP from the retina: Possible role for pannexin hemichannels. Neuroscience *157*, 396-404 PMID:18822352 PMC12692262

Reigada, D., Lu, W., Zhang, X., Friedman, C., Pendrak, K., McGlinn, A., Stone, R.A., Laties, A.M., and Mitchell, C.H. (2005). Degradation of extracellular ATP by the retinal pigment epithelium. American journal of physiology Cell physiology *289*, C617-624.

Resnikoff, S., Pascolini, D., Etya'ale, D., Kocur, I., Pararajasegaram, R., Pokharel, G.P., and Mariotti, S.P. (2004). Global data on visual impairment in the year 2002. Bulletin of the World Health Organization *82*, 844-851.

Rhee, S.H. (2011). Basic and translational understandings of microbial recognition by toll-like receptors in the intestine. J Neurogastroenterol Motil *17*, 28-34.

Ringheim, G.E., Burgher, K.L., and Heroux, J.A. (1995). Interleukin-6 mRNA expression by cortical neurons in culture: evidence for neuronal sources of interleukin-6 production in the brain. J Neuroimmunol *63*, 113-123.

Sanderson, J., Dartt, D.A., Trinkaus-Randall, V., Pintor, J., Civan, M.M., Delamere, N.A., Fletcher, E.L., Salt, T.E., Grosche, A., and Mitchell, C.H. (2014). Purines in the eye: recent evidence for the physiological and pathological role of purines in the RPE, retinal neurons, astrocytes, Muller cells, lens, trabecular meshwork, cornea and lacrimal gland. Experimental eye research *127*, 270-279.

Sappington, R.M., and Calkins, D.J. (2006). Pressure-induced regulation of IL-6 in retinal glial cells: involvement of the ubiquitin/proteasome pathway and NFkappaB. Investigative ophthalmology & visual science *47*, 3860-3869.

Sappington, R.M., Chan, M., and Calkins, D.J. (2006). Interleukin-6 protects retinal ganglion cells from pressure-induced death. Invest Ophthalmol Vis Sci *47*, 2932-2942.

Satrawaha, S., Wongkhantee, S., Pavasant, P., and Sumrejkanchanakij, P. (2011). Pressure induces interleukin-6 expression via the P2Y6 receptor in human dental pulp cells. Arch Oral Biol *56*, 1230-1237.

Scemes, E., Spray, D.C., and Meda, P. (2009). Connexins, pannexins, innexins: novel roles of "hemi-channels". Pflugers Archiv : European journal of physiology *457*, 1207-1226.

Scheller, J., Garbers, C., and Rose-John, S. (2014). Interleukin-6: from basic biology to selective blockade of pro-inflammatory activities. Seminars in immunology *26*, 2-12.

Schindelin, J., Rueden, C.T., Hiner, M.C., and Eliceiri, K.W. (2015). The ImageJ ecosystem: An open platform for biomedical image analysis. Mol Reprod Dev *82*, 518-529.

Schroder, K., Sagulenko, V., Zamoshnikova, A., Richards, A.A., Cridland, J.A., Irvine, K.M., Stacey, K.J., and Sweet, M.J. (2012). Acute lipopolysaccharide priming boosts inflammasome activation independently of inflammasome sensor induction. Immunobiology *217*, 1325-1329.

Seminario-Vidal, L., Okada, S.F., Sesma, J.I., Kreda, S.M., van Heusden, C.A., Zhu, Y., Jones, L.C., O'Neal, W.K., Penuela, S., Laird, D.W.*, et al.* (2011). Rho signaling regulates pannexin 1-mediated ATP release from airway epithelia. J Biol Chem *286*, 26277-26286.

Shahidullah, M., Mandal, A., and Delamere, N.A. (2012). TRPV4 in porcine lens epithelium regulates hemichannel-mediated ATP release and Na-K-ATPase activity. American journal of physiology Cell physiology *302*, C1751-1761.

Shieh, C.H., Heinrich, A., Serchov, T., van Calker, D., and Biber, K. (2014). P2X7-dependent, but differentially regulated release of IL-6, CCL2, and TNF-alpha in cultured mouse microglia. Glia *62*, 592-607.

Shigemoto-Mogami, Y., Koizumi, S., Tsuda, M., Ohsawa, K., Kohsaka, S., and Inoue, K. (2001). Mechanisms underlying extracellular ATP-evoked interleukin-6 release in mouse microglial cell line, MG-5. Journal of neurochemistry *78*, 1339-1349.

Sigal, I.A., and Ethier, C.R. (2009). Biomechanics of the optic nerve head. Experimental eye research *88*, 799-807.

Silinsky, E.M. (1975). On the association between transmitter secretion and the release of adenine nucleotides from mammalian motor nerve terminals. J Physiol *247*, 145-162.

Silverman, W., Locovei, S., and Dahl, G. (2008). Probenecid, a gout remedy, inhibits pannexin 1 channels. American journal of physiology Cell physiology *295*, C761-767.

Silverman, W.R., de Rivero Vaccari, J.P., Locovei, S., Qiu, F., Carlsson, S.K., Scemes, E., Keane, R.W., and Dahl, G. (2009). The pannexin 1 channel activates the inflammasome in neurons and astrocytes. J Biol Chem *284*, 18143-18151.

Snoeck, M. (2012). Articaine: a review of its use for local and regional anesthesia. Local and regional anesthesia *5*, 23-33.

Sofroniew, M.V. (2009). Molecular dissection of reactive astrogliosis and glial scar formation. Trends in neurosciences *32*, 638-647.

Solle, M., Labasi, J., Perregaux, D.G., Stam, E., Petrushova, N., Koller, B.H., Griffiths, R.J., and Gabel, C.A. (2001). Altered cytokine production in mice lacking P2X(7) receptors. The Journal of biological chemistry *276*, 125-132.

Sperlagh, B., and Illes, P. (2014). P2X7 receptor: an emerging target in central nervous system diseases. Trends Pharmacol Sci *35*, 537-547.

Sperlagh, B., Vizi, E.S., Wirkner, K., and Illes, P. (2006). P2X7 receptors in the nervous system. Progress in neurobiology *78*, 327-346.

Spooren, A., Kolmus, K., Laureys, G., Clinckers, R., De Keyser, J., Haegeman, G., and Gerlo, S. (2011). Interleukin-6, a mental cytokine. Brain Res Rev *67*, 157-183.

Stutz, A., Golenbock, D.T., and Latz, E. (2009). Inflammasomes: too big to miss. J Clin Invest *119*, 3502-3511.

Suadicani, S.O., Iglesias, R., Wang, J., Dahl, G., Spray, D.C., and Scemes, E. (2012). ATP signaling is deficient in cultured Pannexin1-null mouse astrocytes. Glia *60*, 1106-1116.

Surprenant, A., and North, R.A. (2009). Signaling at purinergic P2X receptors. Annual review of physiology *71*, 333-359.

Takeda, K., and Akira, S. (2004). Microbial recognition by Toll-like receptors. J Dermatol Sci *34*, 73-82.

Tamai, M., Kobayashi, N., Shimada, K., Oka, N., Takahashi, M., Tanuma, A., Tanemoto, T., Namba, H., Saito, Y., Wada, Y.*, et al.* (2017). Increased interleukin-1beta and basic fibroblast growth factor levels in the cerebrospinal fluid during human herpesvirus-6B (HHV-6B) encephalitis. Biochem Biophys Res Commun *486*, 706-711.

Taruno, A., Vingtdeux, V., Ohmoto, M., Ma, Z., Dvoryanchikov, G., Li, A., Adrien, L., Zhao, H., Leung, S., Abernethy, M.*, et al.* (2013). CALHM1 ion channel mediates purinergic neurotransmission of sweet, bitter and umami tastes. Nature *495*, 223-226.

Tehrani, S., Davis, L., Cepurna, W.O., Choe, T.E., Lozano, D.C., Monfared, A., Cooper, L., Cheng, J., Johnson, E.C., and Morrison, J.C. (2016). Astrocyte Structural and Molecular Response to Elevated Intraocular Pressure Occurs Rapidly and Precedes Axonal Tubulin Rearrangement within the Optic Nerve Head in a Rat Model. PLoS One *11*, e0167364.

Tehrani, S., Johnson, E.C., Cepurna, W.O., and Morrison, J.C. (2014). Astrocyte processes label for filamentous actin and reorient early within the optic nerve head in a rat glaucoma model. Invest Ophthalmol Vis Sci *55*, 6945-6952.

Thornberry, N.A., Bull, H.G., Calaycay, J.R., Chapman, K.T., Howard, A.D., Kostura, M.J., Miller, D.K., Molineaux, S.M., Weidner, J.R., Aunins, J., *et al.* (1992). A novel heterodimeric cysteine protease is required for interleukin-1 beta processing in monocytes. Nature *356*, 768-774.

Thundyil, J., and Lim, K.L. (2015). DAMPs and neurodegeneration. Ageing Res Rev *24*, 17-28.

Totan, Y., Guler, E., and Dervisogullari, M.S. (2014). Brilliant Blue G assisted epiretinal membrane surgery. Scientific reports *4*, 3956.

Tsakiri, N., Kimber, I., Rothwell, N.J., and Pinteaux, E. (2008). Mechanisms of interleukin-6 synthesis and release induced by interleukin-1 and cell depolarisation in neurones. Mol Cell Neurosci *37*, 110-118.

Tsukimoto, M., Maehata, M., Harada, H., Ikari, A., Takagi, K., and Degawa, M. (2006). P2X7 receptor-dependent cell death is modulated during murine T cell maturation and mediated by dual signaling pathways. Journal of immunology (Baltimore, Md: 1950) *177*, 2842-2850.

Valentin, J.L., Lopez, D., Hernandez, R., Mijangos, C., and Saalwachter, K. (2009). Structure of Poly(vinyl alcohol) Cryo-Hydrogels as Studied by Proton Low-Field NMR Spectroscopy. Macromolecules *42*, 263-272.

van Aubel, R.A., Smeets, P.H., Peters, J.G., Bindels, R.J., and Russel, F.G. (2002). The MRP4/ABCC4 gene encodes a novel apical organic anion transporter in human kidney proximal tubules: putative efflux pump for urinary cAMP and cGMP. J Am Soc Nephrol *13*, 595-603.

Vetter, I., Mozar, C.A., Durek, T., Wingerd, J.S., Alewood, P.F., Christie, M.J., and Lewis, R.J. (2012). Characterisation of Na(v) types endogenously expressed in human SH-SY5Y neuroblastoma cells. Biochemical pharmacology *83*, 1562-1571.

Virginio, C., MacKenzie, A., North, R.A., and Surprenant, A. (1999). Kinetics of cell lysis, dye uptake and permeability changes in cells expressing the rat P2X7 receptor. The Journal of physiology *519 Pt 2*, 335-346.

Walsh, J.G., Muruve, D.A., and Power, C. (2014). Inflammasomes in the CNS. Nat Rev Neurosci *15*, 84-97.

Weber, A., Wasiliew, P., and Kracht, M. (2010). Interleukin-1 (IL-1) pathway. Sci Signal *3*, cm1.

Wildman, S.S., Unwin, R.J., and King, B.F. (2003). Extended pharmacological profiles of rat P2Y2 and rat P2Y4 receptors and their sensitivity to extracellular H+ and Zn2+ ions. British journal of pharmacology *140*, 1177-1186.

Wilson, G.N., Inman, D.M., Dengler Crish, C.M., Smith, M.A., and Crish, S.D. (2015). Early pro-inflammatory cytokine elevations in the DBA/2J mouse model of glaucoma. Journal of neuroinflammation *12*, 176.

Winston, F.K., Macarak, E.J., Gorfien, S.F., and Thibault, L.E. (1989). A system to reproduce and quantify the biomechanical environment of the cell. J Appl Physiol *67*, 397-405.

Xia, J., Lim, J.C., Lu, W., Beckel, J.M., Macarak, E.J., Laties, A.M., and Mitchell, C.H. (2012a). Neurons respond directly to mechanical deformation with pannexin-mediated ATP release and autostimulation of P2X7 receptors. The Journal of physiology *590*, 2285-2304.

Xia, J., Lim, J.C., Lu, W., Beckel, J.M., Macarak, E.J., Laties, A.M., and Mitchell, C.H. (2012b). Neurons respond directly to mechanical deformation with pannexin-mediated ATP release and autostimulation of P2X7 receptors. The Journal of physiology *590*, 2285-2304.

Xiao, L., Xu, H.G., Wang, H., Liu, P., Liu, C., Shen, X., Zhang, T., and Xu, Y.M. (2016). Intermittent Cyclic Mechanical Tension Promotes Degeneration of Endplate Cartilage via the Nuclear Factor-kappaB Signaling Pathway: an in Vivo Study. Orthop Surg *8*, 393-399.

Yang, H., Downs, J.C., and Burgoyne, C.F. (2009). Physiologic intereye differences in monkey optic nerve head architecture and their relation to changes in early experimental glaucoma. Invest Ophthalmol Vis Sci *50*, 224-234.

Yang, S.H., Gangidine, M., Pritts, T.A., Goodman, M.D., and Lentsch, A.B. (2013). Interleukin 6 mediates neuroinflammation and motor coordination deficits after mild traumatic brain injury and brief hypoxia in mice. Shock *40*, 471-475.

Yilmaz, O., and Lee, K.L. (2015). The inflammasome and danger molecule signaling: at the crossroads of inflammation and pathogen persistence in the oral cavity. Periodontol 2000 *69*, 83-95.

Yoneda, S., Tanihara, H., Kido, N., Honda, Y., Goto, W., Hara, H., and Miyawaki, N. (2001). Interleukin-1beta mediates ischemic injury in the rat retina. Experimental eye research *73*, 661-667.

Yu, J., Sheung, N., Soliman, E.M., Spirli, C., and Dranoff, J.A. (2009). Transcriptional regulation of IL-6 in bile duct epithelia by extracellular ATP. American journal of physiology Gastrointestinal and liver physiology *296*, G563-571.

Zenkel, M., Lewczuk, P., Junemann, A., Kruse, F.E., Naumann, G.O., and Schlotzer-Schrehardt, U. (2010). Proinflammatory cytokines are involved in the initiation of the abnormal matrix process in pseudoexfoliation syndrome/glaucoma. Am J Pathol *176*, 2868-2879.

Zhang, M., Hu, H., Zhang, X., Lu, W., Lim, J., Eysteinsson, T., Jacobson, K.A., Laties, A.M., and Mitchell, C.H. (2010). The A3 adenosine receptor attenuates the calcium rise triggered by NMDA receptors in retinal ganglion cells. Neurochem Int *56*, 35-41.

Zhang, X., Li, A., Ge, J., Reigada, D., Laties, A.M., and Mitchell, C.H. (2007). Acute increase of intraocular pressure releases ATP into the anterior chamber. Experimental eye research *85*, 637-643.

Zhang, X., Zhang, M., Laties, A.M., and Mitchell, C.H. (2005). Stimulation of P2X7 receptors elevates Ca2+ and kills retinal ganglion cells. Invest Ophthalmol Vis Sci *46*, 2183-2191.

Zhang, X., Zhang, M., Laties, A.M., and Mitchell, C.H. (2006). Balance of purines may determine life or death of retinal ganglion cells as A3 adenosine receptors prevent loss following P2X7 receptor stimulation. Journal of neurochemistry *98*, 566-575

Zhi, Z., Cepurna, W.O., Johnson, E.C., Morrison, J.C., and Wang, R.K. (2012). Impact of intraocular pressure on changes of blood flow in the retina, choroid, and optic nerve head in rats investigated by optical microangiography. Biomedical optics express *3*, 2220-2233.

Zode, G.S., Kuehn, M.H., Nishimura, D.Y., Searby, C.C., Mohan, K., Grozdanic, S.D., Bugge, K., Anderson, M.G., Clark, A.F., Stone, E.M.*, et al.* (2011). Reduction of ER stress via a chemical chaperone prevents disease phenotypes in a mouse model of primary open angle glaucoma. J Clin Invest *121*, 3542-3553.

Zode, G.S., Kuehn, M.H., Nishimura, D.Y., Searby, C.C., Mohan, K., Grozdanic, S.D., Bugge, K., Anderson, M.G., Clark, A.F., Stone, E.M.*, et al.* (2015). Reduction of ER stress via a chemical chaperone prevents disease phenotypes in a mouse model of primary open angle glaucoma. J Clin Invest *125*, 3303.